NANO-COMPOSITE MATERIAL COATING TO IMPROVE THE SOLAR CELL EFFICIENCY IN HOT WEATHER CONDITION

THESIS

SUBMITTED TO THE DEPARTMENT OF MECHANICAL ENGINEERING TECHNIQUES OF POWER
IN PARTIAL FULFILLMENT OF THE REQUIREMENTS FOR THE DEGREE OF MASTER THERMAL TECHNOLOGIES IN MECHANICAL ENGINEERING TECHNIQUES OF POWER (M.TECH.)

BY

ALI MAJID ABBOOD

Supervised by

Prof. Dr. Qahtan Adnan Abed

August/2022

بسم الله الرحمن الرحيم

﴿ اقْرَأْ بِاسْمِ رَبِّكَ الَّذِي خَلَقَ (١) خَلَقَ الْإِنْسَانَ مِنْ عَلَقٍ (٢) اقْرَأْ وَرَبُّكَ الْأَكْرَمُ (٣) الَّذِي عَلَّمَ بِالْقَلَمِ (٤) عَلَّمَ الْإِنْسَانَ مَا لَمْ يَعْلَمْ (٥) ﴾

صدق الله العلي العظيم

سورة العلق: ألايه ١-٥

DISCLAIMER

I confirm that the work in this thesis is entirely mine and has not been submitted to another organization or for any other degree, except perhaps properly cited quotations and summaries.

Signature:

Name: Ali Majid Abbood

Date: /   / 2022

ACKNOWLEDGMENTS

SUPERVISORS CERTIFICATION

I certify that this thesis titled **"Nano-Composite Material Coating to Improve the Solar Cell Efficiency in Hot Weather Condition"** which is being submitted by **Ali Majid Abbood** has been prepared under my supervision at the Department of Mechanical Engineering Techniques of Power, College of Technical Engineering-Najaf, AL-Furat Al-Awsat Technical University, as partial fulfillment of the requirements for the Master's degree in Thermal Engineering Techniques.

Signature:

Name: **Prof. Dr. Qahtan Adnan Abed** (Supervisor)

Date: /   / 2022

In view of the available recommendation, I forward this thesis for debate by the examining committee.

Signature:

Name: **Dr. Ahmed Salim Naser Almurshdi**

Head of Mechanical Eng. Tech of Power Dept.

Date: /   / 2022

COMMITTEE CERTIFICATION

We certify that we have read the thesis titled " **Nano-Composite Material Coating to Improve the Solar Cell Efficiency in Hot Weather Condition** " submitted by **Ali Majid Abbood** and, as the examining committee, examined the student's thesis in its contents. In our opinion, is adequate as a thesis for the degree of Master of Techniques in Thermal Engineering.

Signature:

Name: **Dr. Qahtan Adnan Abed**

Title: Professor

(Supervisor)

Date: /   / 2022

Signature: Signature:

Name: **Dr. Wisam A. Abd Al-wahid**   Name: **Dr. Sahib Shihab Ahmed**

Title: Assistant Professor   Title: Assistant Professor

(Member)   (Member)

Date: /   / 2022   Date: /   / 2022

Signature:

Name: **Dr. Ahmed Hashim Yousif**

Title: Professor

(Chairman)

Date: /   / 2022

Approval of the Engineering Technical College- Najaf

Signature:

Name: **Asst. Prof. Dr. Hassanain Ghani Hameed**

Dean of Engineering Technical College- Najaf

Date: /   / 2022

IV

LINGUISTIC CERTIFICATION

This is to certify that this thesis "**Nano-Composite Material Coating to Improve the Solar Cell Efficiency in Hot Weather Condition**" was reviewed linguistically. Its language was amended to meet the style of the English language.

Signature:

Name:

Date: /   / 2022

ABSTRACT

Solar energy is a crucial green energy source since, in contrast to carbon-emitting fossil resources, it is renewable and easily accessible to the general citizens.

One of the most promising methods for collecting solar energy is the use of photovoltaic systems (PVs), which semiconductors that convert solar energy into an electric current by using photons from the sun to excite electrons. When a PV solar cell is exposed to light, voltage and current are generated. The photovoltaic panel's efficiency suffers from a noticeably reduced solar energy conversion with the rise of the solar cell surface temperature, with about 0.45% dropping efficiency for each 1 °C rise in its working solar cell surface temperature. In addition, the reflection of the sun's irradiance from the panel typically accounts for approximately 35% of the entire amount of sunlight, leading to a reduction in the electrical efficiency of PV modules.

This research specifically investigates way to minimize the impact of temperature increase and reflection losses on polycrystalline silicon solar cells. The method utilized for that is coating the top surface of the solar cell with nanocomposite thin-films made of polymer-polymethyl methacrylate (PMMA), zinc oxide (ZnO) with nano-sized (40–50nm) particles. Different concentrations of (ZnO) and (PMMA) have been used (0.25 wt%, 0.5 wt%, 0.75 wt%, and 1 wt%) and (0.625 wt%, 1.25 wt%, 2.5 wt%, 3.125 wt%, and 3.75 wt%) respectively, in order to prepare four concentrations of ZnO/PMMA nanocomposite coating (3.375 wt%, 3.625 wt%, 3.875 wt%, and 4.125 wt%).

Based on the electrical properties of solar cells test and through the tests (U-V Spectrophotometer device), the results observed that the PMMA affects an Ultraviolet blocking system and thus decreases the solar

cell surface temperature & the ZnO as an anti-reflection coating and reducing the reflection losses. The best concentration of the PMMA was (3.125 wt%) in terms of its ability to absorb the greatest intensity of Ultraviolet solar radiation. The (0.75 wt%) of the ZnO was the best concentration was chosen in terms of its capability to reduce the reflection losses so the best ZnO/PMMA concentration was (3.875 wt%). 8.6 ⁰C was the maximum temperature difference yielded as compared to without coating solar cell, and 5.6% reflection losses was the minimum reflection losses obtained as compared to 35% reflection losses without coating solar cell. The solar cell had an improvement in the efficiency of +3.8%.

CONTENTS

IX

LIST OF FIGURES

XIII

LIST OF TABLES

NOMENCLATURE

Symbol	Description	Unit
A	Absorbance	A.U
ARC	Anti-reflection coating	-
b	Light path length	cm
C	Concentration	Mol/L
C-Si	Crystalline Silicon	-
c	Speed of light	m/s
D	Density	g/cm^3
DW	Distilled water	-
d	Thickness of material	mm
E	Photon Energy	Joule (J)
E_g	Energy band gap	Electron volte (eV)
FF	Fill Factor	-
h	Planck's constant	J.s
I_{SC}	Short Circuit Current	Ampere (A)
I_{mp}	Maximum power Current	Ampere (A)
I_L	light-generated current	Ampere (A)
I_o	Dark saturation current	Ampere (A)
IR	Infrared radiation	-
Mono-Si	Monocrystalline silicon	-
NPs	Nanoparticles	-
n	Refractive index	-
P	Power	Watt (W)
P_{inc}	Incident light power	Watt (W)
PV	Photovoltaic	-
PVA	Polyvinyl alcohol	-

PMMA	Polymethyl Methacrylate	-
Poly-Si	Polycrystalline silicon	-
R	Reflection	A.U
STC	Standard Test Condition	-
Si	Silicon	-
T	Transmittance	A.U
UV	Ultraviolet radiation	-
v	Photon frequency	Hertz (Hz)
V$_{OC}$	Open Circuit Voltage	Voltage (V)
V$_{mp}$	Maximum power voltage	Voltage (V)
wt%	Weight percent	-
ZnO	Zinc Oxide	-
α	Absorption coefficient	cm^{-1}
ε	Molar attenuation coefficient	M^{-1}. cm^{-1}
λ	Wavelength	Nanometer (nm)
ŋ	Electrical Efficiency	Percent (%)

Chapter One
Introduction

Introduction

1.1 Introduction

One of the most significant renewable sources of energy is the solar energy because of its minimal environmental effect and easy accessibility. In comparison to carbon-emitting fossil resources, solar energy is renewable and readily available to the general public, making it a critical green power source [1]. Solar cells are comprised of semiconductors which utilize photons from the sun to excite the electrons, resulting in a direct electric current and the conversion of energy from the sun light, whenever a PV cell is exposed to light, voltage - current are produced [2]. Photovoltaic systems (PVs) are one of the most potential solar energy harvesting approaches, but the PV technology power generation system does have certain basic issues, such as hail, dust, and the operating temperature, that can reduce the generator system's efficiency [3]. Solar cells usually operate in a temperature range of 50 °C to 55 °C or higher. Not all solar radiation absorbed by PV solar cell is converted into electricity, a large part of it converts into heat that causes the solar cell to heat up [4].

For example, solar cells made of crystalline silicon, each increase in surface temperature by 1 °C leads to about 0.45% reduction in efficiency, as a result, the heat dissipation of a solar panel is critical to lowering its temperature, which has a severe impact on energy output [5]. Normally PV solar cells are comprised of silicon (Si), which may be the second most prevalent substance found on the earth's mantle and has a high surface reflection characteristic. Accordingly, after striking the PV panel, approximately 35% of the entire amount of sunlight reflects, according to recent developments, either micro coating or nano-composite coating of antireflection compounds on the PV panel improves solar energy

conversion and compounds that are fluorescent to lower the conversion rate capabilities can be used to solve the high temperature problem [6].

1.2   Solar Radiation Spectrum

The sun is located 150 million kilometers away with solar radiation constant 1367 W/ m^2, this number changes by ±3% depending on how far the earth is from the sun. The light daily is only a small portion of the total energy generated by the sun, it is electromagnetic waves that extend from gamma rays to radio rays, among which are X-rays, ultraviolet, visible, infrared, and microwave rays as shown in the figure 1.1, the photon's energy and the wavelength of light are inversely related [7]. the figure 1.2 shows how much of the incoming solar energy is reflected and absorbed (the earth's energy budget), the sunlight in ground level consists of 44% visible light, 3% ultraviolet light and the remaining is infrared light. Since the atmosphere blocks 77% of the sun's UV-radiation [2].
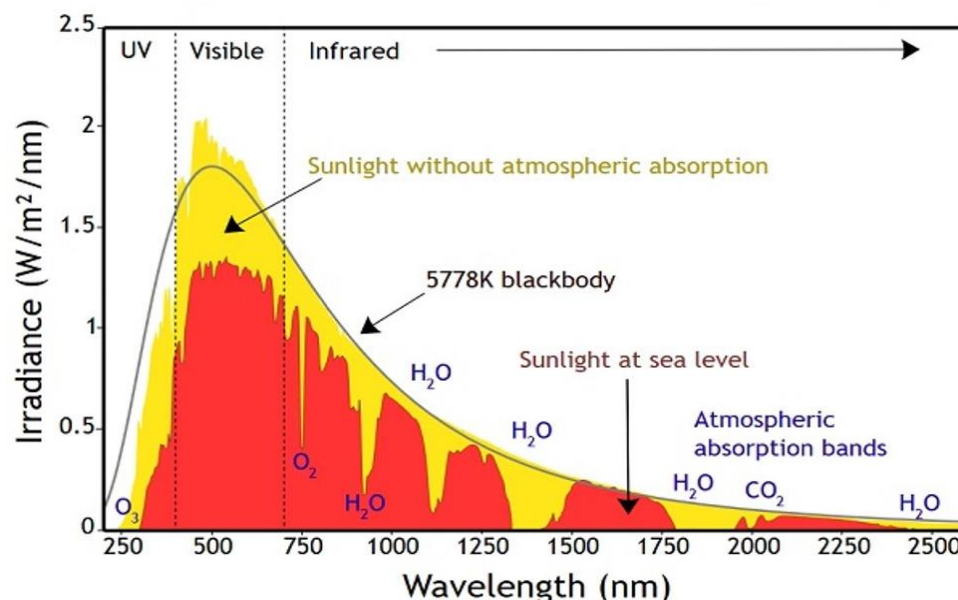
Figure 1.1. Spectrum of Solar Radiation (Earth) [7]
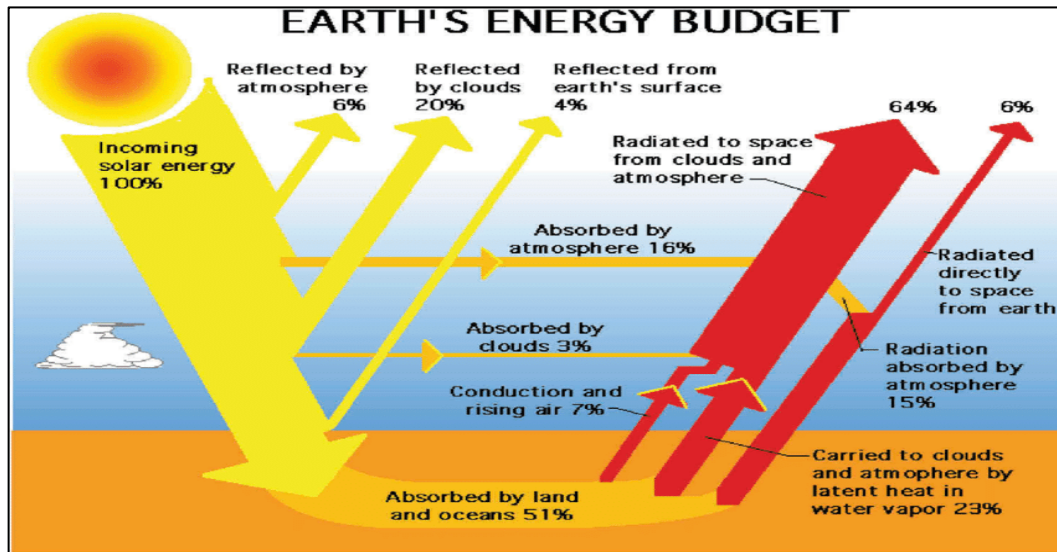
Figure 1.2. Percentage of solar energy incoming, absorbed, and reflected [2].

1.3   Photovoltage Solar cell (PV)

A photovoltaic cell is a semiconductor device that converts sunlight into electricity. It's comprised of highly pure silicon wafers that have been doped with substances that produce an abundance of electrons and holes in the crystalline lattice.

1.4   Working Principles of the PV Solar Cell

The Solar cells have comprised of semiconductors which utilize photons from the sun to excite the electrons, resulting in a direct electric current and the conversion of energy from the sun. Whenever a PV cell is exposed to light, voltage - current are produced. Although the connection between absorbed light and electricity generated production is linear, numerous factors influence the solar cell performance, as a result, its output power. The operating temperature has a great impact on the efficiency of the PV cell. The photovoltaic cell's produced electrical current passes across a P-N junction. As a result, only photons with energies equal to or greater than the band-gap energy is engaged, see figure 1.3. Whenever the energy of a photon exceeds the energy bandgap,

3

electrons are liberating, and the excess is transformed into heat, raising the temperature of the solar cell, so about 20% of overall light is transformed into electrical energy, and the remaining 80% is wasted as light reflects, and as heat in the silicon semiconductor, or light that passes along the photovoltaic cells without being absorbed or reflected. The formation of electrical charge in solar cells is caused by the activation of the semi-conducting of sunlight electrons, which may maximize the efficiency by collecting the complete solar spectra inside that range's band without sacrificing any energy [8].
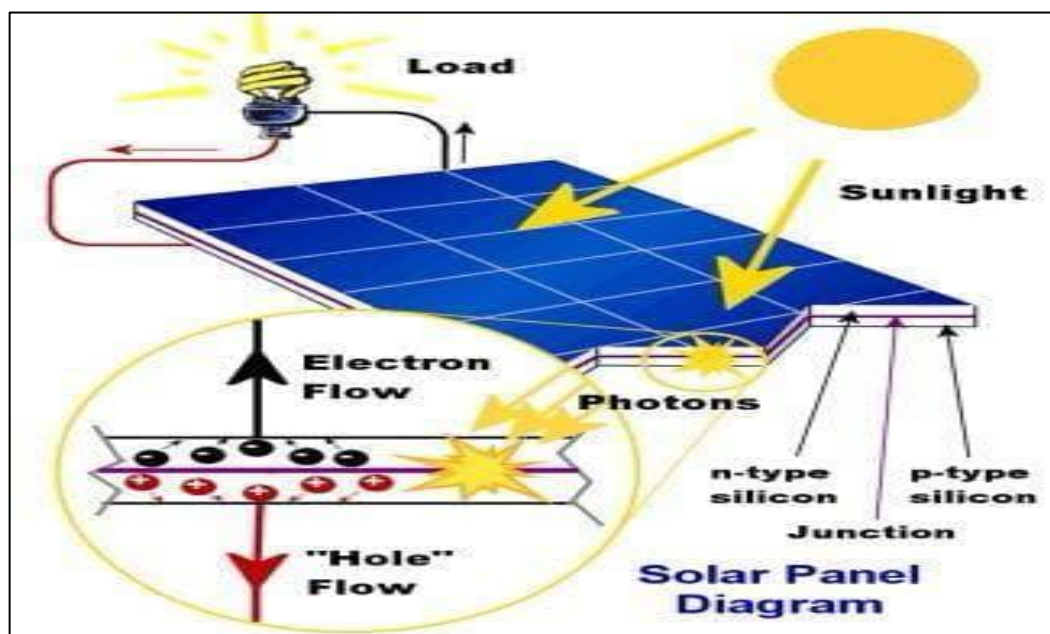
Figure 1.3. Silicon solar cell [8].

Therefore, the process of absorbing high-energy photons, such as ultraviolet photons, is one of the factors causing the rising the temperature of the solar cell. Ultraviolet rays (UV) are divided into three regions based on their intensity (A, B, and C) within the wave range of 200–400 nm, where UV-C has the highest energy within the range of 200–280 nm, where it has electron energy of about 4.43 to 4.4 electron volts (eV), and it causes the most generating thermal energy that causes the heat of the solar cell [9].

1.5 Monocrystalline Silicon Solar Cells (Mono-Si)

In general, crystalline silicon p–n junctions are used. A single-crystalline material is used to create monocrystalline silicon, employing the Czochralski technique of cultivation. This particular solar cell model became the most popular, accounts for roughly 80% of the market, and will remain at the top until another efficient and economical PV technology is created. Current efforts to increase efficiency are constrained by the quantity of electricity the photons generate since it declines at higher wavelengths and silicon is a major component in the construction process of monocrystalline solar cells. Additionally, longer wavelength radiation causes heat loss, which in turn warms up solar cells and therefore lowers their efficiency. Under standard test conditions (STC), a single-crystal silicon cell's efficiency might reach a maximum of approximately 23%, while the highest possible level ever observed was 24.7% (STC). Energy inefficiencies are produced as a result of the solar cells' resistance, the sun's rays being reflected, as well as the metal interface on that upper section [10]. Due to their continuous design, monocrystalline solar cells offer the advantage of not requiring grain boundaries; nevertheless, their principal drawbacks are production costs, material loss, and absorbance issues [6].

1.6 Polycrystalline Silicon Solar Cells (Poly-Si)

A single polycrystalline solar cell, sometimes called as poly-silicon or poly-Si, often consists of several distinct crystals bonded together. Solar cells made of polycrystalline silicon, which are created by condensing a graphite form filled with molten Si, may be processed more inexpensively, there are many grain barriers in poly-Si cells that prevent the extra electrons from flowing continuously into the silicon, decreasing efficiency [6]. Currently, polycrystalline silicon solar cells are among the most

widely used solar cells. Different crystal forms are created as the molten silicon solidifies. Despite being less expensive to manufacture than solar panels made of monocrystalline silicon, these are less effective between 12-14 % [11]. See table 1.1 and figure 1.4, for comparison between two types photovoltaics.

Table 1.1. Comparison between two types of photovoltaics: Monocrystalline and Polycrystalline solar panels.

PV solar panel type	Mono-crystalline solar panels	Poly-crystalline solar panels
Material	A single crystal of pure silicon	Various silicon fragments melting together
Body shape	Squares of uniform darkness with two sharp corners	No-rounded-edged blue squares
Conversion Efficiency	15-20 %	13-16 %
Temperature Coefficient	-0.3% to -0.5% / ℃	-0.3% to -1% / ℃
Expected life span	40 years	35 years
Recyclability	yes	yes
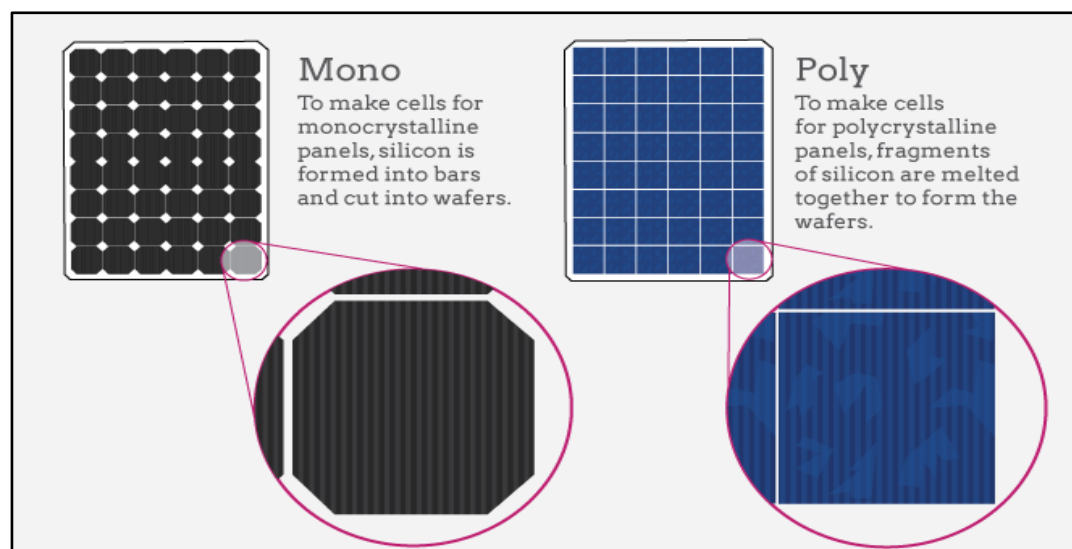
Figure 1.4. Photovoltaic system cells classification [12].

1.7 Nanomaterial

According to standard definitions, nanomaterials are those that have structural or surface features with one or several dimensions in the range of sizes of 1–100 nm. Since of their tiny size and high surface (area to volume ratio), nanoparticles are seen as different from their bulk counterparts and are made up of unique chemical and physical features. A new phase in the development of nanotechnology has emerged during the past two decades as a result of the obvious benefits of employing nanoparticles for many applications. As these sectors continue to produce items with distinctive components and geometries [13]. One, two, or three dimensions may be considered nanoscale for nanomaterials, see figure 1.5. They come in spherical, cylindrical, or irregular shapes, and can be found individually, amalgamated, aggregated, or agglomerated. Nanotubes, fullerenes, and quantum dots are forms of typical nanomaterial structures [14].

- **Zero-dimensional**: All dimensions (x, y, z) are at nanoscale, i.e., no dimensions are greater than 100 nm. It includes nanospheres and nanoclusters (the form of spheres and clusters, etc.).
- **One-dimensional**: Two dimensions (x, y) are at nanoscale and the other is outside the nanoscale. This leads to needle shaped nanomaterials. It includes nanofibres, nanotubes, nanorods, and nanowires.
- **Two-dimensional**: Dimension (x) is at nanoscale and the other two are outside the nanoscale. The 2D nanomaterials exhibit plate-like shapes. It includes nanofilms, nanolayers and nanocoatings with nanometre thickness.
- **Three-dimensional** These are the nanomaterials that are not confined to the nanoscale in any dimension.

(a) Zero-dimensional.   (b) One-dimensional.

(c) Two-dimensional.   (d)Three-dimensional.
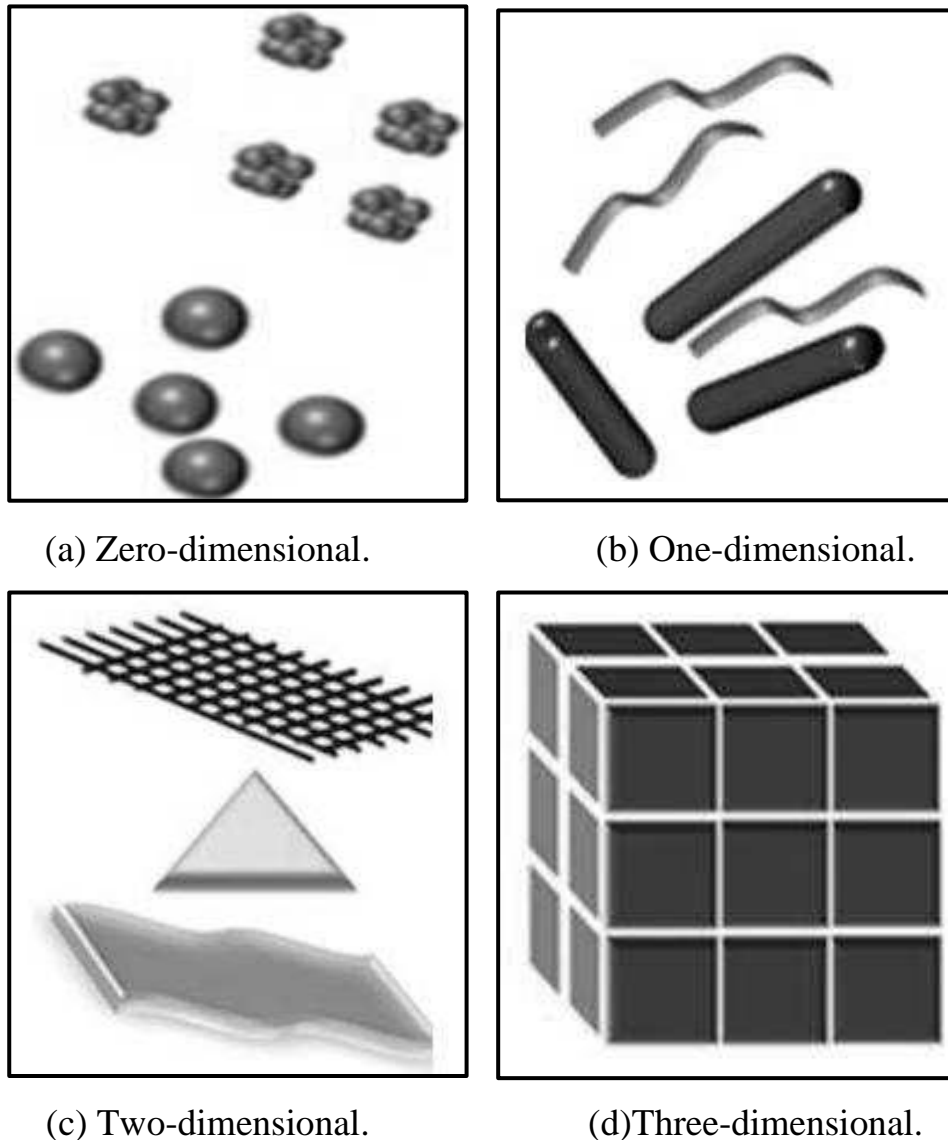
Figure 1.5. Classifications of nanomaterial based of dimensions. [14].

1.8 Nanocomposite Coating

A practical way to integrate inorganic and organic elements to create a hybrid nanocomposite material is through inorganic and organic elements. Since organic–inorganic nanocomposites, sol–gel hybridization techniques have emerged as an exciting new field of research in material science. The creation of innovative organic-inorganic hybrid multi-purpose coating systems with intriguing physiochemical properties for potential application is the result of increased scientific research in this

sector [15]. Figure 1.6. Nanocomposite coating is used in a variety of applications, including corrosion protection, anti-fog coating, anti-reflective coating, self-cleaning coatings, anti-stain coatings, and water repellent anti-static coatings, etc.
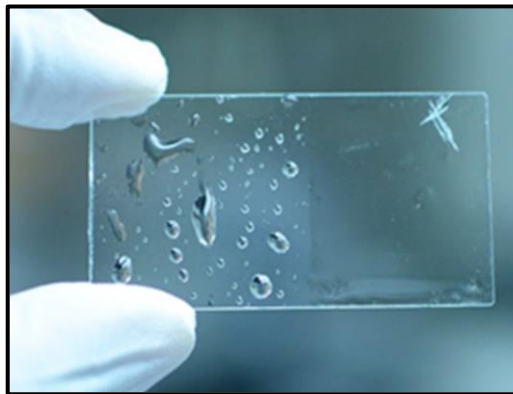
Self-cleaning coating on glass   Water-repellent antistatic coatings
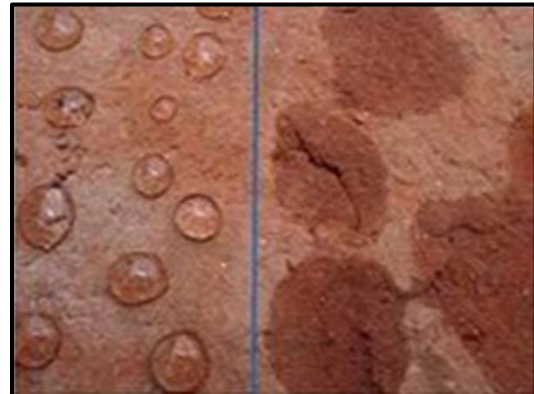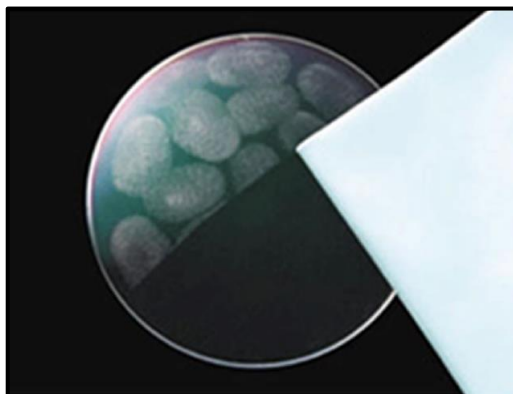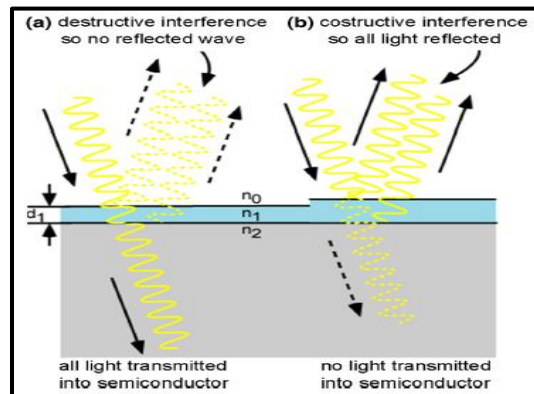
Anti-stain coatings   Antireflective coating

Figure 1.6. Nanocomposite coating applications [15].

1.9   Problem Statement

The PV technology power generation system does have certain basic issues, such as light reflection and increased operating temperature, that can reduce the generator system's efficiency. The main two problems that are focused on in this thesis are the high solar cell surface temperature and the high reflection light of PV solar cells. In hot weather, solar cell surfaces can reach temperatures of nearly 50 °C to 55 °C or higher. Not all solar radiation absorbed by PV solar cells is converted into electricity; a large part of it is converted into heat that causes the solar cell to heat up.

The second parameter is the high surface reflection of PV solar cells, so normally PV solar cells are comprised of silicon (Si) has a high surface reflection characteristic. As a result, after striking the PV panel, approximately 35% of the entire amount of sunlight is reflected, which led to a decrease in the PV cell's efficiency and energy production.

1.10 The Scope of the Study

1. Reducing the effect of the surface temperature of polycrystalline silicon solar cells on the efficiency.

2. lowering the polycrystalline silicon solar cell's issue with reflected light losses, which accounts for around 35% of the overall irradiance.

3. Examining the impact of applying polymerized Polymethyl methacrylate (PMMA) as a coating layer on the top surface of polycrystalline silicon solar cells in order to reduce the solar cell temperature.

4. Studying the impact of applying Zinc Oxide/polymerized Polymethyl methacrylate (ZnO/PMMA), with a 40-50 nm nanoparticles size of ZnO, as a nanocomposite coating layer on the top surface of polycrystalline silicon solar cells in order to reduce reflection losses.

1.11 Objective

The study's main aim is to look at how PV solar cells are affected by temperature changes and reflection losses. Therefore, the objective of this experimental effort is to reduce the elements that adversely impact the solar cell's functioning to raise the solar cell's efficiency, which in turn leads to an increase in energy output.

The below mentioned points provide a summary of the main goals that this study attempted to accomplish.

1. Lowering the polycrystalline silicon solar cells' surface temperature although working in hot weather conditions.

2. Reducing of the amount of light that reflects intensely in polycrystalline silicon solar cell.

3. Blocking ultraviolet (UV) light in the wavelength range (200-400) away from the solar cells, which is one of the reasons solar cells get heated.

4. Producing and applying a thin film nanocomposite coating Zinc oxide/Polymethyl methacrylate (ZnO/PMMA) on the top surface of the polycrystalline silicon solar cell.

5. The efficiency of the polycrystalline solar cell is being increased by the aforementioned elements, which raises the output of energy.

1.12 Outline of the Thesis

Chapter One: Provides a brief introduction to solar energy, the solar spectrum, and some of photovoltaic technologies, as well as the definition and classification of nanomaterials. It also provides the problem statement, objective and the scope of the study.

Chapter Two: Presents a summary of previous studies that dealt with the use of nanocomposite coatings on the photovoltaic solar cell to reduce reflection losses and reduce cell surface temperature in order to increase the efficiency of the solar cell.

Chapter Three: The important scientific concepts of the activities that have been studied will be covered in this chapter, including the equations for calculating the power and efficiency of solar cells, the phenomena of reflection, and the impact of temperature and radiation variations on solar cells.

Chapter Four: In this chapter, the preparation and application steps of nanocomposite coating on the PV solar cells are explained in detail, and the devices listed in the process of preparing and examining nano-coating and the performance of the PV solar cells.

Chapter Five: This chapter covers all the experimental findings, including those related to absorbance, reflectivity, and band gap values for polymer and nanocomposite coatings. examining the polycrystalline silicon solar cells' electrical and thermal characteristics, and comparing the findings to previous studies and analysis of the cost and feasibility.

Chapter Six: This chapter provides the most significant conclusions that can be extracted from the whole of this experimental study. and provide a list of suggestions for further study.

Chapter Two

Literature Review

Literature Review

2.1 Introduction

PV solar cells are composed of silicon (Si), which has a high surface reflection characteristic of light that significantly lowers the conversion efficiency of PV solar cells. To address silicon's reflecting feature, a lot of researches has been done on coatings for PV panels. According to recent developments, either micro coating or nano-composite coating of antireflection compounds on the PV panel improves solar energy conversion [6]. Depending on the examination, the following materials are commonly used as anti-reflective coatings (ARCs) in Si- solar cells:

- Titanium dioxide (TiO_2).

- Zinc sulfide (ZnS).

- Zinc oxide (ZnO)

- Carbon nanotube (CNT).

- Aluminum iso-propoxide ($C_9H_{21}AlO_3$).

- Aluminum oxide Al_2O_3

- Silicon dioxide (SiO_2).

- Silicon carbide/ silicon dioxide $SiC–SiO_2$.

- Magnesium fluoride (MgF_2).

- Silicon nitride (SiN).

- Silicon oxynitride (SiON).

Passive cooling is applied to increase the performance of photovoltaic modules, and cooling photovoltaics doesn't need any special power. As a result, passive cooling technologies are regarded as useful in lowering PV cell temperatures since they are very simple and cost-effective to manufacture. To drive natural convection cooling, passive cooling may incorporate supplementary components such as a heat pipe, sink, or

14

exchanger. Active cooling necessitates the use of a coolant such as air or water, as well as the use of fans or pumps [16]. To manage and maintain the working temperature, coolant liquid, air, and other fluids (typically water or glycol) are used. A crucial economic aspect is whether or not improved power production by active cooling would offset power consumption. Water cooling and air cooling are types of passive and active cooling technology and may require extra parts such as pipes, sinks, and exchangers [17]. Depending on what is listed above, the cooling technique using thin-film nanocomposite coating is very useful and without any expensive extra components.

2.2   PV Solar Cell Nano-Composite Coating Techniques

2.2.1   Studies on Antireflective Properties

The experimentally study investigated the usage of single-layer silicon nitride (SiNx) films as anti-reflection coating (ARC) by **Shubham Duttagupta et al.** [18] on polished and textured mono-Si wafers to optimize SiNx antireflection coatings for silicon wafer solar cells. The SiNx films' refractive index (n) has been increased from 1.9 to 2.7. SiNx films with n = 2.0 (at λ=633.3 nm) and a thickness of 70 nm on textured mono-Si wafers have a WAR1000 (weighted average reflectance) of less than 2.5 % and a WAT1000 (weighted average transmission) of greater than 97%, figure 2.1-a, resulting in total photon losses of less than 3%. Anti-reflecting coatings made of silicon nitride (SixNx) are commonly utilized anti-reflective coatings for commercial Si solar cells.

Azmira Jannat et al. [19] A crystalline silicon solar cell's was experimentally coated with a silicon carbide/silicon dioxide (SiC-SiO2) nanocomposite layer antireflection coating (ARC) (very thin coating of

41.6 nm). Figure 2.1-b, shows the reflectance of the (SiC–SiO2) nanocomposite anti-reflective coating placed on a silicon wafer and matte Si-wafers at 350°C and 450°C heat up temperatures. The results show that the minimum reflection was 7.08% in the wavelength range (750–950) nm and a significant reduction in the reflectance of SiC–SiO2–450 °C in the wavelength range (1000–1400) nm in comparison to other items (textured Si wafer and SiC–SiO$_2$–350°C). That reduction could be linked to the Si wafer's black surface, which could be the result of carbon scraps left over from the sol-gel coated wafer's annealing. The performance of the manufactured crystalline silicon solar cell with SiC–SiO$_2$ nanocomposite antireflection layer was extremely equivalent to that of commercial Si solar cells with SixNx antireflection coating, with an energy conversion efficiency of 16.99% (18.24%). As a result, the SiC–SiO$_2$ antireflection coating on silicon wafers might be regarded as a novel and promising technology for producing silicon solar cells with high efficiency and low cost.

(a)   (b)
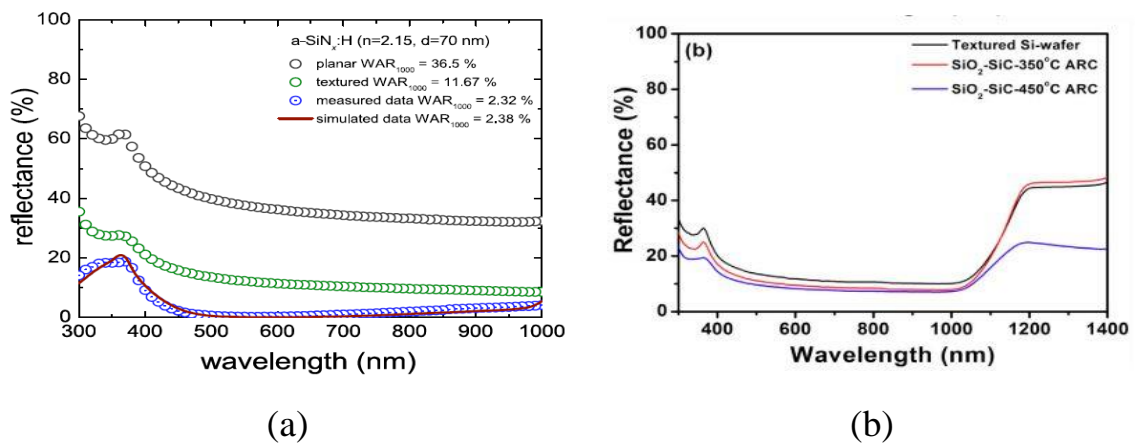
Figure 2.1. (a)- The reflectance percentage for different situations of the silicon wafer with and without coating[18]. (b)- Wavelength (nm) vs. reflectance (%) for 350 ℃ and 450 ℃ annealing temperatures of SiC–SiO2 nanocomposite AR deposited on a Si wafer and textured Si wafer. [19]

Dhadala Karthik et al. [20] Experimental study of mesoporous MgF_2 nanoparticles from Ink bottles as a high-performance broad-band antireflective coating, see figure 2.2. and dispersion (3wt%) in a 90:10 of isopropoxyethanol and ethanol mixture. The AR coating had nearly 97% transmittance (3% R) in the invisible range (400–1500)nm**,** the use of an anti-reflective (AR) coating on the glass cover of crystalline silicon solar cells resulted in a net efficiency boost of 6% for photovoltaic modules.

(a)   (b)   (c)
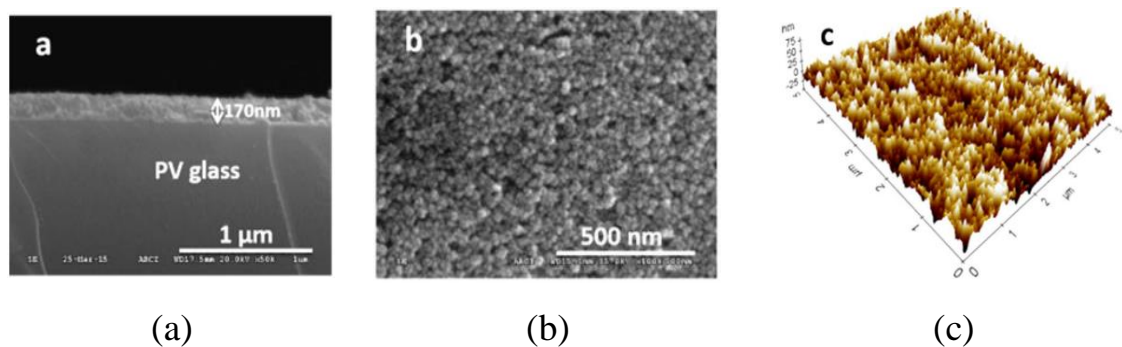
Figure 2.2. (a)- Field emission scanning electron microscopy (FE-SEM) view of cross section for the coating layer (**b**)- FE-SEM view for the roughness of the surface. (**c**)- Antireflective mesoporous ink-bottle type profile of the surface.[20]

Vandana Kaler et al. [21] prepared a nano-composite coating mixture of TiO_2/PVA by mixing polyvinyl alcohol (PVA) after being dissolved in distilled water (DW) and adding different concentrations of titanium dioxide (TiO_2) nanoparticles. It was applied to the top surface of the solar cell to block ultraviolet (UV) radiation and reduce the reflection of visible light, which led to enhancing the optical properties in order to achieve higher efficiency. The results show absorbance, figure 2.3-a, for the maximum UV spectrum (200-400 nm) when 0.25 wt% titanium dioxide is used in the TiO_2/PVA nanocomposite, figure 2.3-b. In comparison to pure PVA, the melting point value of the TiO_2/PVA nanocomposite increased significantly. The highest heat stability of the TiO_2/PVA

nanocomposite was found to be 0.25 wt%. As a result, TiO_2/PVA nanocomposites have superior thermal stability to PVA.

(a)   (b)
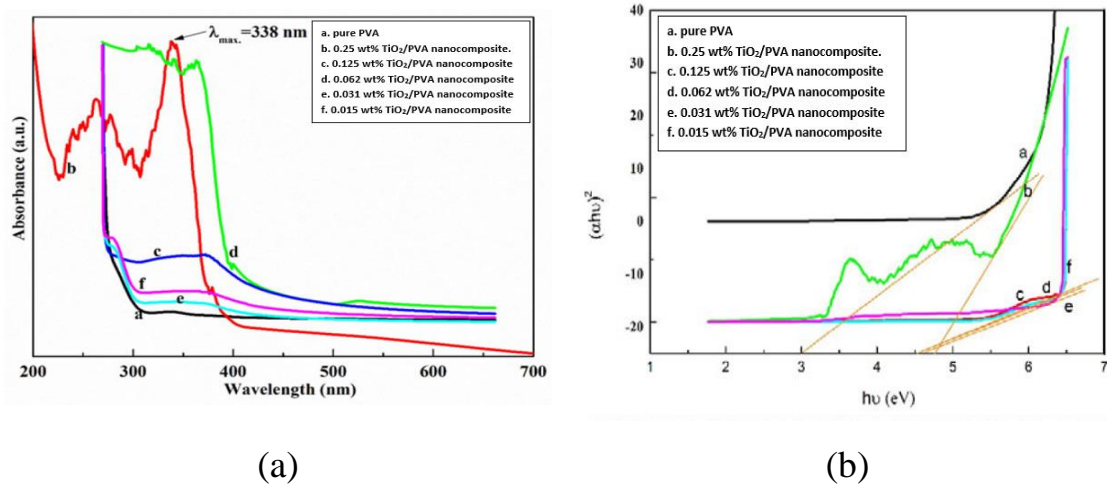
Figure 2.3. (a)- the UV-Vis spectrum absorbance properties. (b)- Bandgap energy for various solutions[21].

B.Ashok kumar et al. [2] experimentally study the usage of nano-composite materials with antireflection properties coated the silicon solar cell item with Aluminum Iso-propoxide, Carbon Nano Tube (CNT), Zinc Sulphide, Tetra-ethoxy Silane, and a mixture of Silver Nitrate and Aluminum Iso-propoxide in order to boost solar cell efficiency, the results shows that the maximum power was 72mW indicated, figure 2.4-a and the best improvement is 31.25 % for CNT-TiO_2-SiO_2 as comparison to non - coated cells.

Jinsu Jung et al. [22] By using spin coating sol–gel precursors experimentally, a double layers ARC of TiO_2/Al_2O_3 was effectively synthesized on single silicon solar cell. When compared to single layer titanium dioxide (TiO_2), and single layer aluminium oxide (Al_2O_3), double layers ARC of (TiO_2/Al_2O_3) on silicon substrate figure 2.4-b, showed the minimum reflectance result of 3.02% at 970 nm is confirmed by the double-layer TiO2/Al_2O_3 ARC, which has an average reflection of 4.74 %

18

in the 400–1000 nm wavelength area, as well as a high refractive index (n) 2.89. Silicon solar cells with a double layer TiO_2/Al_2O_3 anti-reflection coating had a 13.95 % higher conversion efficiency than single layer TiO_2 and Al_2O_3 anti-reflection coating.

(a)   **(b)**
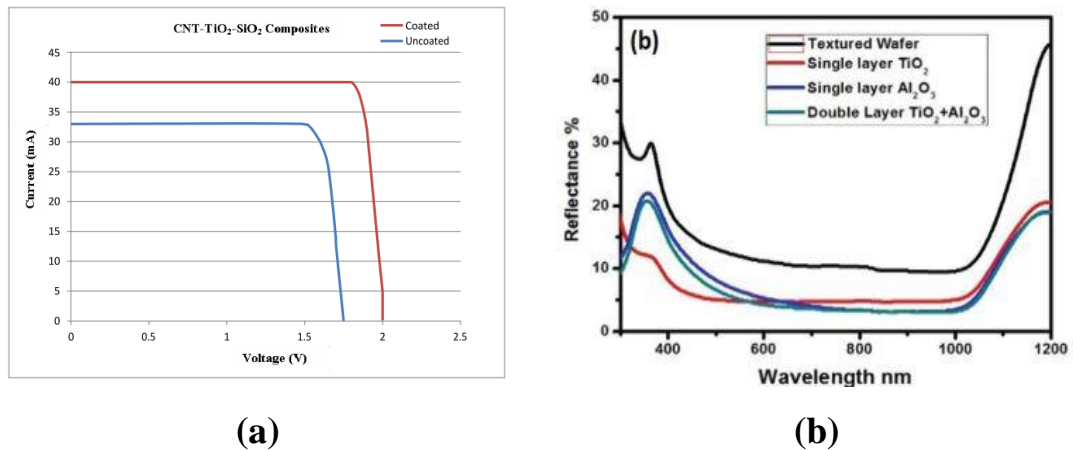
Figure 2.4. (a)- I-V curve for coated and uncoated solar cells[2]. **(b)-** Reflectance spectra of single and double layer TiO2.[22]

Hala J. El-Khozondar et al [23] numerically study a multi-layer antireflection coating with a nano-composite layer put on top of the silicon nitride SiNx antireflection coating layer has been modelled in figure 2.5-a. It is assumed that the nanoparticle-composite layer is gold (Au)-silver (Ag) embedded in a polyacrylic acid host medium. Both normal and angular incidents are considered, the effect of the SiNx layer's refractive index and the volume percent of silver (Ag) to gold (Au) nanoparticles on reflectance were investigated. The best results of antireflection were found at a volume fraction of nanoparticle Ag = 1 and Au = 1.8, as per figure 2.5-b, and the value of y-axis where the lowest reflection (R) occurs, shifts blue as the proportion of Au decreases. because Ag has a larger absorptivity. They discovered that by adjusting the reflectivity of the SiNx layer or modifying the Ag/Au ratio, we can control the lowest reflectance

19

and even the wavelength at which it occurs. It's also worth noting that the narrower the angle of incidence, the lower the reflectance value.

(a)   (b)
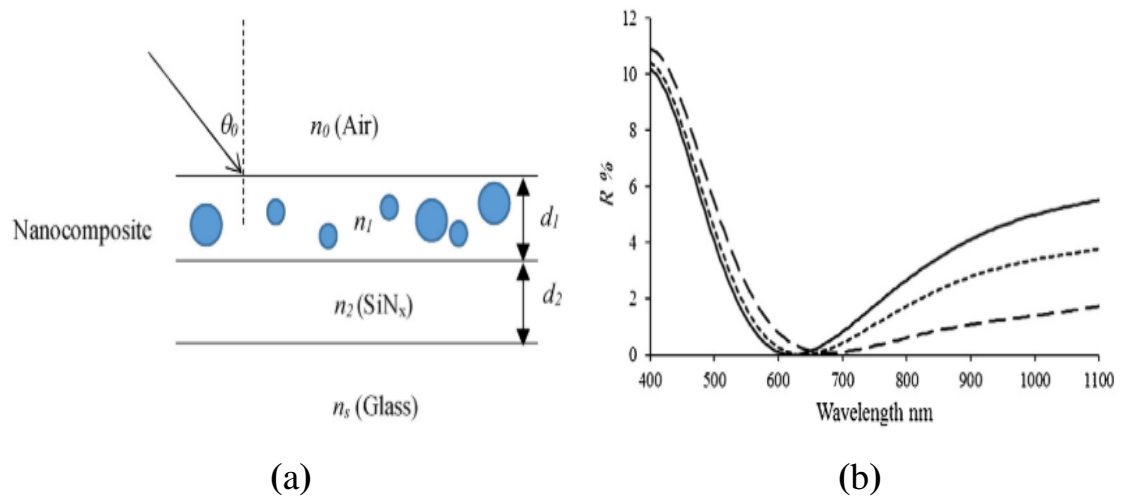
Figure 2.5. (a)-The suggested design of a solar cell. (b)- Wavelength(nm) relative with reflectance(%) for Ag-Au fraction equals 1:1.8 (___),1: 6 (-- ---), 1:3.4(.....).[23].

Alireza Jalali et al. [24] investigated experimentally the presence of a thin ZnO layer on silicon by using spin-coating technique was used to enhance light absorption, increase the number of produced excitons. The results showed that in the addition of the antireflection ZnO layer, the efficiency of the fabricated solar cell was 9.19 % and without the antireflection ZnO layer was 5.29 %. As a result, it was determined that depositing ZnO nanoparticles on silicon might improve the performance of solar cells significantly, a hexagonal ZnO was reported to operate as an antireflection coating, improving the electrical features and performance of the solar cells, figure 2.6-a. Furthermore, the findings revealed that the concentration of the sol–gel solution has a significant impact on the solar cell's efficiency.

Hrishikesh Dhasmana[25] experimentally investigate single and multilayer spin coating of zinc oxide nanoparticles (NPs) with a simple and low-cost technique to improve Si-surface lowering the reflectivity for improving efficiency of solar cells. Preparation of ZnO by two methods: hydrothermal (Hy) and continuous spray pyrolysis (SP). In figure 2.6-b, using the ZnO (SP) four layers, ZnO (Hy) double and four layers, and compared with textured Si, the result shows that the ZnO (SP) double layer has the best light absorption, by using ZnO (Hy) four layers, these ZnO nanorod structure thin films in the 350–370 nm wavelength region can reduce the reflectivity of Si surfaces change from 25 to 2.5 %. The study also suggests that spray pyrolysis (SP) creates a porous structure in ZnO NPs, which helps reduce Si surface reflectance.

(a)   **(b)**
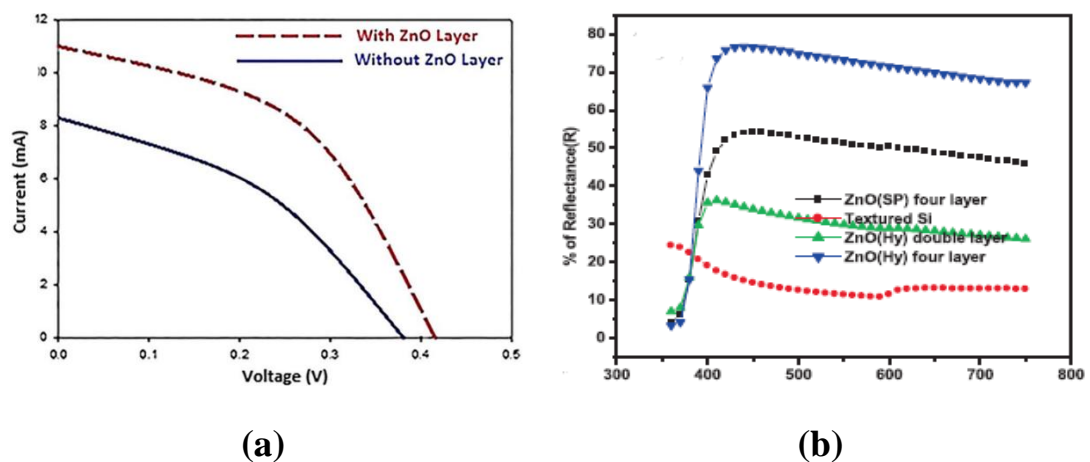
Figure 2.6. (a)- The I-V curve of PVs with and without ZnO layer[24]. (b)- The reflectance of ZnO (Hy) and ZnO (SP) layers on the textured silicon.[25].

Shaheer A. Khan et al. [26] worked on improving the efficiency of solar cells by using PVA/ZnO nano-composite coating thin film. The films were made with different zinc oxide (ZnO) nanoparticles concentrations in a Polyvinyl alcohol (PVA) and used a solution casting process. The results show a very significant difference between the

performance of solar cells with and without PVA/ZnO nanocomposite coating, with the results identifying 13.57% and 10.07%, respectively. It is worth noting that the nano mixture that achieved the best result was composed of 14.25 % (ZnO) weight percent and 85.75 % (PVA).

Abd El-Hady B. Kashyout et al.[27] investigated the effect on the efficiency of the solar cell by applying multilayer nanocomposite coatings up to a four-layer of polythiophene(PT) with gold nanoparticles (PT-Au) as the first test and also with palladium nanoparticles (PT-Pd) as the second test, applied to the rear surface of the silicon solar cell by using the spin coating technique. The testing found that the UV area had a large absorbance, figure 2.7-a. The energy gap was 2.65 electron volts (eV) for (PT-Pd 5%), 2.9 electron volts (eV) for (PT), and 3.05 electron volts (eV) for (PT-Au 5%), figure 2.7-b. The results reported a decrease in load resistance and a maximum efficiency boost of up to 7.25 %.

Hussein A. Elsayed et al. [28] A theoretical study on the effect of adding an anti-reflective coating on the top surface and a back reflector to a solar cell revealed that the coating was designed to operate as an anti-reflector and a back reflector. A one-dimensional (1D) quadrant photonic crystal single period (binary, ternary, and quadrant layers from different materials such as Al_2O_3, Zns, or MgF_2 and ten periods of one-dimensional (1D) binary photonic crystals were added by using the finite element approach as well as the transfer matrix approach, figure 2.8-a. The results show that the greatest absorbance is 97% in the wavelength range (400-640) nm for both the back reflector and the anti-reflecting coating, figure 2.8-b.

(a)   (b)
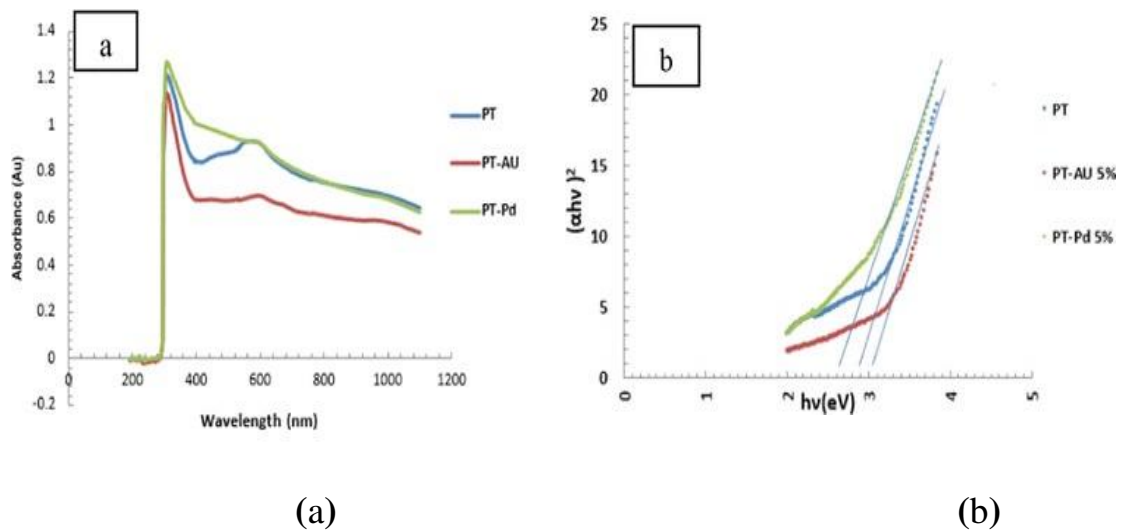
Figure 2.7. (a)- the UV-Vis spectrum absorbance properties. (b)-
Bandgap energy for various solutions[27].

(a)   (b)
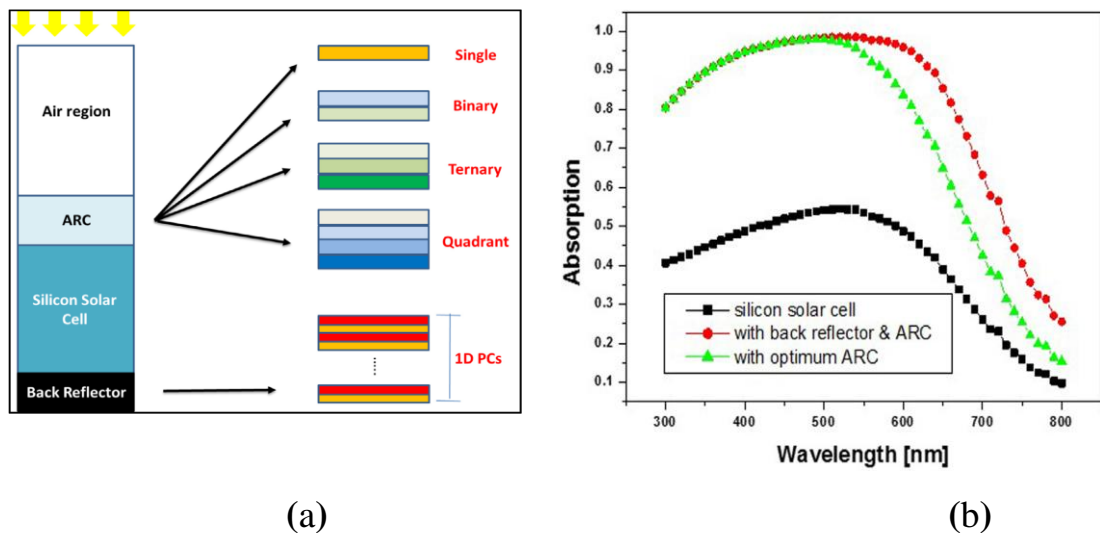
Figure 2.8. (a)- A simulation model of a silicon solar cell with a back
reflector and an antireflection coating (ARC). (b)-Absorption of silicon
solar cell, with antireflection coating (ARC) and with back reflector &
ARC[28]

2.2.2 Studies Included the Temperature Reduction

In this section, we included most studies that refer to the temperature
redaction for solar cells in the case of coating and without coating.
Huanzhi Zhang et al. [9] investigated the UV-blocking and temperature-

23

regulating properties of composite films made of polyvinyl chloride (PVC), entrapped phase-change materials (micro-PCMs), and TiO_2 nanoparticles (nano-TiO_2), as well as multi-films prepared with different concentrations. Results of the experiment found that the films prepared with 6 wt% for both (micro-PCMs) and (nano-TiO_2) recorded the best results in ultraviolet (UV) blocking, figure 2.9, only 9.68% of UV transmittance in the wavelength range (250–400) nm and promising temperature regulation.

Wei Li et al. [29], applied experimentally on the upper surface of a silicon solar cell, layers that alternate of (Al_2O_3 / SiN/ TiO_2/ SiN) with irregular thickness arrangements, with just a single layer of SiO_2 on top for anti-reflection, figure 2.10. The results showed that the solar spectrum and UV were greatly reflected, and the solar panel may reduce the temperature of the cell with over 5.7 °C, figure 2.11-a. The absolute efficiency gain from this temperature drop is expected to be roughly 1 %.

(a)   (b)
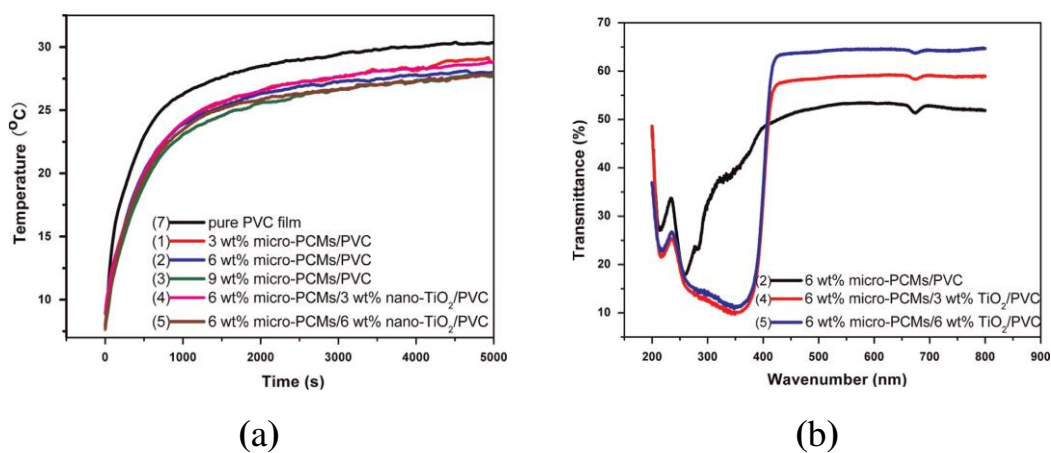
Figure 2.9. (a)- The temperature varies with time for different concentrations of micro-PCMs and nano-TiO2 fims. (b)- The transmittance (UV-visble) of the prepared films is composed of 6 wt% micro-PCMs with varying concentrations of nano-TiO2[9].

(a)   (b)   (c)
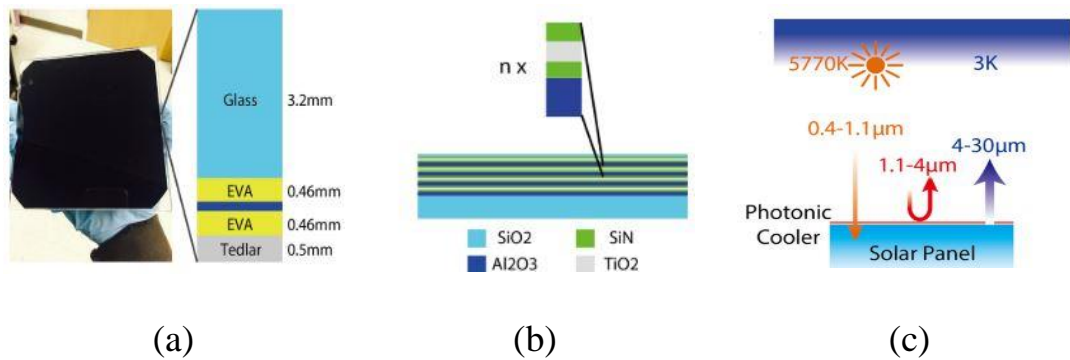
Figure 2.10.(a)- A graphic of a photovoltaic cells. (b)- A multilayer insulating stack makes up a photonic cooler. (c)- The effectiveness of the photonic cooler on the surface of the solar cell..[29]

Ahmad Manasrah et al. [30] examined experimentally the impact of the thermally insulating nanocoating on the output characteristics of (20 × 30) cm solar panels. On a solar module, three different types of shielded coatings were tested. The nanofilms utilized are coated with a combination of carbon and ceramic particles of 25 to 50 nm and, as per the manufacturer's specifications, have a 99 % IR and UV blocking rate. Three nanocoating with thermal insulating properties (20%, 60%, and 80% visible light blocking) were applied individually on 1 mm thick glass layers with the same measurements as the solar cell panels. The nanofilms were then applied to the glass panels, which would then be affixed to the solar cells. Nanocoating 20 % blocking value produced more electrical energy than other solar filters with an efficiency of 21 % at the average PV solar cell surface temperature of 54.3 °C. figure 2.11-b. According to the results, the use of particular nanolayer filters considerably reduced the surface temperature of the solar panel. The surface temperature of the solar cell was tested with various nano-layer filters, and it was found that the solar model's surface temperatures were reduced by a minimum of 5 °C. The minimum temperature recorded for 80% of the nano layer was used, whereas the highest temperature was recorded when no filters were used.

(a)   (b)
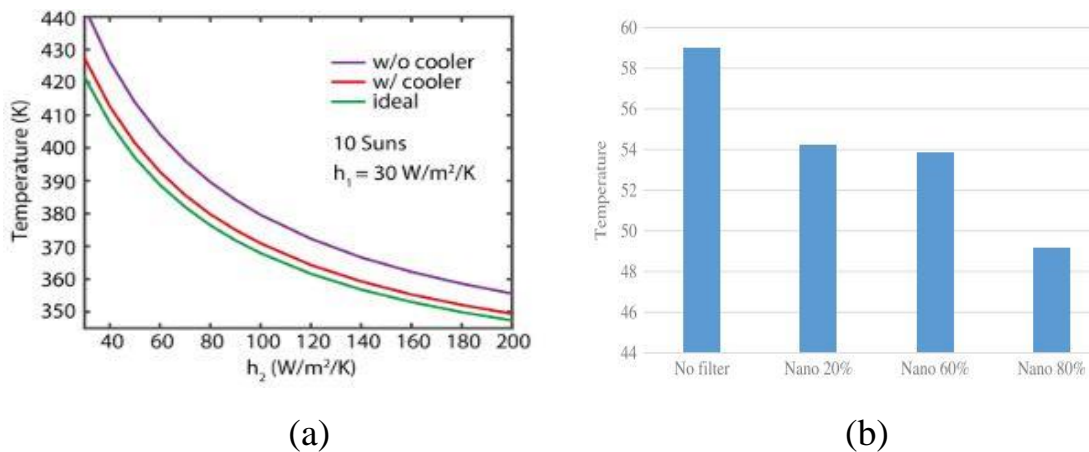
Figure 2.11.(a)- Temperature change during operation with h2 function
at constant h1 = 30 W/m2/K for solar panel with and without cooler
[29]. (b)- The effect of nano-film filters (20%, 60%, and 80% visible
light blocking) on the solar cell's surface temperature [30]

A.Kumar and A. Chowdhury [31] experimentally study for applying
SiO_2, Si_3N_4, Al_2O_3, HfO_2, and TiO_2 anti-reflective coatings in various
thicknesses (100-1000) nm on the top surface of a crystalline solar cell
and decreasing the surface temperature, revealed that using Si_3N_4 at the
(9700 nm) wavelength produced the highest emissivity, and the emissivity
increased with increasing coating thickness, figure 2.12-a. The
temperature of the crystalline solar cell was reduced from 68 °C to 57 °C,
with an anti-reflective coating in the infrared radiation (IR) range varying
from 0 to 1. The temperature recorded is 66 °C when the Si_3N_4 thickness
is 80 nm.

Another published paper by **A. Kumar and A. Chowdhury**[32]
studies, experimentally, the impact of adding the selective radiative
antireflective coating (SR-ARC) on the single and double Si_3N_4-coated
layers of the crystalline silicon solar cell, SiO_2, Si_3N_4 and Al_2O_3 were used
for designing SR-ARC. The results refer to temperature reductions of 5.6
°C and 5.4 °C for double and triple ARC layers, respectively, figure 2.12-
b, compared to a single layer at an ambient temperature of 30 °C, and a

maximum reduction of 6.8 °C found at an ambient temperature of 45 °C with double-layer ARC, and the solar absorbance in the (300–1150) nm wavelength region being constant or rising.

(a)   (b)
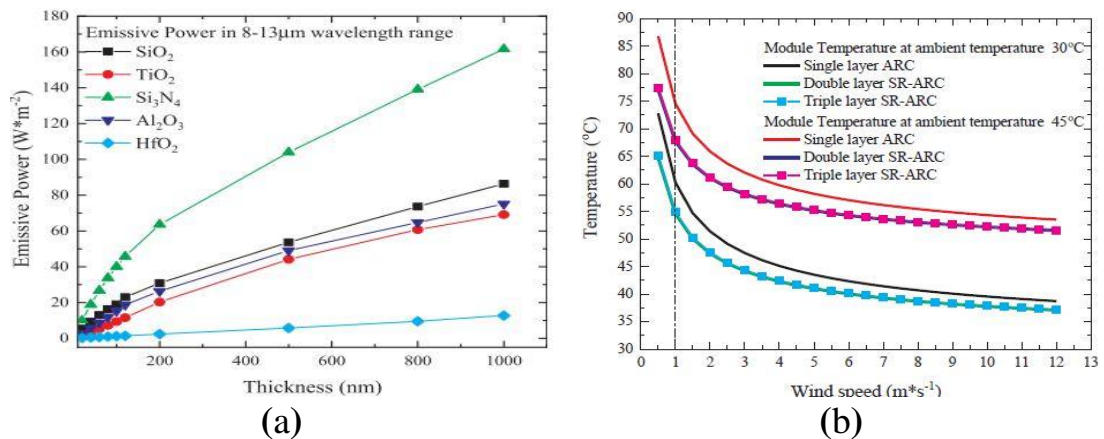
Figure 2.12. (a)- Variation the emissive power with thickness for different ARC.[31] (b)- The temperature value of c-Si module with different layer SR-ARC.[32]

Farah K. Mohd Zaini et. al.[33] conducted an experimental study was conducted to apply a nanocomposite coating on the top surface of a photovoltaic (PV) solar cell to improve temperature-lowering and performance. The nanocomposite coating is made up of TiO_2 nanoparticles with 3-amino propyltriethoxysilane (APTES), Methyltrimethoxysilane (MTMS), and isopropyl alcohol ($CH_3CHOHCH_3$) for the first two samples, and nitric acid (HNO_3) in place of APTES for the remaining two samples. The results were found to refer to increasing the fill factor by about 0.2 for TiO_2 nanoparticles, figure 2.13-a. Also, the coating sample prepared from MTMS/APTES solution and TiO_2 nanoparticles scored the best temperature reduction, approximately 8.93 ºC compared to without coating, figure 2.13-b.

(a)   (b)
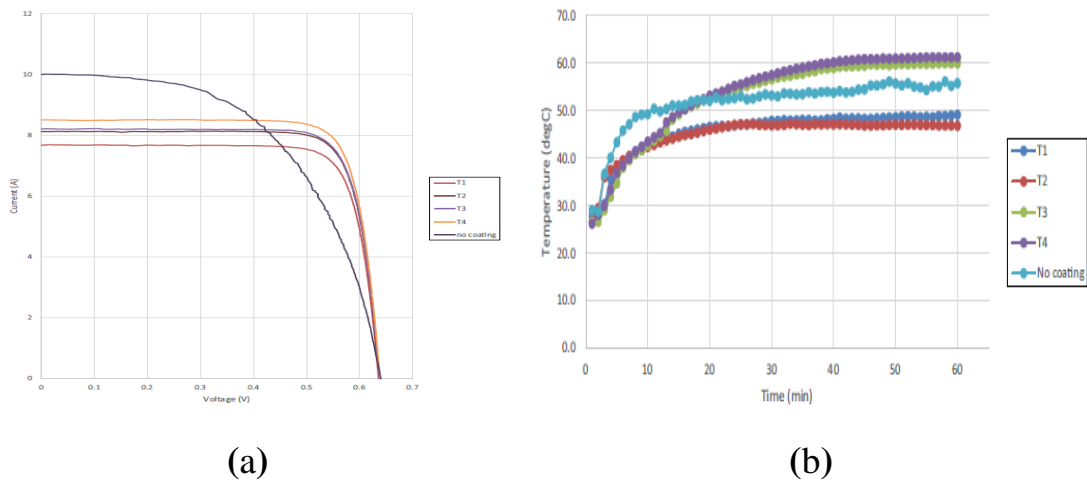
Figure 2.13. (a)- I-V curve for coating and uncoating solar cells. (b)-
Temperature readings for all prepared coatings and without coating in 60
minutes[33].

The results of the experimental test for nanocomposite material
Titanium dioxide (TiO_2) with polymer at different concentrations of single
and double layers as a coating applied on the top surface of the
photovoltaic (PV) polycrystalline solar cell were done by **Dhafer.
Hachim et al.** [34] demonstrated that the first concentration (Co_1) with
two layers performs better than the other instances in the first
concentration (102.7g Ethan, 4.19g Nitro cellulose polymer, 0.93g TiO_2
Nps) and second concentration (Co_2) (102.7g Ethan, 4.19g Nitro cellulose
polymer, 0.12g TiO_2 Nps).The first concentration's efficiency increased at
a rate of 1.11 % with one layer and 2.71 % with two layers (figure 2.14-
a), whereas the second concentration's efficiency increased at a rate of
0.473 % with one layer and 1.59 % with two layers. The critical
concentration of the examined nanoparticles (Nps) was found to be
0.863% TiO_2 Nps in the experiments. When the concentration of Nps
rises, the nanoparticles settle out of the solvent. The application of an eco-
friendly coating is designed to reduce solar cell consumption during hotter
weather, lowering solar cell processing costs. This approach works by
reducing the amount of infrared radiation absorbed, which lowers the PV

temperature. Furthermore, when compared to solar cells without a coating, solar cells coated with nano have better heat dissipation.

Ali kadim et al. [35] Experimentally investigating the nanocomposite Titanium Dioxide/ Polyvinyl Alcohol(TiO_2/PVA), nanoparticle concentration (10-20)nm for coating on the top surface of the crystalline silicon solar cell, the solvent casting process is used. The goal is to see how nanocomposite TiO_2/PVA affects polycrystalline silicon solar cells. It was found that for TiO_2/PVA 0.2wt% nanocomposite, the reflection achieved was 3.9 %, and the improvement in sunlight-based cell proficiency was (+2.3%). figure 2.14-b, when compared to a solar cell without a covering, the surface sun-based cell temperature (9.7 °C) had the most extreme temperature variation.

(a)   (b)
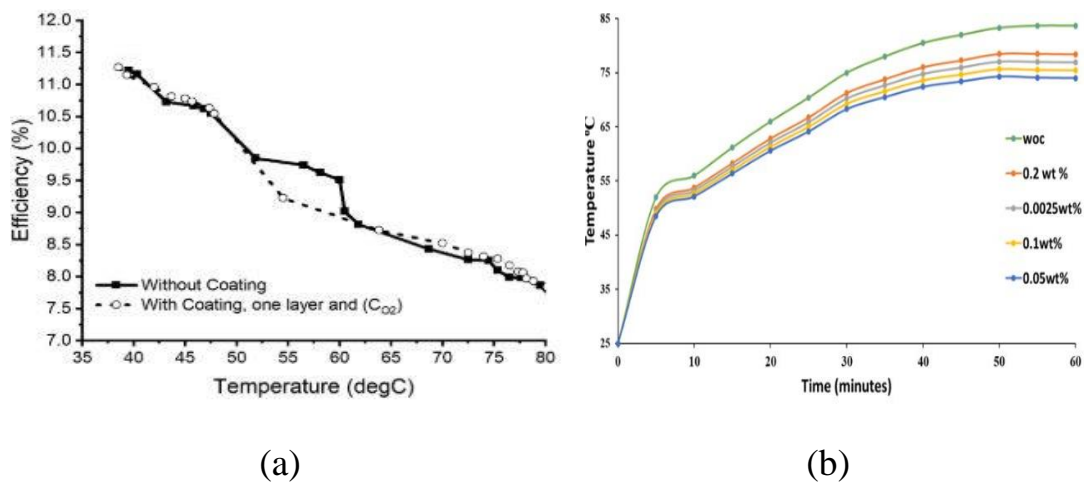
Figure 2.14. (a)- The efficiency of PV coated with two layers of the first concentration (Co_1) coating compared with the non-coated PV cell. [34]. (b)-Temperature changes with time for solar cell coated with PVA/TiO2 nanocomposite coating on the top surface. [35]

V. K. Gobinath et al. [36] experimental investigation into the use of zinc sulphide (ZnS) material as an anti-reflective coating and to lower the surface temperature of commercial polycrystalline solar cells. The ZnS coating is applied by using the Radio Frequency Sputtering technique with different times of 10, 20, 30, and 40 minutes. The results show that the

maximum light transmittance of 85% at the wavelength range of 600–800 nm, and the temperature reduced from 58.6 ℃ to 51.4 ℃, which led to solar cell efficiency increased by +3.24 compared to solar cells without coating for controlled conditions achieved by used 30 minutes (S-III) of ZnS coating deposition, see figure 2.15.

(a)   (b)
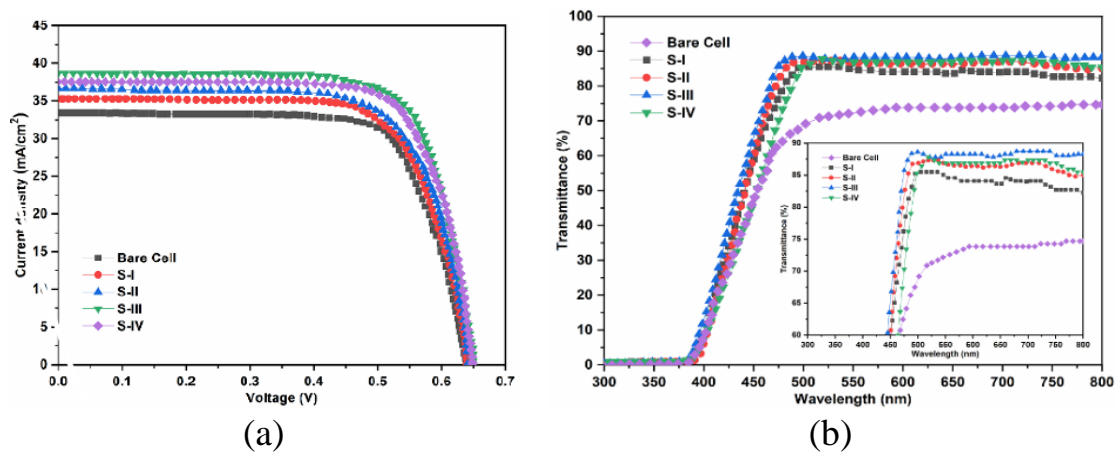
Figure 2.15. (a)- I-V curve for coated and uncoated solar cells. (b)- The light transmittance of solar cells coated with ZnS and without coating[36]

2.2.3 Summarization of the Major Distinctions Between Researchers' Work

Several items summarize the major distinctions between researchers. The utilization of various nanomaterials is the most significant factor. The researchers looked for and tested novel materials and NPs sizes, comparing them to ones that had previously been utilized. They also experimented with utilizing polymers of various molecular weights, functional groups, and concentrations to discover the optimum bonding for the spread and cohesiveness of nanoparticles. Another interesting element of the studies was that the authors used a variety of coating techniques, such as dip-coating, spin coating, and spray coating[37], and different thicknesses of thin film, some of them working with only one layer and comparing the results with the use of many layers to discover the best thickness for optimal performance.

Table 2.1. Summary studies of using Nano-composite coating.

References	Nano- Materials	The Mixing Ratios	Results
Azmira Jannat et al.2016 [19]	$SiC–SiO_2$	(1:4:4) TEOS+ citric acid+ ethylene $SiC–SiO_2$ (41.6nm)	• Provide a lower reflection of 7.08 % at wavelengths in the range from 400 to 1000 nm. • The performance was extremely equivalent to that of commercial Si solar cells with SixNx 16.99 %
Dhadala Karthik et al. 2017 [20]	Ink-Bottle mesoporous MgF_2 Nps	3wt% ethanol and isopropoxyethanol in a 90:10	• The anti-reflection coating had nearly, 97 % Optical transmittance in the visible range (300–1500 nm). • Increase of 6% in efficiency for crystalline silicon solar cells.
Wei Li et al. 2017 [29]	Al_2O_3/SiN/TiO_2/SiN /SiO_2	-	• the solar spectrum and UV were greatly reflected. • and the solar panel may reduce the temperature of the cell with over 5.7 °C. • The absolute efficiency gain from this temperature drop is expected to be roughly 1%.
B.Ashok kumar et al. 2018 [2]	Carbon Nano Tube (CNT). Zinc Sulphide (ZnS). Aluminum Iso-propoxide $C_9H_{21}O_3Al$.	-	• The coated cell of carbon nano tube (CNT) shows the maximum improvement of solar cell efficiency 31.25 %.

Jinsu Jung et al. 2018 [22]	TiO_2/Al_2O_3	Si (51.99 wt.%). Oxygen (39.21 wt.%). Aluminum (0.74 wt.%) Titanium (8.06 wt.%).	• Silicon solar cells with a double layer TiO_2/Al_2O_3 Anti-Reflection Coating had. ➢ Considerable reduction in reflectance (4.74 %) in the wavelength region of (400 to 1000 nm). ➢ 13.95 % higher conversion efficiency than single layer TiO_2 and Al_2O_3 Anti-Reflection Coating.
Hala J. El-Khozondar et al. 2018 [23]	silver (Ag) /gold (Au)	Ag /Au embedded polyacrylic acid SiNx antireflection coating layer.	• Indicate that the reflectance is affected by (nanoparticles ratio, SiNx layer's refractive index and angle of incidence.)
Ahmad Manasrah et al. 2019 [30]	Ceramic and carbon	particles of 25 to 50 nm	• Nano coatings 20 % with a filtering rate produced greater electricity thermal filters with efficiency 21 %. • The solar modules' surface temperatures were recorded when 80 % Nano layer was reduced by at minimum 5 °C.
Alireza Jalali et al. 2020 [24]	ZnO layer on silicon	Zinc acetate (2.74 g). two-methoxy ethanol 47.5 ml solvent. ethanolamine 1.5 mL.	• The efficiency of the fabricated solar cell was 9.19 % and without the antireflection ZnO layer was 5.29 %.

Hrishikesh Dhasmana et al. 2020 [25]	Zinc oxide (ZnO)	Poly Ethylene Glycol (PEG) Methanol, (ZnO)nano powder, (50) mM	• Reduce the reflectivity of silicon surfaces from (25 to 2.5) percent in the (350–370) nm wavelength range which helps reduce Si surface reflectance.
Kumar and A. Chowdhury 2020 [32]	Silicon dioxide (SiO2) Silicon nitride(Si_3N_4) Aluminium oxide (Al_2O_3)	-	• Temperature reductions of 5.6 °C and 5.4 °C for double and triple ARC layers, respectively compared to a single layer at an ambient temperature of 30 °C. • Maximum reduction of 6.8 °C found at an ambient temperature of 45 °C with double-layer ARC.
Farah K. Mohd Zaini et. al. 2020 [33]	Titanium dioxide (TiO_2)	propyltriethoxysilane (APTES), Methyltrimethoxysilane (MTMS). Isopropyl alcohol (CH3CHOHCH3) Nitric acid (HNO3)	• Increasing the fill factor (FF) by about 0.2. • The best temperature reduction, approximately 8.93 C compared to without coating.
Dhafer M. Hachim et al. 2020 [34]	Titanium dioxide (TiO_2)	4.19g Nitro cellulose polymer, 0.93g TiO2 Nps	• Efficiency increased at a rate of 2.71 % with two layers. • Compared to solar cells without a coating, solar cells coated with nano have better heat dissipation.

|			
Shaheer A. Khan et al. 2021[26]	Zinc oxide (ZnO)	85.75% Polyvinyl Alcohol (PVA). 14.25 % (ZnO).	• The efficiency of solar cells identified with and without coating is 13.57% and 10.07%, respectively.
Abd El-Hady B. et al.2021[27]	Gold (Au) Nps Palladium (Pd)Nps	Polythiophene(PT) PT-Au PT-Pd	• The maximum efficiency boost of up to 7.25 %.
Hussein A. Elsayed et al.2021 [28]	Al2O3, Zns, and MgF2	-	• The results show that the greatest absorbance is 97% in the wavelength range (400-640) nm for both the back reflector and the anti-reflecting coating.
Ali Kadim et al. 2021 [35]	Titanium Dioxide (TiO_2)	0.2wt% Titanium Dioxide (TiO_2)/ Polyvinyl Alcohol (PVA)	• Reduced reflection obtained was 3.9 %. • Improvement in sunlight-based cell proficiency was (+2.3%) • The greatest significant temperature change was seen in the surface sun-based cell temperature (9.7 °C).
V. K. Gobinath et al. 2021 [36]	zinc sulphide (ZnS) material	-	• The results show that the maximum light transmittance of 85% at the wavelength range of 600–800 nm. • The temperature reduced from 58.6 ℃ to 51.4 ℃. • The solar cell efficiency increased by +3.24 compared to solar cells without coating for controlled conditions achieved by used 30 minutes (S-III) of ZnS coating deposition.

Chapter Three
Theoretical Principle

Theoretical Principle

3.1   Introduction

This chapter explains the mathematical basis of the operations performed on the solar cell to enhance power and efficiency by lowering the solar cell's temperature and light reflection, as well as how to calculate the magnitude of each operation's impact. Additionally, a calculation of the solar cell's electrical characteristics is analyzed.

3.2   Semiconductor's Optical Properties

Intrinsic   effect   is   connected   to   a   semiconductor's   optical characteristics. The formation of electron-hole pairs can take place direct or indirect depending on where the head of the valence band (V.B) as well as bottom of the conduction band (C.B.) are intrinsically located inside the band structure shown in Figure (3.1) [38].
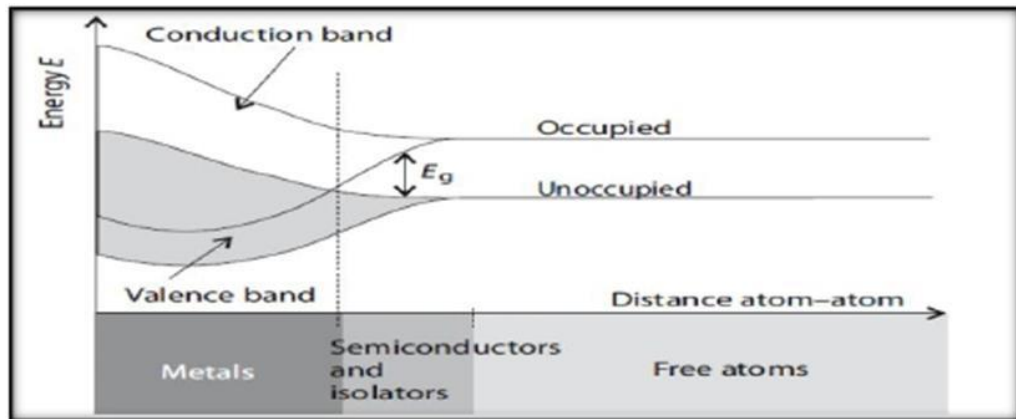
Figure 3.1. Silicon lattice crystalline band structure synthesis [38].

3.3   The Optical Edge Absorption

The basic absorption, which includes the movement of electrons out from valence to the conduction band and manifests itself by an increase in absorption, has to be the most significant absorption activity. It is used to calculate the semiconductor's energy gap [39].

The semiconductor absorbs photons of the incoming light; the absorbance is dependent on the photon energy (hv), (h = Planck's constant and v = the frequency of the incoming photons); the absorption is connected to the electron excitation between the valence band (V.B) and the conduction band (C.B) in the substance, beginning first at the energy gap, which is equivalent to the lowest energy difference (Eg) between the least C.B minimum and the highest V.B maximum.

When the photon's energy (hv) is equal to or greater than the bandgap energy (Eg), it can make contact with a valence electron, elevating into the C.B. and producing an electron-hole. The incoming photon's maximal wavelength (λc), which produces an electron-hole pair, may be represented as follows [40]:

$$\lambda c(\mu m) = \frac{hc}{Eg} = \frac{1.24}{Eg(eV)} \dots\dots\dots\dots\dots\dots\dots\dots\dots\dots\dots\dots\dots(3.1)$$

$$A = \mathcal{E}bC \dots\dots\dots\dots\dots\dots\dots\dots\dots\dots\dots\dots\dots\dots\dots(3.2)$$

$$E_{g=}hv\dots\dots\dots\dots\dots\dots\dots\dots\dots\dots\dots\dots\dots\dots\dots\dots(3.3)$$

Where: λc = photon's wavelength(nm), h = planck's constant, v = photon frequency(hz), c = speed of light(m/s), Eg = energy bandgap(eV), A= absorbance (A.U), b =path length(cm), and C = concentration (mol/L).

Planck's constant (h) = 6.63×10^{-34} J.s

Speed of light (c) = 3×10^{8} m/s
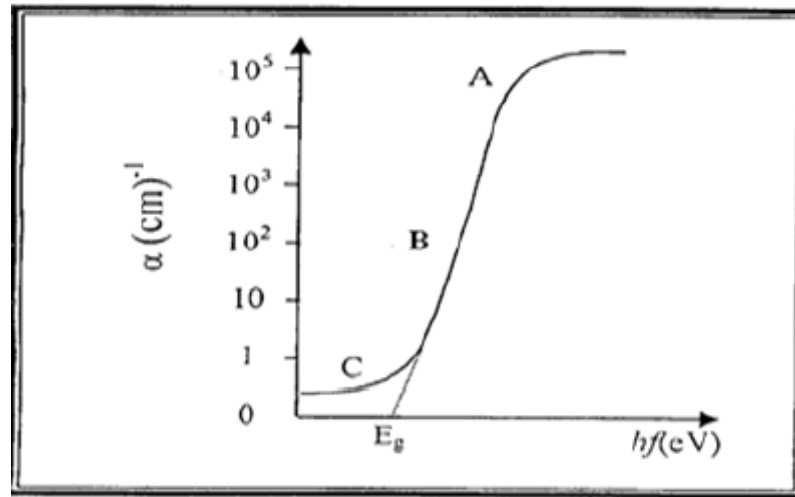
Figure 3.2. Crystal semiconductor absorption edge [40].

The relationship between the intensity of the photon flux with distance is exponentially dependent on equation (3.4) [40].

$$I = I_0 \times e^{-\alpha d} \dots\dots\dots\dots\dots\dots\dots\dots\dots\dots\dots\dots\dots\dots\dots\dots\dots(3.4)$$

Where: I = transmitted photons, I_o = incident photons, α = absorption coefficient, and d = thickness of the material.

3.3.1 Reflection (R)

Reflection is the term for transforming the pathway of radiation moving from one medium to another having an index of refraction, and it is represented by the symbol (R). Additionally, each material has a specific reflection coefficient based on its physical properties, Eq. 3.5.

3.3.2 Transmittance (T)

The percentage of incoming light of a certain wavelength that passes through a sample is known as transmittance. The descriptors visible transmittance & visible refractive indices refer to the corresponding proportions for the visible spectrum of light [41].

$$R(\%) = 1 - A - T \dots\dots\dots\dots\dots\dots\dots\dots\dots\dots\dots\dots\dots\dots\dots\dots\dots.(3.5)$$

3.4   Electrical Characteristics of Photovoltaic Cell

The current-voltage (I-V) characteristic curve of a photovoltaic (PV) silicon solar cell describes the electrical performance of the solar cell by containing several variables such as short circuit current (I_{SC}), open-circuit voltage (V_{OC}), fill factor (FF), maximum power (P_{max}), and efficiency (ɳ). The below figure 3.3 shows the electrical circuit of PV solar cell.
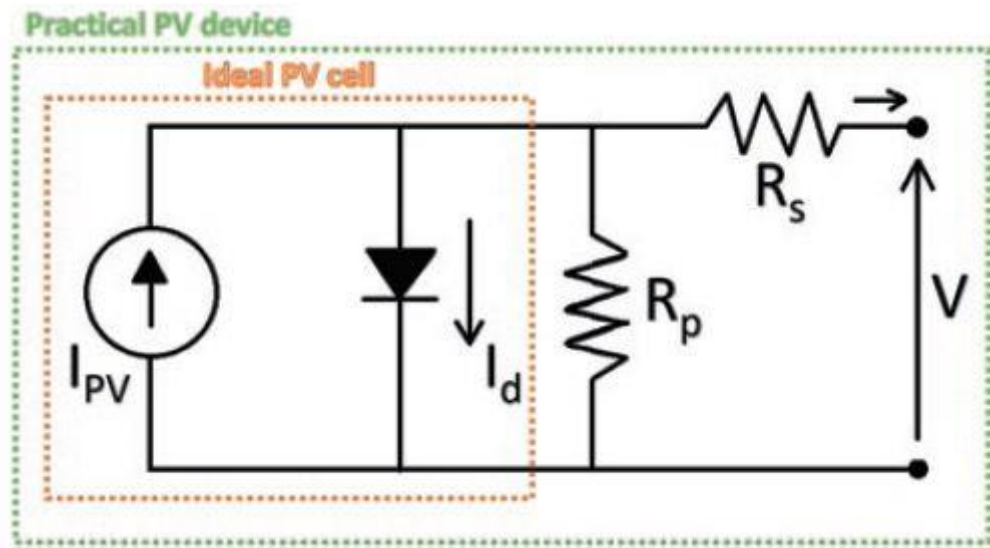
Figure 3.3. Electrical circuit of photovoltaic solar cell [7].

3.4.1 Open Circuit Voltage (V_{OC})

The open-circuit voltage (V_{OC}) represents the maximum voltage that a solar cell can produce when the current is zero. Variables like solar irradiation and solar cell temperature affect its value. The V_{OC} at zero can be calculated using equation (3.6) [7].

$$V_{OC} = \frac{nk\mathcal{T}}{q} \ln(\frac{I_L}{I_O} + 1)\dots\dots\dots\dots\dots\dots\dots\dots\dots\dots\dots\dots\dots(3.6)$$

Where: (I_L) is the light-generated current and (I_O) is the dark saturation current, (K) is the constant of Boltzmann, ($\mathcal{T}$) is the absolute temperature, (q) is the absolute value of electric charge, and (n) is the ideality factor.

3.4.2 Short Circuit Current (I_{SC})

The short-circuit current (I_{SC}) is the maximum current that a solar cell can produce when its voltage is zero (i.e., when it is short-circuited), as this current results from the accumulation and creation of carriers made from light photons. I_{SC} is affected by solar irradiation and solar cell temperature. Can be calculated using equation (3.7) [7].

$$I_{SC} = I_O \left[\exp\left(\frac{qV}{nkT}\right) - 1 \right] - I_L \dots\dots\dots\dots\dots\dots\dots\dots\dots\dots\dots\dots(3.7)$$
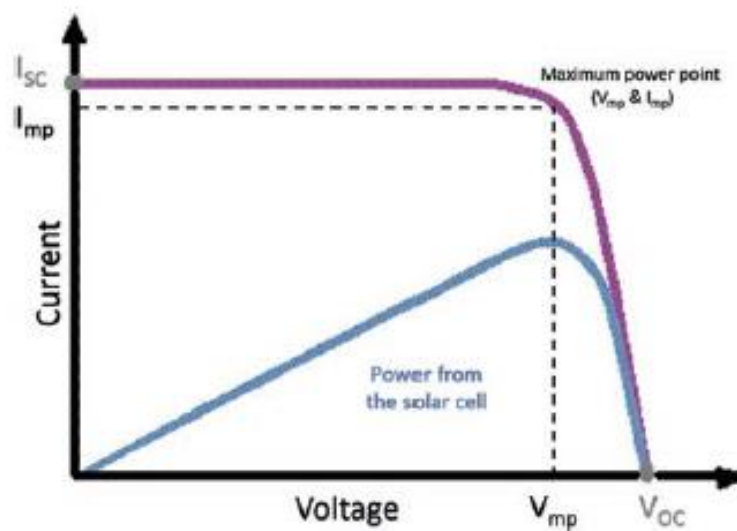
Figure 3.4. Current-Voltage (I-V) curve and Power curve(P-V) [7].

3.4.3 Fill factor (FF)

The ratio of the solar cell's maximum power to the total value of Voc and Isc is known as the fill factor (FF). The area of the greatest rectangle that will fit inside the current-voltage (I-V) curve and a graphic representation of the squareness of the solar cell are both represented by the FF. Can be calculated using equation (3.8) [7].

$$FF = \frac{I_{mp} V_{mp}}{I_{sc} V_{oc}} \dots\dots\dots\dots\dots\dots\dots\dots\dots\dots\dots\dots\dots\dots(3.8)$$

The power output from the photovoltaic effect is zero at both of the operational points that relate to short-circuit current (I_{SC}) and open-circuit voltage (V_{OC}). The variable known as the FF, along with Voc and Isc, defines the maximum power output from a photovoltaic.
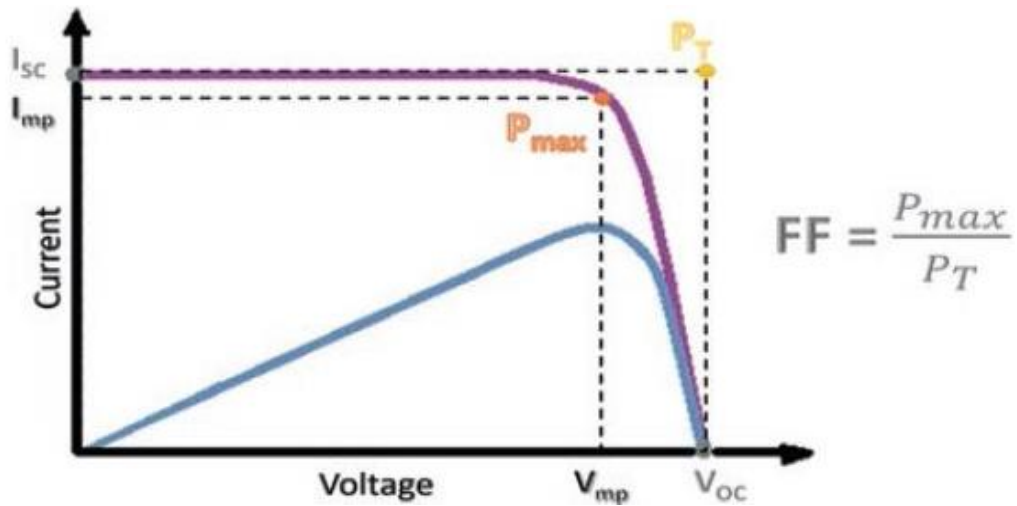
Figure 3.5. Fill factor (FF) of the photovoltaic solar cell [7].

3.4.4 Power and Efficiency

The efficiency (η) of the solar cell, or what is sometimes called the power conversion efficiency (PCE), represents the ratio of dividing the highest power point (Pmax) of the solar cell at the I-V curve divided by the power of incident light, which is usually done in standard conditions at (AM 1.5 G) [42]. By measuring the efficiency of the solar cell, it is possible to know the extent of its effectiveness in converting photons of light into electrical energy [42].

$$P_{max} = V_{OC} \times I_{sc} \times FF \dots\dots\dots\dots\dots\dots\dots\dots\dots\dots\dots\dots\dots(3.9)$$

$$\eta = \frac{V_{OC} \times I_{SC} \times FF}{P_{inc}} \dots\dots\dots\dots\dots\dots\dots\dots\dots\dots\dots\dots\dots\dots(3.10)$$

Where: P_{inc} is the incident light power, that calculated by multiple the overall irradiance (W/m^2) by the effectively illuminated region(m^2).

3.5 Anti - reflective Concept

When light interferes from one medium to another suddenly, it leads to a change in the direction of its wave path. This phenomenon is called "reflection." The coefficient of reflection is related to the speed of light in the reflected medium and the speed of light in a vacuum.

A change in the refractive index will cause an optical interruption, meaning that some of the incident light will be transformed into reflection (neglecting the effects of absorption and dispersion). This process is known as Fresnel reflection loss.

The principle operation of the anti-reflective thin-film coating is that this film has a refractive index (n) lower than the refractive index (ns) of the coated substrate, as shown in Figure (3.6). The reflection of incident light is determined by the following equation (3.11)[37].

$$R = \left| \frac{(n_0 n_s - n^2)}{(n_0 n_s + n^2)} \right|^2 \dots\dots\dots\dots\dots\dots\dots\dots\dots\dots\dots\dots\dots\dots\dots(3.11)$$

Where: n, n_0, n_s are the reflective index of thin film, substrate, and air respectively.
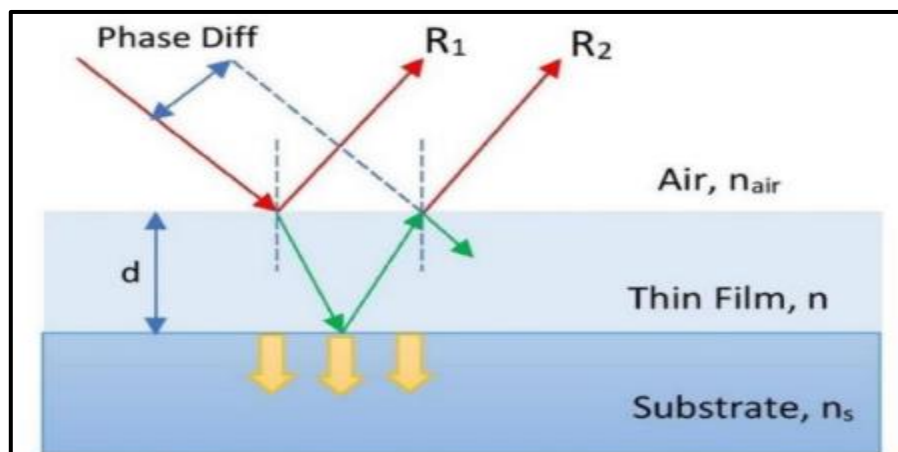
Figure 3.6. Thin film coating's reflection effect [37].

3.6 Temperature Effect on Solar Cell

As a semiconductor, solar cells are sensitive to temperature. As the temperature of semiconductors rises, the band gap will be reduced, and this reduction is caused by an increase in the energy of the material's electrons. Therefore, when the temperature rises, the electrical characteristics of the solar cell experience a slight increase in current and a large drop in voltage, which results in a reduction in the amount of power generated and a corresponding drop in efficiency[43].

PV solar cell output varies inversely with temperature; as the temperature drops, more electricity is produced; as the temperature rises, less energy is produced. With a temperature increase of 1 °C higher than 25 °C (standard test condition temperature STC), the output changes by 0.4% to 0.5%, figure 3.7. [44].
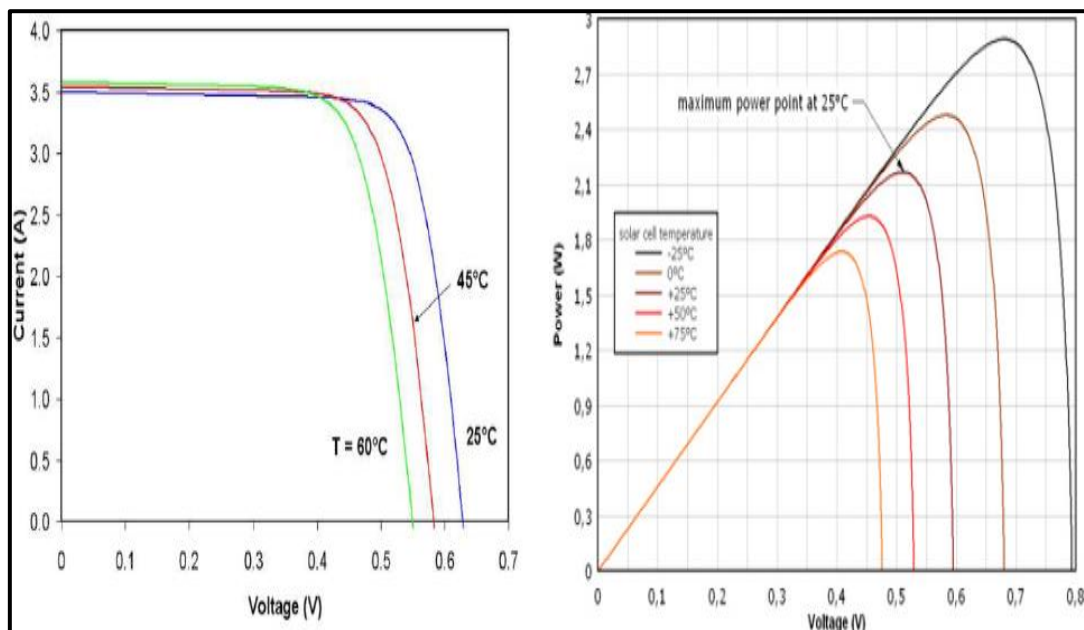
Figure 3.7. The temperature effect on the solar cell output parameters[44].

3.7 Irradiation Effect on Solar Cell

Irradiance, which is measured in watts per square meter (W/m^2), is described as the quantity of solar energy received in a certain area. In contrast, the total energy of sunlight is measured by irradiance. Solar radiation incidence is a term that refers to solar elements. With the increasing solar radiation, both the V_{OC} and I_{SC} rise, and as a result, the P_{max} changes as the solar insolation changes throughout the day [45].

From figure 3.8. It is clearly apparent that the incident light's process of producing current is influenced by irradiance; the greater the radiation exposure, the higher the current. On the other hand, Voltage is nearly constant or has slight change. It is evident that irradiation has an impact on maximum power point; the greater the irradiation, the greater the maximum power point[46].
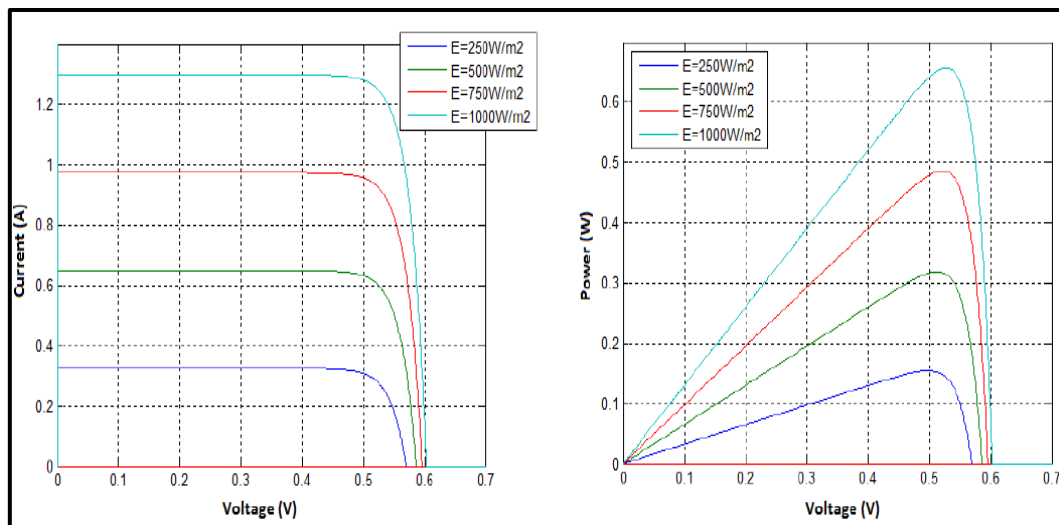
Figure 3.8. The irradiation effect on the solar cell output
parameters[46].

Chapter Four

Experimental Work

Experimental Work

4.1 Introduction

The steps of the preparation process of the nano-coating and its application to commercial polycrystalline silicon solar cells, the type and specifications of materials used such as polymers, nano-materials, and the solvent will be included. The devices used in this experiment of the preparation, such as the sensitive balance, magnetic stirrer, ultrasonic devices for examination of nano-coatings and the device that measured the electrical properties of the silicon solar cells, will be mentioned in detail in this chapter. The measurement devices include UV- Visible spectrophotometer, thermal imaging infrared Camera, temperature data logger, coating thickness gauge, and solar module analyzer, for investigations of the effect of coatings on the performance of solar cells.

4.2 Materials Used

4.2.1 Polymethyl Methacrylate (PMMA)

A white powder of PMMA (polymethyl methacrylate) has a 1.18 g/cm^3 density and a 160 °C melting point. Table 4.1, shows some of the physical and chemical properties of Poly (methyl methacrylate). PMMA is one of the most well-known and well-established polymers with the chemical formula $(C_5H_8O_2)_n$. PMMA was formerly thought to be a viable alternative to glass in a number of applications, and it is now widely utilized in glazing. It's one of the most rigid polymers with a stiff the substance that is transparent, and weather-resistant. PMMA is colorless and transparent by nature. Visible light transmittance is extremely great (about 99%). PMMA matrix materials are well-known for their use in technological applications[47].

Figure 4.1. polymethyl methacrylate (PMMA).

Table 4.1. Physical and chemical properties of polymethyl methacrylate (PMMA).

Property	Polymethyl methacrylate (PMMA)	Unit
Color	White	-
Density	1.18	g/cm^3
Melting point	160	°C
Thermal conductivity	0.12	W/m.k
Surface hardness	M90	Rockwell
Refractive index	1.4	-
Chemical formula	$(C_5H_8O_2)_n$	-
Organic solvents	Acetone, Chloroform and Toluene	-

4.2.2 Zinc Oxide (ZnO)

Zinc oxide has the formula ZnO and is an inorganic substance. It is a white powder that is water insoluble. ZnO may be found in many different forms, including nanoengineered, nanoparticles, nanostructured, and nan-building materials. It's also simple to change the qualities of a nanostructure by changing its shape and size, so the Zinc oxide crystallizes mostly in wurtzite, zinc-blende, and rock salt cubic regimes[48]. They have outstanding optoelectronic characteristics and can be readily manufactured into various geometries, making them potential

photovoltaic solar cell possibilities. ZnO nanoparticles have a low reflectivity, which increases optical absorption. Nanostructures of ZnO are commonly used as the anti-reflective coating in photovoltaic systems, Appendix-A.

Table 4.2. Zinc Oxide general specifications

Property	Zinc Oxide
Chemical formula	ZnO
Color	White
Molar mass	81.406 g/mol
Melting point	1974 °C
Density	5.5 g/cm^3
Band gap	3.3 eV
Refractive index	2.013

4.2.3 Polycrystalline Silicon Solar Cell

A commercial polycrystalline silicon solar cell was used with the specifications shown in table (4.3) and figure (4.2) to test the effect of the nanocomposite coating. The solar cell, with dimensions of (39×22) mm, forms part of the solar module that contains several cells connected in series.
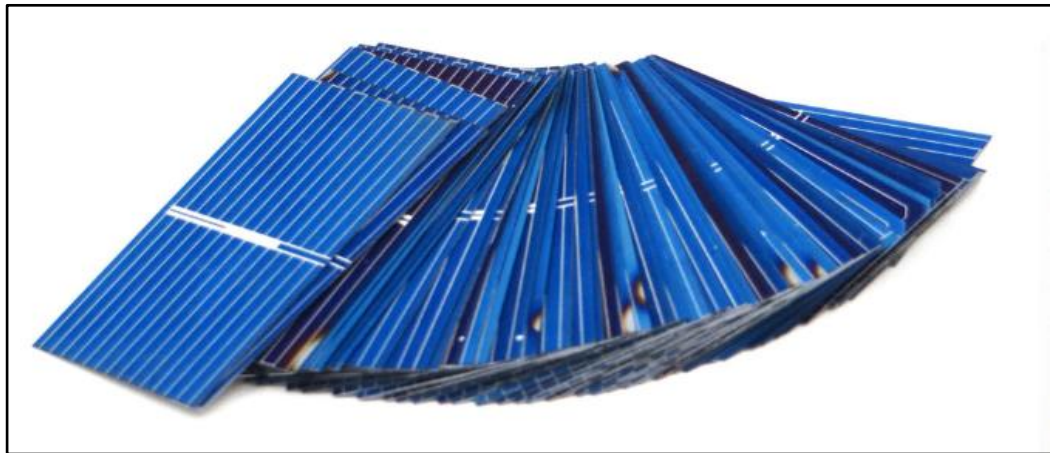
Figure 4.2. The commercial polycrystalline silicon solar cell.

Table 4.3. Commercial Polycrystalline Silicon Solar Cell Properties.

Item	Description
Type	Polycrystalline silicon
Size	(39×22) mm
Area	858 mm^2
Maximum power (P_{max})	0.14 W
Rated Voltage	0.5 V
Rated Current	0.28 A
Standard test conditions (STC)	1000 W/m^2, 25 °C

4.3 Preparation of PMMA/ZnO Nano-coating.

The nanocomposite coating was prepared in two stages: first, the PMMA polymer is dissolved in acetone solvent to make the matrix combination, and then the nano-material is prepared and added to the polymer solution, as listed below:

4.3.1 Preparation of Polymethyl Methacrylate (PMMA)

Five amounts of PMMA polymer were prepared, weighed by using a sensitive balance, and then the acetone solution was added to each weighted amount to prepare the five PMMA concentrations shown below.

- ➢ 0.25 gram PMMA powder + 40 ml (acetone solvent): 0.625 wt%
- ➢ 0.50 gram PMMA powder + 40 ml (acetone solvent): 1.25 wt%
- ➢ 1.00 gram PMMA powder + 40 ml (acetone solvent): 2.5 wt%
- ➢ 1.25 gram PMMA powder + 40 ml (acetone solvent): 3.125 wt%
- ➢ 1.50 gram PMMA powder + 40 ml (acetone solvent): 3.75 wt%

Five amounts of PMMA were selected (0.25 g, 0.5 g, 1 g, 1.25 g, and 1.5 g). So, 0.5 g as a sample of preparation steps. Fill a vial with 40 ml of acetone solvent, then add 0.5 g and seal it. Place the PMMA solution on the magnetic stirrer at 400 RPM and a temperature of 60 ºC for about an hour until it is fully dissolved, see figure 4.3. The same procedure used for

other PMMA amounts to get the weighted percent concentrations of 0.625%, 1.25 wt%, 2.5 wt%, 3.125 wt%, and 3.75 wt%.
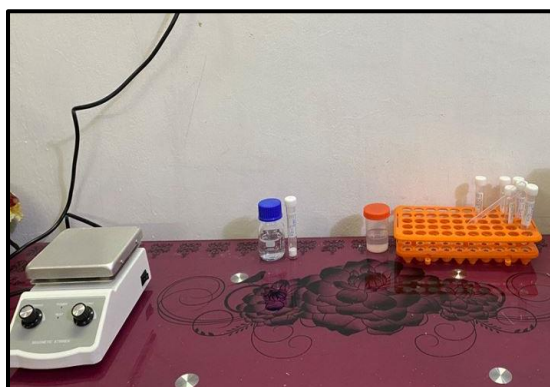
(a). PMMA & Accetone solvent.   (b). Stirrer & PMMA concentations.
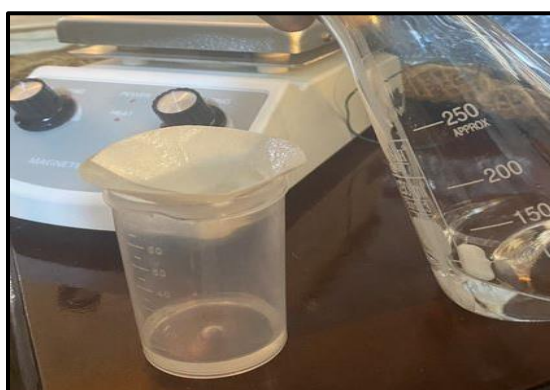
(c). Mixing solution.   (d). Filtering the final solution.

Figure 4.3. The preparation steps for the PMMA coating solution.

4.3.2 Preparation of Zinc oxide solution (ZnO)

The four amounts of ZnO nanoparticles powder (0.1 g, 0.2 g, 0.3 g, and 0.4 g) were weighed by using a sensitive balance, and then 40 ml of the acetone solution was added to each weighted amount to prepare the four different concentrations as shown below.

➢ 0.1 gram ZnO powder +40 ml (acetone): 0.25 wt%

➢ 0.2 gram ZnO powder +40 ml (acetone): 0.5Wt%

➢ 0.3 gram ZnO powder +40 ml (acetone): 0.75 wt%

➢ 0.4 gram ZnO powder +40 ml (acetone): 1 wt%

48

The four different concentrations (0.25 wt%, 0.5 wt%, 0.75 wt%, and 1 wt%) were prepared by weighing four different amounts of ZnO nanoparticles, size 40-50 nm, (0.1 g, 0.2 g, 0.3 g, and 0.4 g), using a sensitive balance, and then adding 40 ml of the acetone solution to each weighted sample. To disperse the ZnO nanoparticles in the solution, the four created varied concentrations (0.25 wt%, 0.5 wt%, 0.75 wt%, and 1 wt%) were placed individually in the ultrasonic device, type NT-628, for six hours (total time for preparing one sample of nanocomposite). The preparation of ZnO is shown in Figure 4.4.

| (a). ZnO white powder. | (b).Mixing & Sample weight. |

| (c). Sonicating step. | (d). Final solution. |
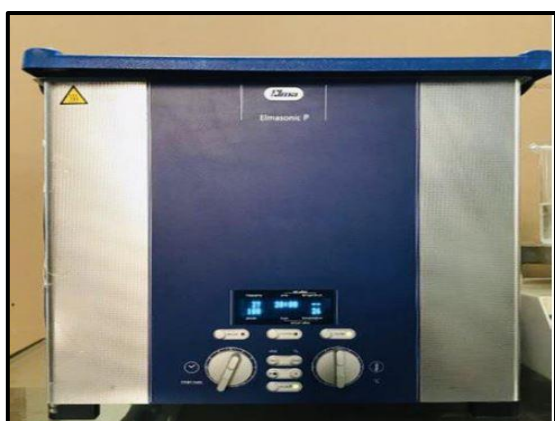
Figure 4.4. The preparation steps for the ZnO solution.

4.3.3 Preparation of PMMA/ZnO Nanocomposite Coating

The best concentration of the five PMMA concentrations was chosen based on UV-Visible absorbance; the (3.125 wt%) concentration had the best UV absorption and was made with (1.25 g); more details are available in Chapter 5. (Results and discussion). The four ZnO concentrations prepared were doped with a 1.25 g PMMA amount in order to prepare the four concentrations ZnO/PMMA (3.375 wt%, 3.625 wt%, 3.875 wt%, and 4.125 wt%) as below listed. Figure 4.5, 4.6.

➢ (1.25 g PMMA/40ml acetone)+(0.1 g ZnO /40 ml acetone):3.375 wt%

➢ (1.25 g PMMA/40ml acetone)+(0.2 g ZnO /40 ml acetone):3.625 wt%

➢ (1.25 g PMMA/40ml acetone)+(0.3 g ZnO /40 ml acetone):3.875 wt%

➢ (1.25 g PMMA/40ml acetone)+(0.4 g ZnO /40 ml acetone):4.125 wt%
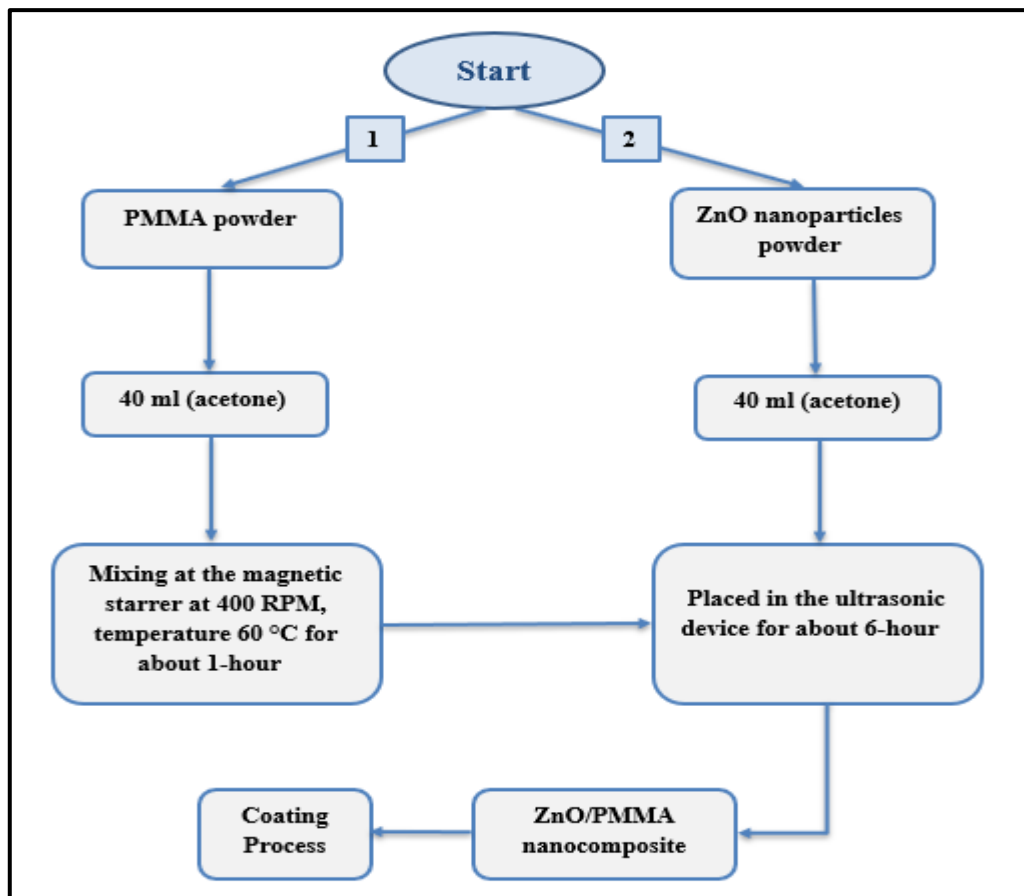
Figure 4.5. Flowchart for the production of ZnO/PMMA nanocomposites coating.
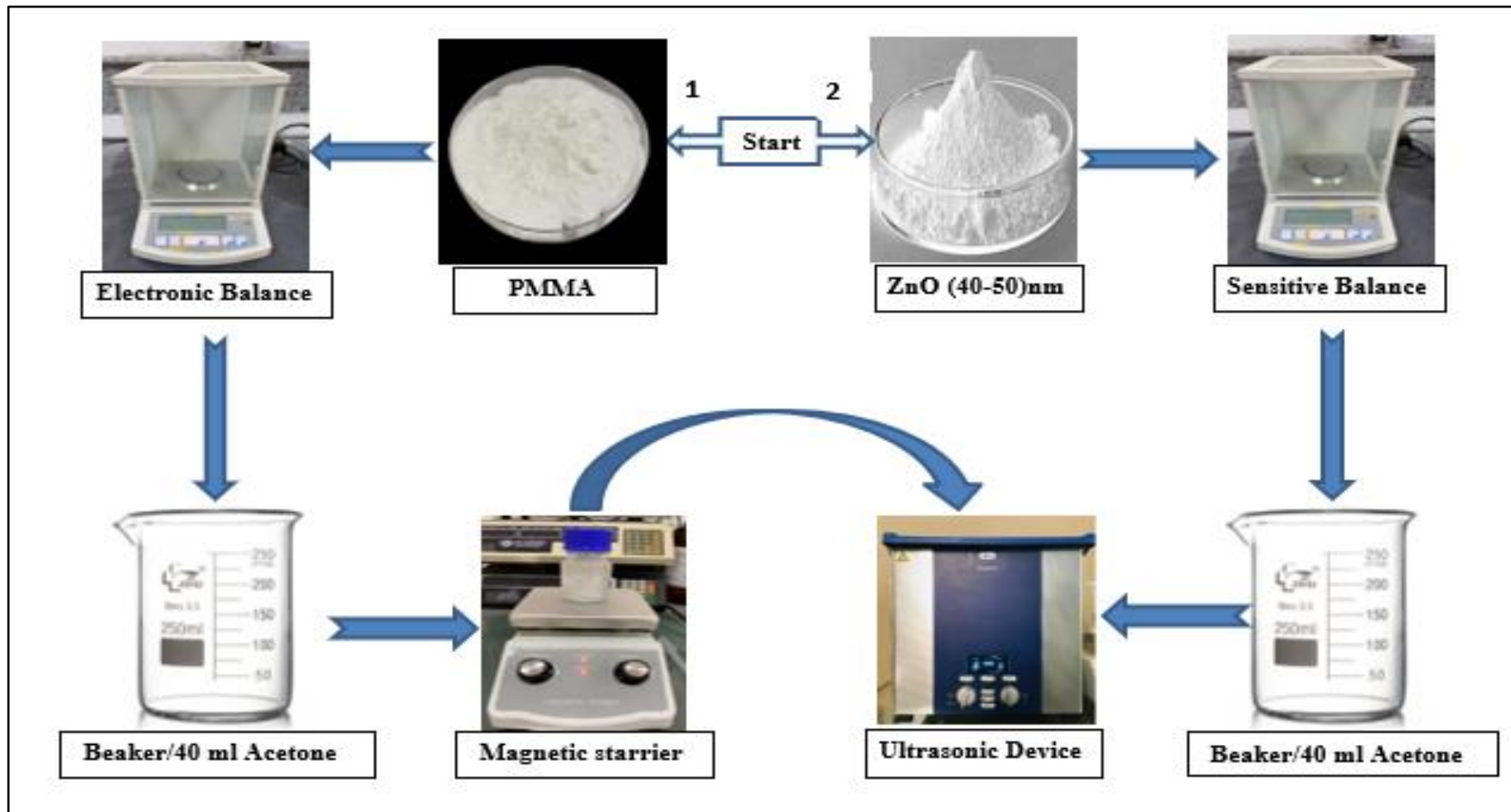
Figure 4.6. The production of ZnO/PMMA nanocomposites coating.

4.4   Coating Application Process

4.4.1 Surface Preparation of Polycrystalline Silicon Solar Cell

The first step of the coating process is the cleaning and surface preparation for commercial polycrystalline silicon solar cells of size (39×22) mm. This is done by placing a number of cells in a beaker and adding 20 ml of distilled (DI) water, sonicating in the ultrasonic device, for 10 minutes, as shown in figure 4.7, and repeating the procedure with acetone instead of DI water. The cells were then allowed to dry at an ambient temperature. As a result, the polycrystalline silicon solar cells are free from dust and pollutants and are ready for coating.

4.4.2   Coating method

There were several techniques used to coat the silicon solar cells, but the casting procedure was the most economical and easiest one[21]. 0.5 ml of ZnO/PMMA nanocomposite coating was enough to coat one of the commercial polycrystalline silicon solar cells with a size of (39×22) mm, so by using a pipe tube, 0.5 ml of coating was applied to the top surface of the solar cell. The coating was then moved to cover the entire solar cell, where the coating layer was formed with an even thickness, as conformed by measuring the coating thickness using a dry film thickness gauge (DFT). And then the solar cell is left at room temperature for 30 minutes to dry the coating, see figure 4.7.
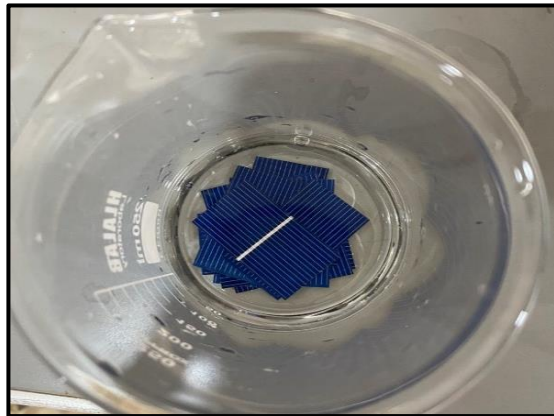
(a). Cleaning the PV solar cells   (b). The coating & pipe tube.
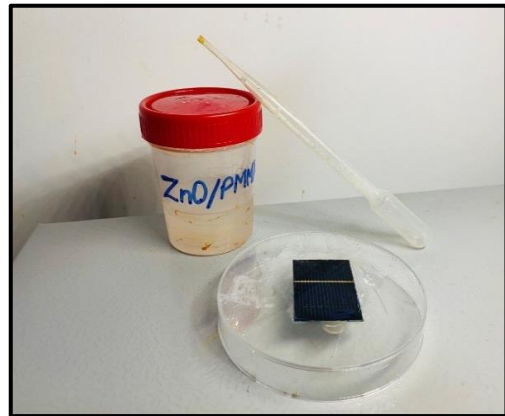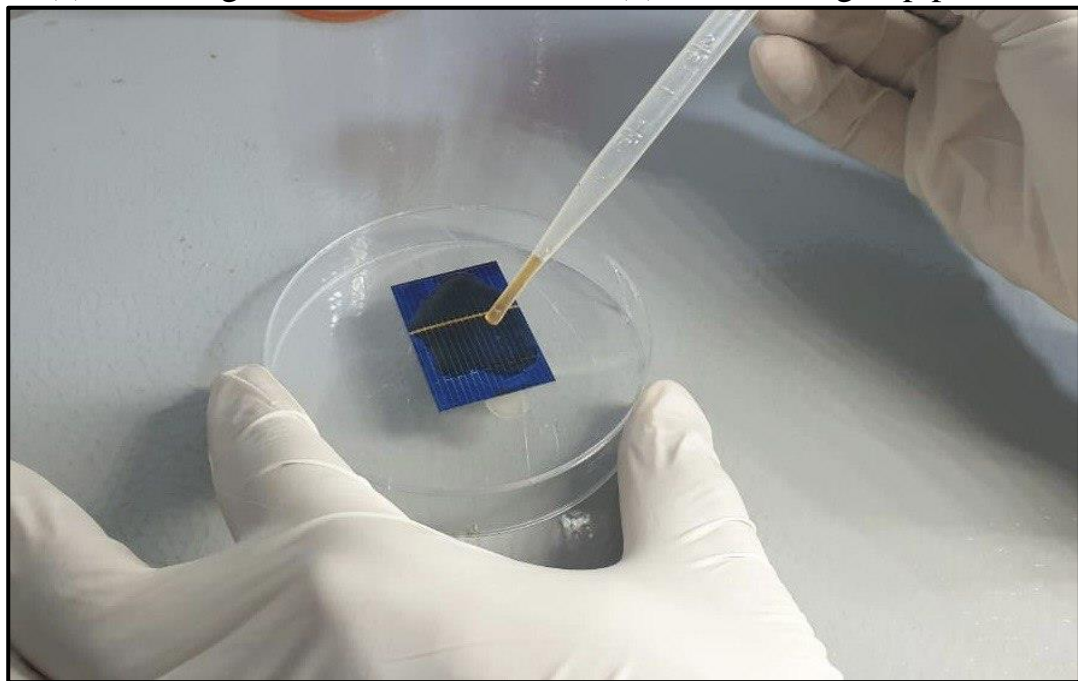
(c). Applying the coating to the top surface of the PV solar cell.
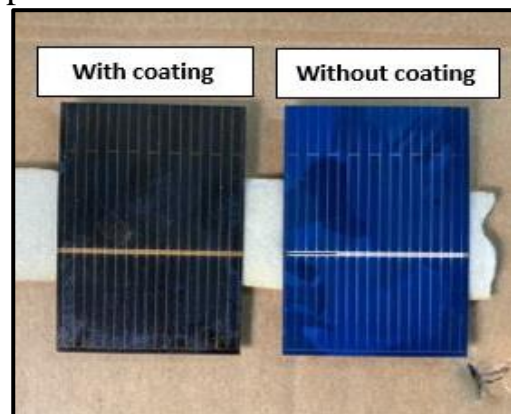
(d). ZnO/PMMA thin film.   (e). Coated and uncoated cells.

Figure 4.7. Coating application process

4.5   Devices used

4.5.1 Sensitive Electronic Scale

To accurately weigh the quantities of material to be used in the experiment, a sensitive Electronic Scale type KERN-ABS, manufacturer Kern & Sohn, figure 4.8, was used with digit sensitive (d=0.1 mg) and a maximum weight of 220 g.

Figure 4.8. KERN-ABS Sensitive electronic scale

4.5.2 Magnetic Stirrer

The magnetic stirrer, model SH-2, rotational speed 200-1600 rpm device is used to dissolve and mix the PMMA with acetone (figure 4.9). The work principle of the magnetic stirrer depends on the coil inside the device that generates a magnetic field. This field stirs a small iron placed inside the mixture and also contains a heater that heats the mixture through the external plate, where the device provides a speed and temperature controller.

Figure 4.9. The magnetic stirrer, model SH-2.

4.5.3 Ultrasonic Device

The principle of the device's work is to generate ultrasonic waves with specific frequencies as they collide with the mixture that is placed inside the device to disperse the nanoparticles in the mixture. where Elmasonic P-180H device, manufactured in Germany by Elma Ultrasonic, shown in figure 4.10, was used. The device has been used to disperse apart particle clusters, scatter the nanoparticles, and create their dispersion in the basic fluid. It's an important device that's used to prepare the nanocomposite coating. Place the closed beaker filled with the nano mixture inside the basin filled with water of the device, where the water level is higher than the level of the mixture inside the beaker. It disperses the nanoparticles to avoid their aggregation to form a homogeneous nano-mixture. Appendix-B.

Figure 4.10. Elmasonic P-180H device.

4.5.4 Coating Thickness Gauge

The most essential metric in protective coatings operations is dry film thickness, which is defined and monitored in almost every coating application. Modern digital gauges allow for the rapid and precise collection of readings, providing a full image of the coating job[49]. The gauge operates according to the measurement principles of eddy pulsed magnetic inducement.

After the coating dried and cured, the thickness of the film was measured by using a digital thickness gauge in several different locations on the solar cell. The thickness of the coating layer was measured by the coating thickness gauge TT-260, with accuracy 0.1%, shown in figure 4.11 and appendix-C for device information's. The tests were carried out at Engineering College-University of Babylon. Some of the thickness readings recorded were 1.4 μm, 1.7 μm, 1.8 μm, and 2.1 μm so the average reading for ZnO/PMMA thin film coating was found in the range of 1-2 μm, and the average reading was 1.75 μm.

Figure 4.11. Digital coating thickness gauge TT-260.

4.5.5 Ultraviolet-Visible Spectrometer (UV-Vis)

The study of a light beam's attenuation after passing through a sample or after reflecting off of a sample surface is known as ultraviolet and visible (UV-Vis) absorption spectroscopy. Various measures of absorption, transmittance, and reflectance in the UV region, visible, and near-infrared (IR) spectrum bands are together referred to as UV-Vis spectroscopy. The measurements are made across a wide spectral range or at a single wavelength. UV-Vis spectrophotometers utilize a source of light to shine light onto a sample that spans the UV to visible wavelength range (usually 190-900 nm). The devices then calculate the amount of light at each wavelength that is absorbed, transmitted, or reflected by the sample [50]. Where a Double Beam UV-visible spectrophotometer, type (Mega-2100), manufactured by SCINCO, shown in figure 4.12, was used to measure the absorption, transmittance, and reflectance in the wavelength region (200–700) nm. The tests were carried out at Kufa University's Physics College.
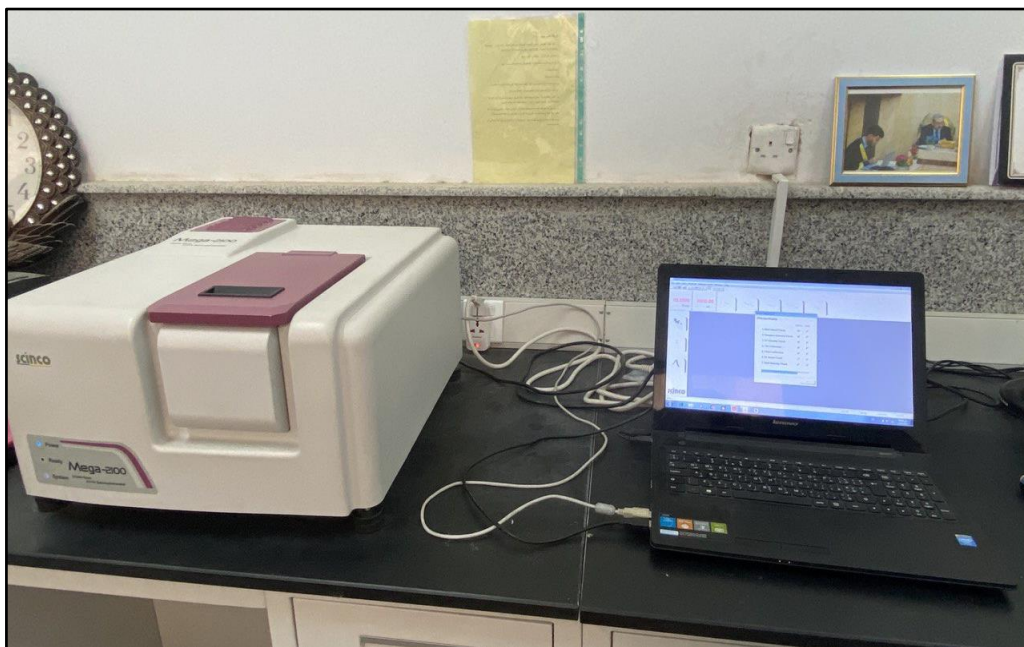
Figure 4.12. The Double Beam UV-visible spectrophotometer, type (Mega-2100).

4.5.6 Solar Intensity Meter

Easy operable device for measuring of solar radiation intensity in W/m^2. Provides for quick and reliable control of efficiency of photovoltaic or solar devices. Where a solar intensity meter DT-1307 type, manufactured by CEM, shown in figure 4.13 and appendix-D for device information's, was used to measuring of solar irradiation intensity during the experimental test.
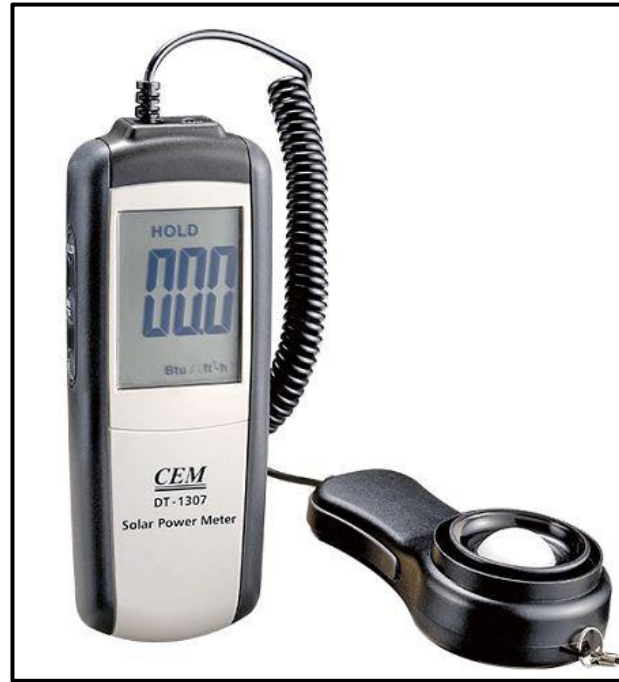
Figure 4.13. The solar intensity meter DT-1307.

4.5.7 Thermometer

It is a device for measuring temperature with dual channels by connecting k-type thermocouples in its channels; on the other hand, the thermocouples (type-k) are fixed on the back surface of the polycrystalline solar cell, so the device displays the temperature of the coated and uncoated solar cells at the same time. To know the temperature difference for the appearance of the effect of the nanocomposite coating in reducing the temperature of the solar cells, a UT-320D thermometer brand UNI-T, with the accuracy of reading ($\pm$ (0.5%＋1)), figure 4.14 and appendix-E.

Figure 4.14. Mini Dual-channel K/J Thermometer, UT-320D type.

4.5.8 Thermal Imaging Infrared Camera

Any body above absolute zero will produce infrared radiation (IR) by the black radiation law. Its properties may be utilized to determine the temperature. The infrared radiation that an item emits is therefore captured by infrared measuring instruments, which then convert it into an electrical signal. The Thermal Imaging Infrared Camera can display the items' detected radiation and can be used to spectral the temperature of the objects [51]. In the present experimental work, a Thermal Imaging Infrared Camera, FLIR E-30bx type, was used, figure 4.15 and appendix-F, to measure the temperature of the coating/un-coating polycrystalline solar cells to confirm the readings measured by the Data-Logger device.

Figure 4.15. Thermal Imaging Infrared Camera, FLIR E-30bx.

4.5.9 Solar Module Analyzer

It is a device used to measure the electrical properties of solar cells, such as the I-V curve, P-V curve, and efficiency. The PROVA-200A solar module analyzer is made by PROVA INSTRUMENTS COMPANY (INC), shown in figure 4.16 and appendix-G, was used at Kufa University's Physics College to identify the electrical properties of coated solar cells by different concentrations and compare them to those of uncoated solar cells in order to identify the best concentrations.

Figure 4.16. Solar module analyzer, PROVA-200A.

4.6 Experimental Rig Setup

The study tested electrical properties by the solar module analyzer device for the coated polycrystalline solar cells with different concentrations of ZnO/PMMA nanocomposite coating thin film and compare them to the uncoated solar cell. The tests were carried out indoors by halogen light under standard test conditions (STC) (1000 W/m^2 of solar radiation and a temperature of 25 °C. The experiment was done in the laboratory of the Faculty of Science-University of Kufa, where the standard test conditions (STC) were provided in the laboratory. The temperature of the laboratory was 25 °C, and the polycrystalline solar cells were placed at a distance from halogen light at which the reading of the solar irradiation was 1000 W/m^2 where the solar irradiation was measured using a solar power meter device. Figure 4.17 depicts a test rig for solar cell experiments. The results are indicated by the test analyzer type PROVA-200A which is connected to a personal laptop to collect and save the data. Note that the total error of the reading of PROVA-200A device is 1% ± 0.09V and 1% ± 9mA for voltage and current, respectively.
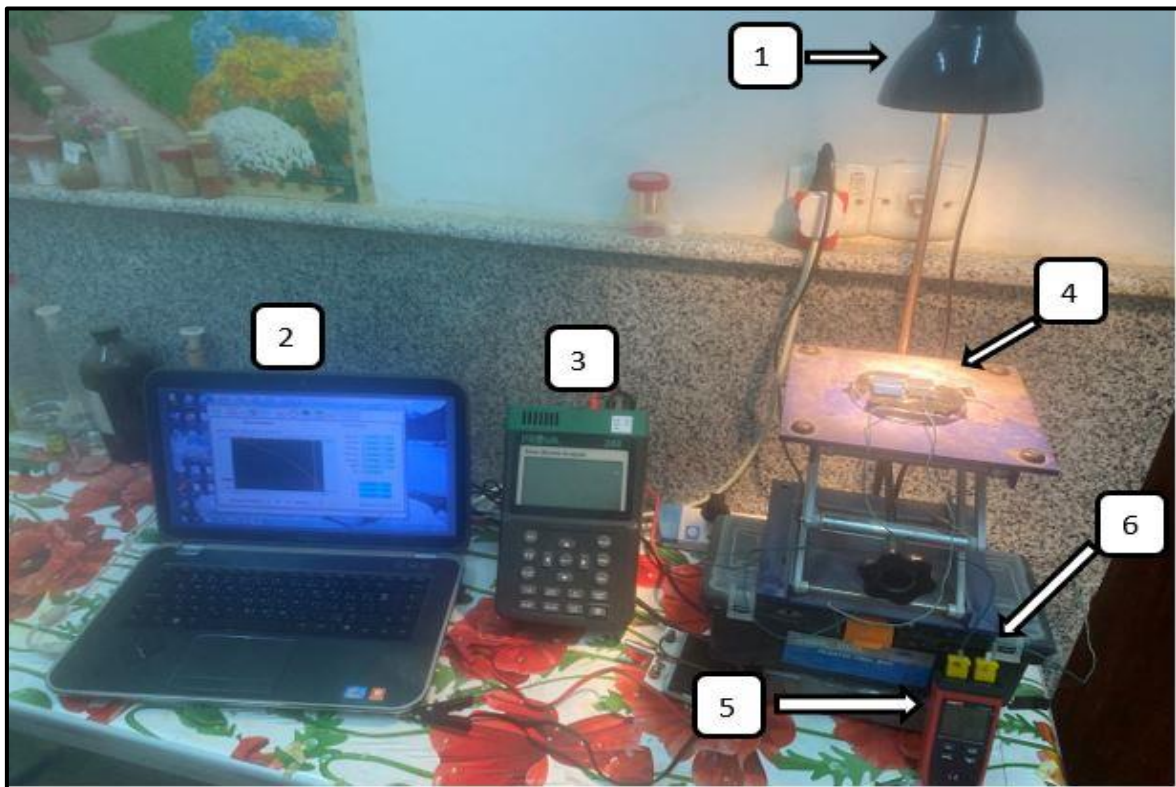
Figure 4.17. Rig Solar cell Test.

1. Halogen Lamp.
2. Personal laptop.
3. Solar cell module analyzer
4. Polycrystalline silicon solar cell/coating – un-coating
5. Thermometer (Data-logger)
6. K-type thermocouples.

Chapter Five

Results and Discussion

Results and Discussion

5.1   Introduction

The impact of nanocomposite coating thin film on polycrystalline silicon solar cell efficiency and energy production was studied in this chapter. The major goals of the study were to reduce the surface temperature and light reflection of the solar cell in order to improve efficiency, which is the main purpose of this study.

A polymethyl methacrylate (PMMA) polymer was used and different concentrations of the Zinc Oxide (ZnO) nanomaterial size (40-50) nm were added to accomplish the nanocomposite coating to use for coating the commercial polycrystalline silicon solar cell size (39×22) mm, the experimental work has been done in the Engineering Technical College of Najaf. Various devices and tests were used to complete the work and obtain the results that were mentioned in this chapter, such as the (UV-visible absorbance, I-V curves, surface temperature detection, and coating thickness measured) tests, and they were done by using the devices (UV-visible spectrometer, solar analyzer, thermocouple data logger, and dry film thickness gauge) respectively.

5.2   Investigate the Influence of Polymethyl Methacrylate on the Performance of Solar Cells.

The effect of adding a Polymethyl Methacrylate (PMMA) polymeric coating on the surface of solar cells was experimentally studied as it was tested in the laboratories of the Engineering Technical College of Najaf under standard test conditions (STC) (Solar irradiance = 1000 W/m^2, and ambient temperature = 25 °C).

In the beginning, the ability of the PMMA polymer to absorb ultraviolet rays (UV) was examined, where different concentrations of the

polymer mixture were prepared. The absorption of ultraviolet and visible rays was tested, and then a layer was applied to the solar cell to measure the effects on the electrical properties and the surface temperature of the cells to find the best concentration that can be used to obtain the highest possible efficiency.

5.2.1 Influence the Polymethyl Methacrylate on Ultraviolet Absorbance

Based on the principle of blocking ultraviolet rays (UV) to reduce the excess energy that is converted into heat in order to reduce the polycrystalline solar cell while maintaining the transmission of visible light, which constitutes the bulk of the energy used by the solar cell to produce electricity. In this practical experiment, five samples were prepared from polymethyl methacrylate (PMMA) polymer with different concentrations (0.625 wt%, 1.25 wt%, 2.5 wt%, 3.125 wt%, and 3.75 wt%). The samples were examined by a UV-visible spectrophotometer. The test was done in the laboratory of Science College at the University of Kufa to test their ability to absorb ultraviolet rays. The results shown in figure 5.1 showed that the examination was conducted within the wavelength (200-700) nm where the UV region (200-400) nm and visible light region (400-700) nm, and the PMMA absorbance intensities results (2.1 AU, 2.3 AU, 3.2 AU, 3.7 AU, 3.5 AU) for the concentrations (0.625 wt%, 1.25 wt%, 2.5 wt%, 3.125 wt%, and 3.75 wt%) respectively. They showed that the absorption of ultraviolet rays increases with the increase in the concentration of the PMMA polymer. The reason for that variation was because of the accumulation of the atoms on top of each other, increasing the concentration over a certain quantity and creating a state of destructive interference with the substance, so the best result of PMMA

64

concentration absorbing ultraviolet rays to the largest possible extent was 3.7 AU when using the concentration of 3.125 wt%.
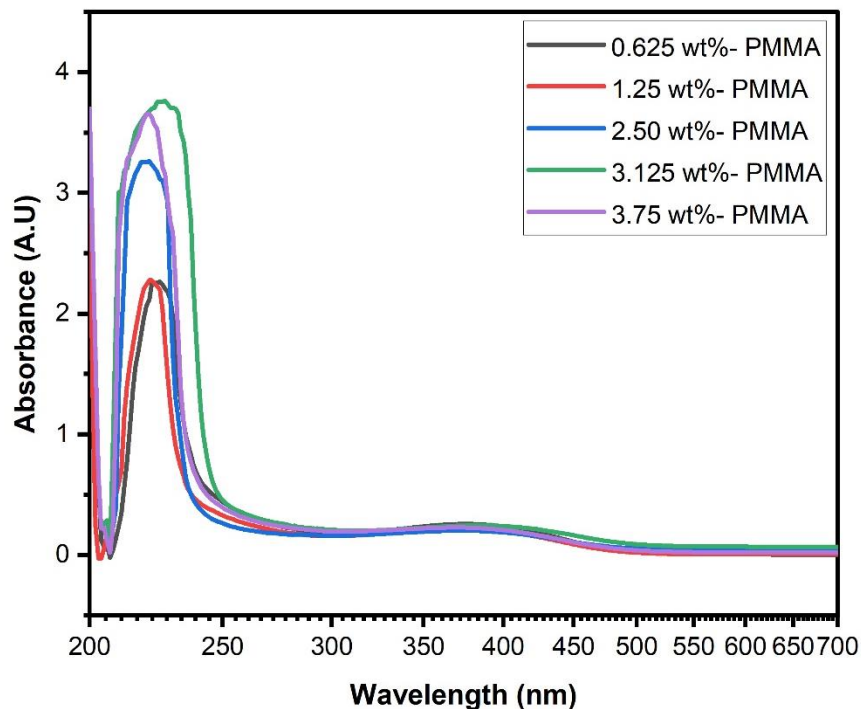
Figure 5.1. UV-Visible absorption of polymethyl methacrylate (PMMA) concentrations.

5.2.2 Influence the Polymethyl Methacrylate on Surface Temperature

As per mentioned in the basic concepts of the experiment, the temperature is affected by the amount of photon energy falling on the solar cell, and ultraviolet rays have an effect and are one of the causes of the rise in the temperature of the solar cells. Therefore, to examine the effect of adding the polymer (PMMA) to the upper surface of the polycrystalline solar cell that has the ability to UV-block, the polycrystalline solar cells were coated with different concentrations of PMMA polymer, and the polycrystalline solar cells without coating were tested, and temperature

readings were recorded for each cell during the test for one hour. Figure 5.2 shows the test results for the temperature change with time for the coated and uncoated cells, where the results were obtained at the end of the test time (78.5 ℃, 77.7 ℃, 76.3 ℃, 74.4 ℃, and 75.2 ℃) for the PMMA polymer concentrations used (0.625 wt%, 1.25 wt%, 2.5 wt%, 3.125 wt%, and 3.75 wt%) respectively, while the uncoated cell was recorded (81.5 ℃), so the temperature variation was recorded in table 5.1, which showed that the maximum temperature redaction was (7.1 ℃) when using the 3.125 wt% concentration. These results were matched and confirmed to the results of UV-absorption, which referred to the PMMA concentration that has the maximum UV-absorption and then the maximum temperature reduction compared to the other PMMA polymer concentrations.
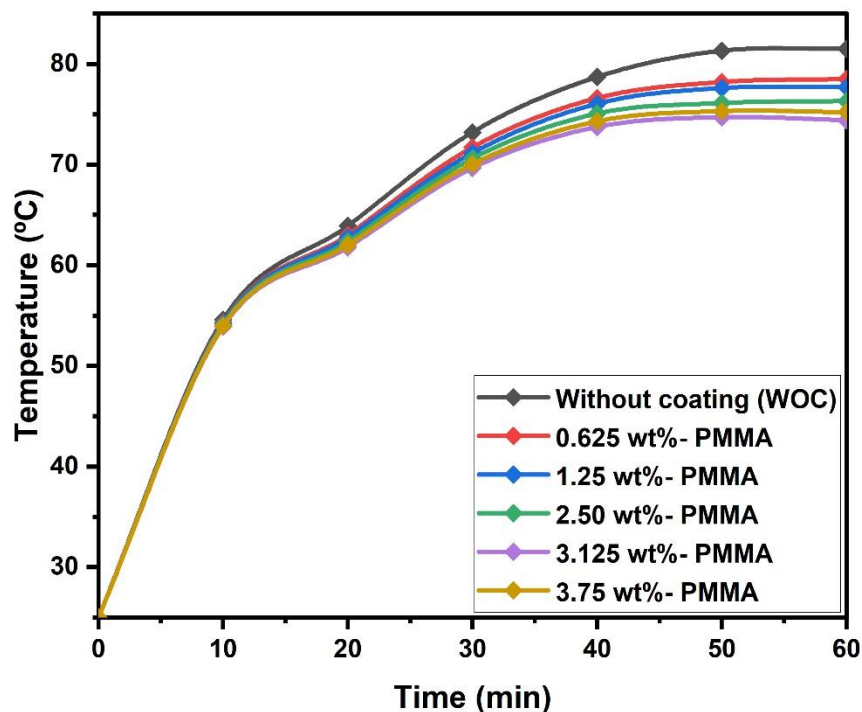
Figure 5.2. Temperature readings obtained during the testing of solar cell samples, with and without PMMA coating

Table 5.1. Temperature variance with the PMMA concentrations of test solar cell.

PMMA concentration (wt%)	Absorbance (AU)	Temperature variance (°C)
0.625 **wt%**	2.1	3.0
1.25 **wt%**	2.3	3.8
2.5 **wt%**	3.2	5.2
3.125 **wt%**	3.7	7.1
3.75 **wt%**	3.5	6.3

5.2.3 Influence of the PMMA on the Solar Cell Electrical Properties and Efficiency

The electrical properties (voltage-current (I-V) curve and power-voltage (P-V) curve), tested by the Solar Module analyzer (PROVA-200) device for the coated polycrystalline solar cells with different concentrations of PMMA thin film and compare them to the uncoated polycrystalline solar cell. The tests were carried out indoors using halogen light with standard test conditions (STC) (1000 W/m^2 of solar radiation and a temperature of 25 °C), where the test was carried out in two stages, the first at the beginning of the test and then after one hour, where the effect of the rising temperature on the efficiency of the solar cell was measured. The results indicated by the test analyzer listed in table 5.2 and figure 5.3 showed the I-V curve and figures 5.4 for the P-V curve and figures 5.5, and 5.6 for efficiency and power, respectively, of the coated and uncoated solar cells (11.4%, 11.6%, 11.8%, 12.1%, and 11.9%), for PMMA concentrations (0.625 wt%, 1.25 wt%, 2.5 wt%, 3.125 wt%, and 3.75 wt%), respectively, and (11.3%) for without coating at the end of the test, where the solar cell with 3.125 wt% PMMA concentration gave the

highest efficiency value of 12.1%, which led to the highest amount of power (104 mW) compared to the other concentrations, and the uncoated solar cell had the least efficient value of 11.3%. The increasing efficiency of the polycrystalline solar cell by using PMMA thin film coating is because the polymer reduces the surface temperature of the polycrystalline solar cell by absorbing part of the ultraviolet (UV) rays and blocking them from passing through the cell, as mentioned previously in this chapter.
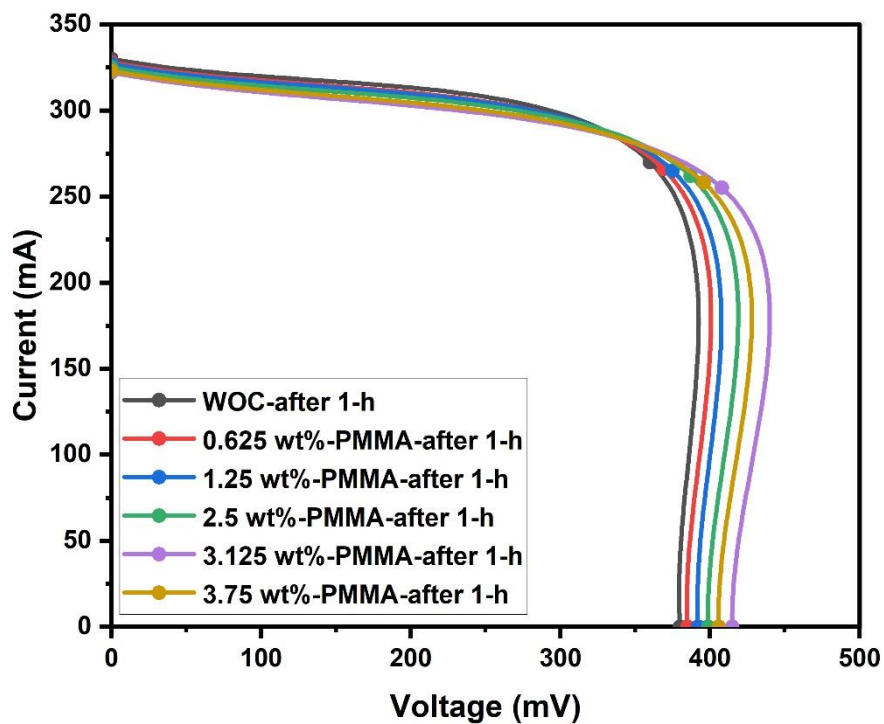
Figure 5.3. Polycrystalline solar cell current-voltage (I-V) curves with and without PMMA coating
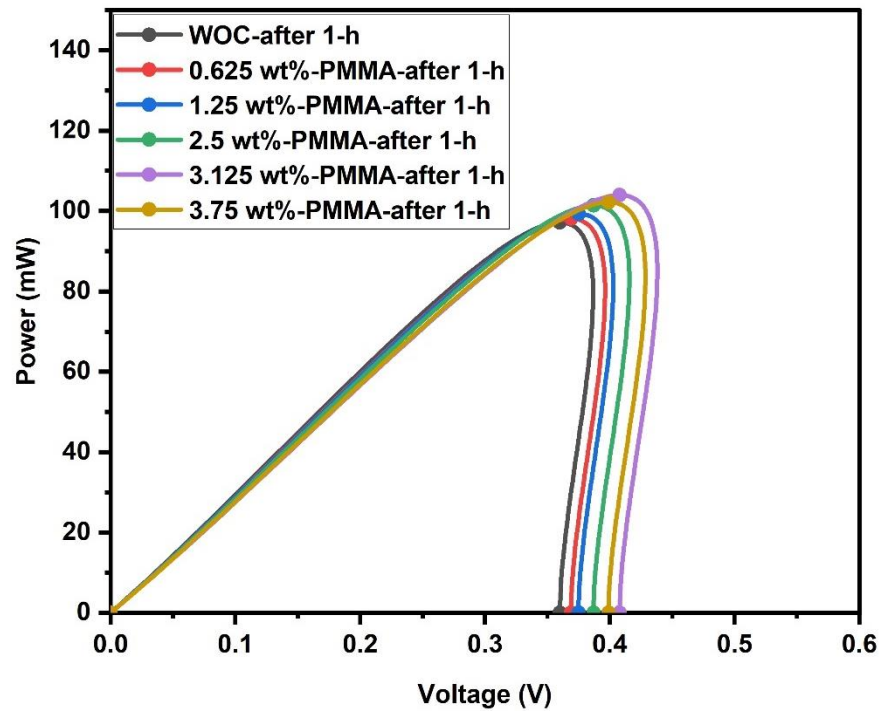
Figure 5.4. Polycrystalline solar cell Power-Voltage (P-V) curves with and without PMMA coating.
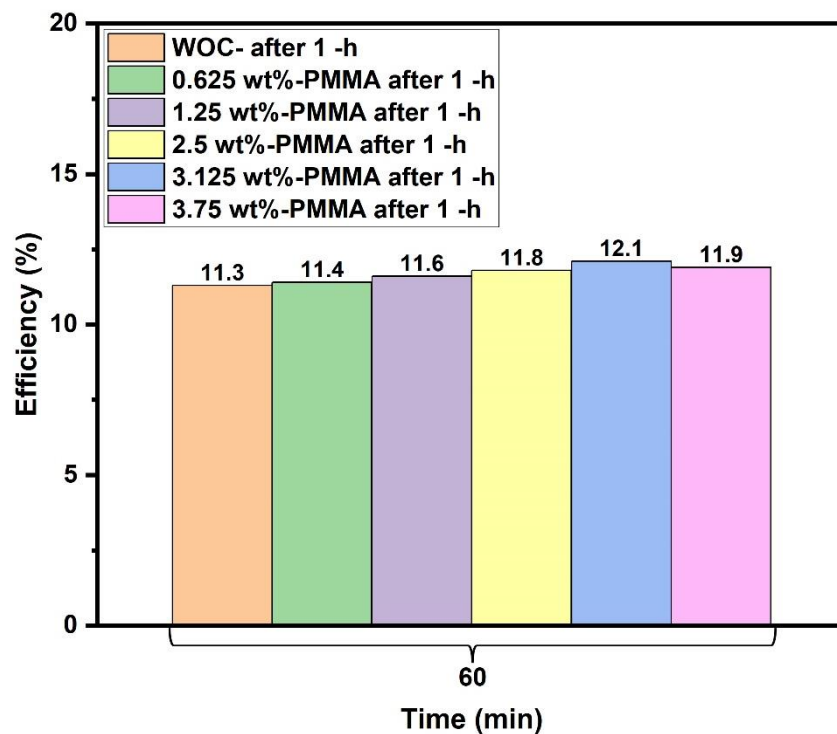
Figure 5.5. The efficiency of Polycrystalline solar cells with and without PMMA coating.
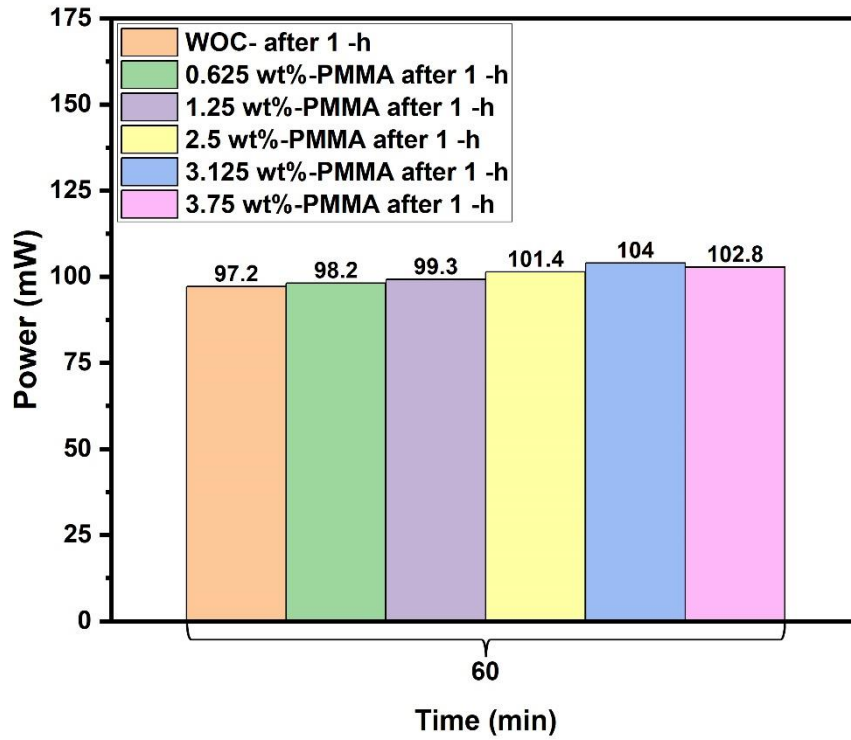
Figure 5.6. Power of Polycrystalline solar cell with and without PMMA coating.

Table 5.2. Electrical characteristics of Polycrystalline solar cells with and without PMMA concentrations coating.

PMMA concentrations	V_{oc} (V)	I_{sc} (mA)	P_{max} (mW)	Efficiency η (%)
WOC-after 1-h	0.380	330	97.2	11.3
0.625 wt%- after 1-h	0.385	328	98.1	11.4
1.25 wt%- after 1-h	0.392	325	99.3	11.6
2.5 wt%- after 1-h	0.399	321	101.4	11.8
3.125 wt%- after 1-h	0.415	311	104	12.1
3.75 wt%- after 1-h	0.406	315	102.8	11.9

5.3   Influence the ZnO/PMMA Nanocomposite on the Performance of Solar Cells

To assess the performance of the nanocomposite coating made from (ZnO/PMMA), zinc oxide (ZnO) has doped in polymethyl methacrylate (PMMA) with various concentrations and applied to the upper surface of the polycrystalline silicon cell, as well as to measure cell efficiency and surface temperature. The nanocomposite passed multiple tests measuring ultraviolet (UV) ray absorption and visible light reflection and transmission.

Four amounts (0.1 g, 0.2 g, 0.3 g, and 0.4 g) of ZnO that were used, and doping with 1.25 g of polymethyl methacrylate (PMMA) to prepare the nanocomposite coating concentrations (3.375wt%, 3.625wt%, 3.875wt%, and 4.125wt%).

5.3.1 Energy Bandgap Analysis of ZnO/PMMA Nanocomposite

The band gap (energy gap E_g) is the energy difference between the conduction and valence (P-region), commonly given in electron volts (eV). The band gap is particularly important in insulation materials and semiconductors, where even a small gap value controls several of the material body's electrical and optical characteristics[52]. Therefore, the bandgap energy of polymethyl methacrylate (PMMA) and ZnO/PMMA nanocomposite was measured using the Tauc plot relation through the absorbance data that was extracted when examining the UV-Visible absorbance. The results shown in Figure 5.7 showed that the examined PMMA polymer at a concentration of 3.125 wt% obtained a band gap of 4.55 eV, while the examined ZnO/PMMA nanocomposite concentrations

71

(3.375 wt%, 3.625 wt%, 3.875 wt%, and 4.125 wt%) recorded higher results (5.16 eV, 5.23 eV, 5.60 eV, and 5.50 eV) respectively.

Based on the above, the value of the energy bandgap is increased by increasing the concentration of the ZnO nano-material until it reaches the steady state point. Compared with the value of the band gap of silicon (Si), the main component of the polycrystalline solar cell, at 1.1 eV, it is low, as raising the band-gap value of the nanocomposite coating works to reduce the reflection light experienced by the silicon cell, so it works as an antireflective coating.
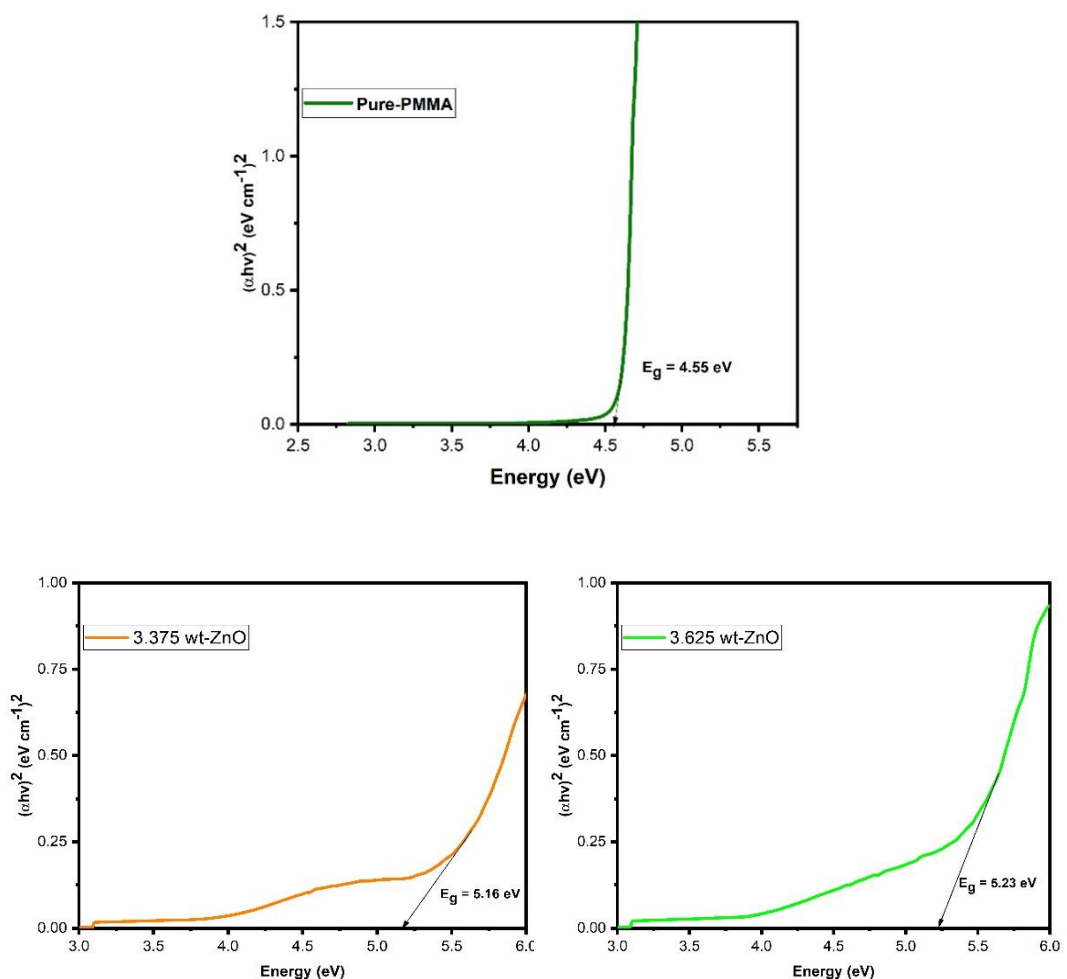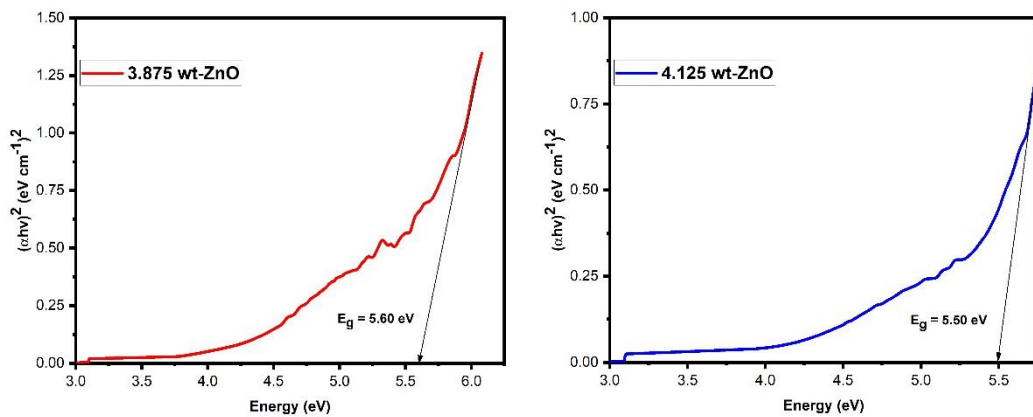
Figure 5.7. The energy band gap (E_g) of the ZnO/PMMA
nanocomposite, Tauc plot relation.

5.3.2 Influence of ZnO/PMMA Nanocomposite on Light Transmission and Reflection Losses

Many researchers have worked to reduce the light reflection that the polycrystalline solar cell suffers since silicon reflects about 35% of sunlight light, and what has been used most is to add a one thin or multiple layers on the front surface of the silicon cell from the nanocomposite as an anti-reflection coating. As mentioned in chapter two of the previous studies.

In this study, a nanomaterial ZnO with different concentrations was added to PMMA, which acts as a matrix for the stability of nanomaterials, where the transmittance of UV-Visible light was tested for the prepared samples of nanocomposite and compared with the reflection of the polycrystalline solar cell without coating by using the UV-Visible spectrometer, type (UV-1800) double beam device. Figure (5.9) shows the transmittance results (86.8%, 89.7%, 94.4%, and 91.3%) for visible light at 600 nm wavelength for the tested ZnO/PMMA concentrations (3.375wt%, 3.625wt%, 3.875wt%, and 4.125wt%) respectively,

73

compared, with the reflectance on the uncoated polycrystalline solar cell at 35%, with a visible light reflection ratio showed in figure (5.8) for the concentrations (13.2%, 10.3%, 5.6%, 8.7%) respectively, the best result was obtained for visible light transmission and reflection (5.6%) at 3.875 wt% of ZnO/PMMA concentrations. Depending on the above, the light reflection is reduced from 35% to 5.6% for the polycrystalline solar cell coated with ZnO/PMMA nanocomposite coating, 3.875 wt% concentration.

The measure that reduced the reflection is an anti-reflective coating that works differently. It typically consists of nanomaterial, such as in this study used 40-50 nm of ZnO deposited on PMMA, and this zinc oxide is optimized in terms of its refractive index, so if a photon traveling through the sky and goes through the air with a reflective index of one ($A_{air} = 1$) and wants to enter the silicon that has a reflective index of approximately four, depending on the wavelength, so for most of the wavelength ($A_{silicon} = 3.8$), if we put a material with an intermediate reflective index between the air and silicon, the light is bends into the material instead of being reflected away, the more abrupt change is in the refractive index, the higher reflection it will have. In this work coating has been put with an intermediate refractive index to minimize reflection. This effect is wavelength-dependent.
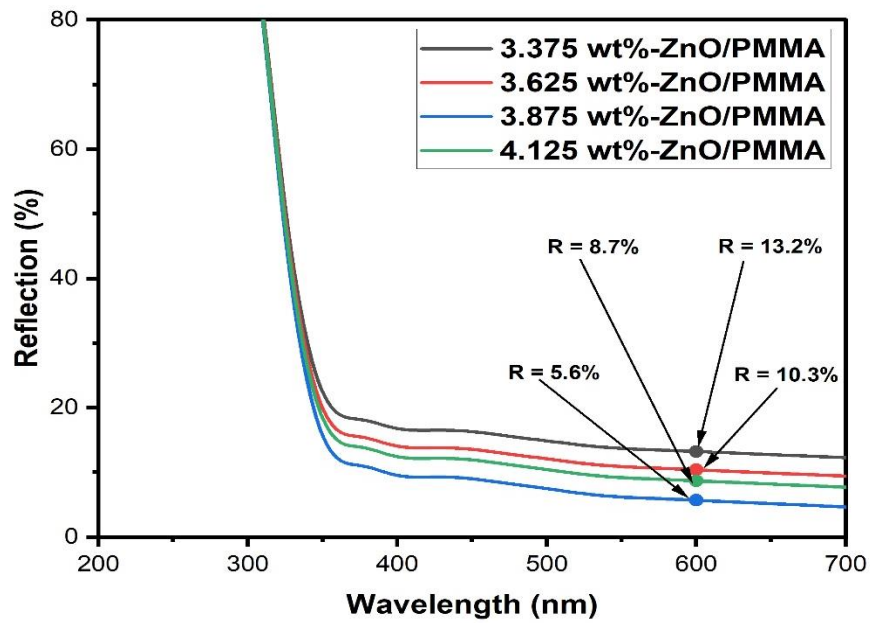
Figure 5.8. Comparison of the reflection for ZnO/PMMA coating concentrations (3.375 wt%, 3.625 wt%, 3.875 wt%, and 4.125 wt%).
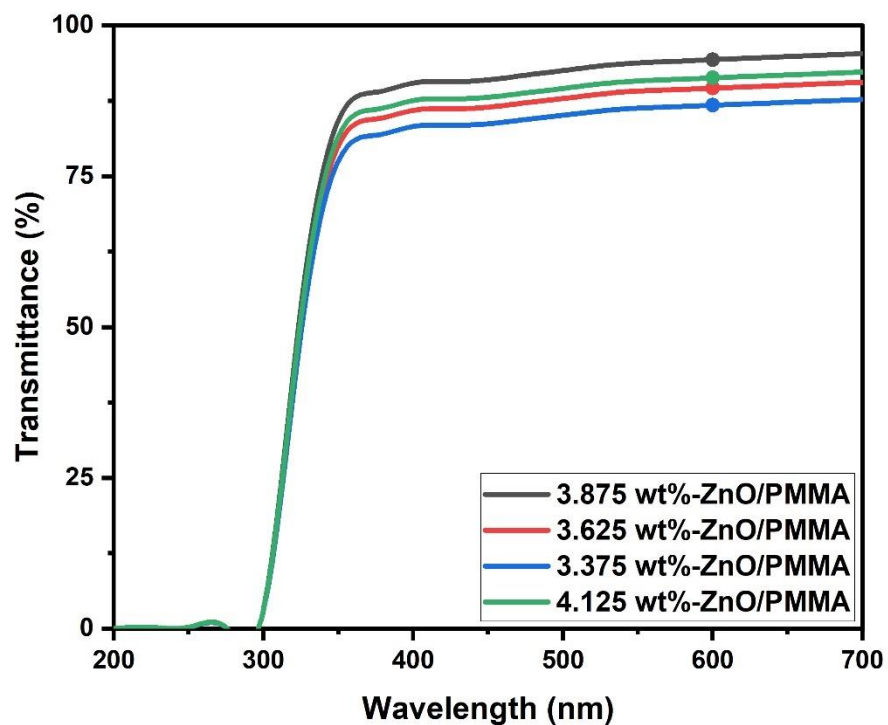
Figure 5.9. Comparison of the transmission for ZnO/PMMA coating concentrations (3.375 wt%, 3.625 wt%, 3.875 wt%, and 4.125 wt%).

Table 5.3. The light transmittance & reflection loss values with the
ZnO/PMMA nanocomposite concentrations.

ZnO/PMMA nanocomposite concentrations (wt%)	Light Transmittance (%)	Reflection losses (%)
Without coating (WOC)	65	35
3.375 wt%	86.8	13.2
3.625 wt%	89.7	10.3
3.875 wt%	94.4	5.6
4.125 wt%	91.3	8.7

5.3.3 Influence the ZnO/PMMA Nanocomposite on Ultraviolet Absorbance

The best concentration of 3.125 wt% of polymethyl methacrylate (PMMA) polymer was chosen as the UV absorber with the highest absorption intensity (3.7 AU) among the other concentrations. To make four samples of the ZnO/PMMA nanocomposite coating, different concentrations of Zinc Oxide (ZnO) nanomaterial (40–50 nm) were used (3.375 wt%, 3.625 wt%, 3.875 wt%, and 4.125 wt%). An absorbance test UV-Vis was conducted to find out the effect of adding the ZnO nanomaterial to the PMMA polymer on the absorption of UV rays. The examination was carried out by the UV-visible spectrophotometer device (Mega-2100) at the University of Kufa, Science College. The results show that the absorbance intensities (1.9 AU, 2.2 AU, 2.7 AU, and 2.4 AU) for the investigated concentrations (3.375 wt%, 3.625 wt%, 3.875 wt%, and 4.125 wt%), respectively, indicating that the nanomaterial increased the absorption area within the UV wavelength range (200-400) nm, with the higher concentration of the nanomaterial, the greater the ultraviolet ray absorption area, as shown in figure 5.10.
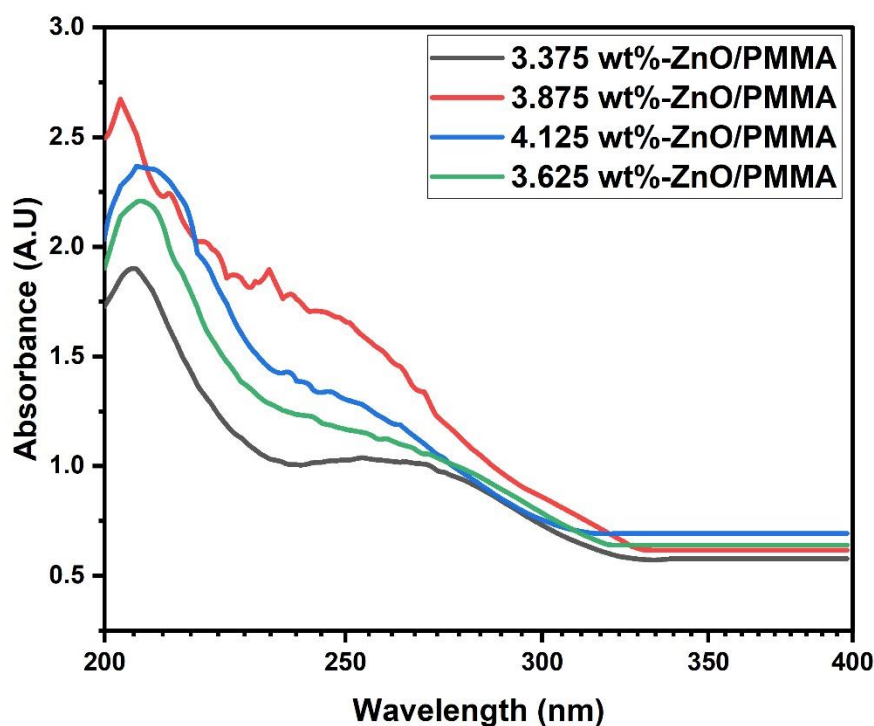
Figure 5.10. Comparison of the Absorption for ZnO/PMMA coating
concentrations used (3.375 wt%, 3.625 wt%, 3.875 wt%, and 4.125 wt%)

Table 5.4. The Absorption values with the ZnO/PMMA nanocomposite
concentrations

ZnO/PMMA nanocomposite concentrations (gram)	Absorbance (AU)	Peak Absorption point (nm)
Without coating (WOC)	Full-transmittance	-
3.375 wt%	1.9	205
3.625 wt%	2.2	208
3.875 wt%	2.7	203
4.125 wt%	2.4	210

5.3.4 Influence the ZnO/PMMA Nanocomposite on the Surface Temperature of Solar Cells

One of the objectives of this work is to reduce the surface temperature of polycrystalline silicon solar cells by applying ZnO/PMMA nanocomposite coatings with different concentrations on the top surface of commercial polycrystalline silicon solar cells, to increase their efficiency. Thermocouples (K-type) were used to measure the temperature of the solar cells by fixing them on back surface of PV solar cells, and the thermocouples were connected to thermometer device (UT-320D) to display temperature results. The test was done in the laboratory by exposing solar cells to solar radiation using halogen light with STC (1000 W/m^2 and 25 °C) and the test duration was one hour after the temperature reaches a steady state.

The experiment was carried out for four polycrystalline silicon solar cells coated with four different concentrations of ZnO/PMMA nanocomposite (3.375 wt%, 3.625 wt%, 3.875 wt%, and 4.125 wt%) and compared to the uncoated polycrystalline cell.

The results showed that the temperature of solar cells at the end of the test time, after 1 hour, was (75.4 °C, 74.3 °C, 72.9 °C, and 73.7 °C) for the concentrations used respectively, while the uncoated solar cell recorded (81.5 °C), where the decrease in temperature for each concentration was (6.1 °C, 7.2 °C, 8.6 °C, and 7.8 °C) compared to the uncoated solar cell, respectively, as shown in the figure (5.11) and the table (5.5), from the results, concluded that the solar cell surface temperature decreases as the concentration of nanomaterials in the nanocomposite coating increases, which leads to increases the amount of UV photons absorption in the wavelength range (200-400)nm, that is one

of the causes of the temperature rising of solar cells as shown in the first part of this theses, and thus its effect on the efficiency of solar cells increases. The highest decrease in temperature was recorded (8.6 °C) when using a concentration (3.875 wt%) of ZnO/PMMA nanocomposite coating.
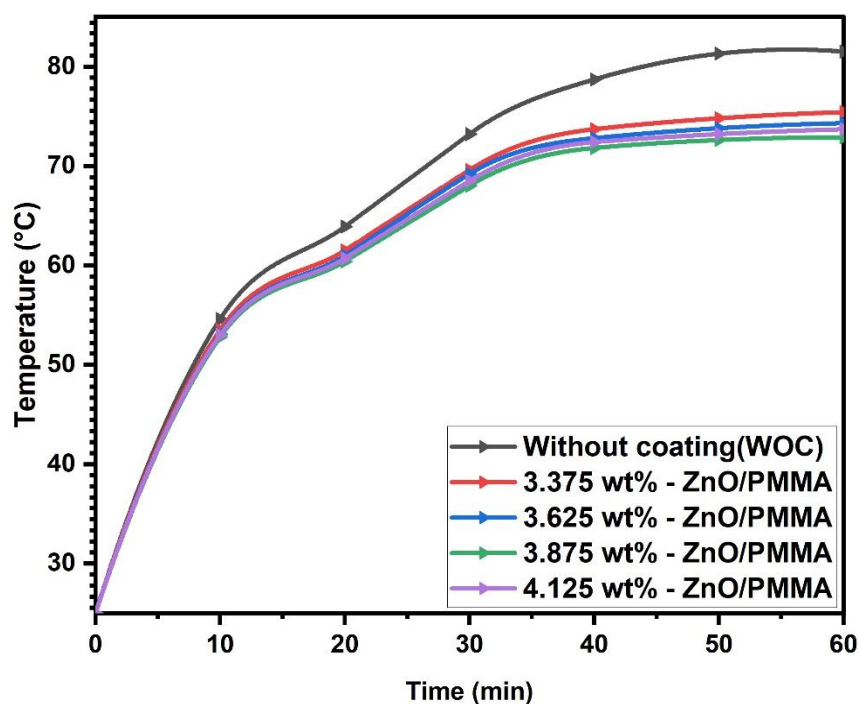
Figure 5.11. Comparison of surface temperatures of coated and uncoated polycrystalline solar cells at (3.375 wt%, 3.625 wt%, 3.875 wt%, and 4.125 wt%) concentration.

Table 5.5. The temperature variance of solar cells with the ZnO/PMMA nanocomposite concentrations.

ZnO/PMMA nanocomposite concentrations	Temperature variance values
Without coating (WOC)	-
3.375 wt%	6.1 °C
3.625 wt%	7.2 °C
3.875 wt%	8.6 °C
4.125 wt%	7.8 °C

To validate the findings, a Thermal Imaging Infrared Camera FLIR E-30bx type was used in the current experiment to monitor the temperature of the coated and uncoated polycrystalline solar cells to verify the temperature readings obtained by the thermometer device. Figure (5.12) illustrates that the results closely resemble those of thermocouples extremely closely.
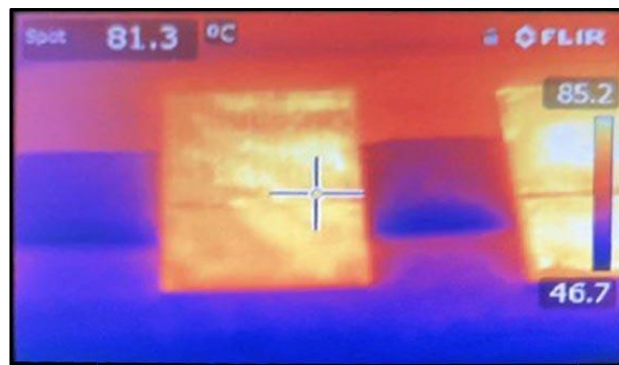
Without coating- after 1-h
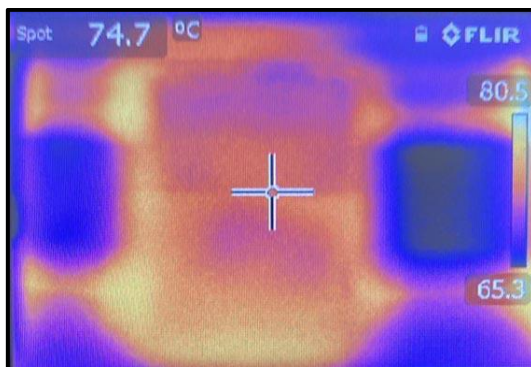
| 3.375 wt% concentration of ZnO/PMMA- after 1-h | 3.625 wt% concentration of ZnO/PMMA- after 1-h |

| 3.875 wt% concentration of ZnO/PMMA- after 1-h | 4.125 wt% concentration of ZnO/PMMA- after 1-h |
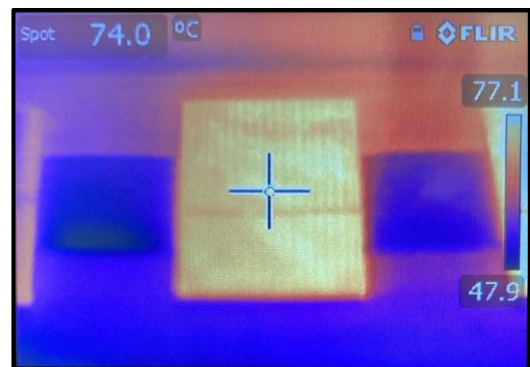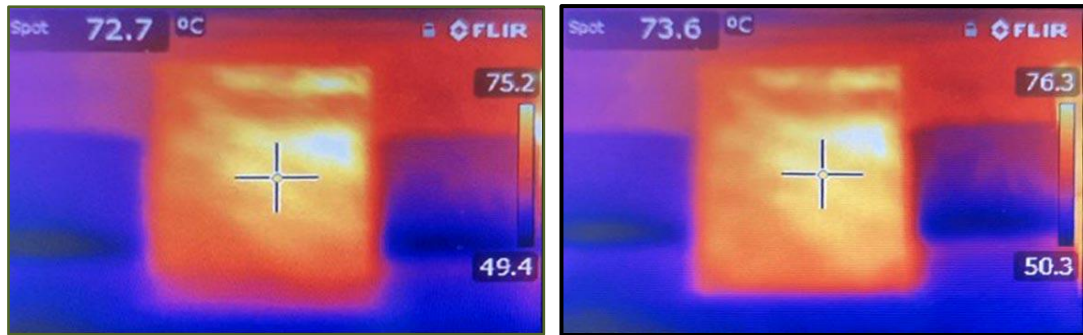
Figure 5.12. Thermal imaging of coated and uncoated polycrystalline solar cells at (3.375 wt%, 3.625 wt%, 3.875 wt%, and 4.125 wt%).

5.3.5 Influence the ZnO/PMMA nanocomposite coating on the Solar Cell Electrical Properties and Efficiency

To test the electrical properties, current-voltage (I-V curve), power voltage (P-V) curve, and efficiency of coated polycrystalline solar cells with different concentrations of ZnO/PMMA nanocomposite thin film coating (3.375 wt%, 3.625 wt%, 3.875 wt%, and 4.125 wt%) were used and compare them to the uncoated polycrystalline solar cell using the Solar Module analyzer (PROVA-200) device. The tests were performed indoors under halogen light with standard test conditions (STC) (1000 W/m^2 of solar radiation and a temperature of 25 °C), the test was conducted in two stages; the first at the start of the test; and the second after one hour of halogen light exposure, where the effect of increasing temperature on the solar cell's efficiency was estimated. Therefore, the parameters of solar cells, short circuit current (Isc), open-circuit voltage (Voc), maximum power output (P$_{max}$), and efficiency (η), refer to the investigation of the performance of polycrystalline solar cells and show the effect of various concentrations of ZnO/PMMA coating and selecting the best result.

5.3.5.1 Impact of ZnO/PMMA Nanocomposite Coating on (I-V) and (P-V) Curves

The optimal increase in the electrical characteristics of the solar cell was attained at zero time, where the reflection losses are carried out. The results show the short circuit current (I_{sc}), open-circuit voltage (V_{oc}), maximum power current (I_{mp}), and maximum power voltage ($V_{mp)}$ for polycrystalline solar cells with the concentrations of ZnO/PMMA nanocomposite coating (3.375 wt%, 3.625 wt%, 3.875 wt%, and 4.125 wt%), and compared to the polycrystalline solar cell without coating.

According to presented data in table (5.6), the maximum effect of antireflection coating when used at the (3.875 wt%) concentration reduces reflection from 35% for polycrystalline solar cells without coating to only 5.6%. After one hour, the second test was performed where the temperature effects were carried out (increased surface temperature of the tested solar cells). The electrical performance results of polycrystalline solar cells with the concentrations of ZnO/PMMA nanocomposite coating (3.375 wt%, 3.625 wt%, 3.875 wt%, and 4.125 wt%), and compared to the polycrystalline solar cell without coating. According to the data presented in the table (5.6), the maximum effect of the antireflection coating when used the 3.875 wt% concentration, reduces the surface temperature from 81.5 °C for polycrystalline solar cells without coating to 72.9 °C, which leads to the maximum current and voltage ($I_{mp} = 0.317$ A, $V_{mp} = 0.412$ V).

Figures (5.13 and 5.14), show the I-V and P-V curves, while Table (5.6) shows the results of studies for all polycrystalline solar cells with various nanocomposite coatings and without coating.

Figure 5.13. Comparison of I-V curves for polycrystalline solar cells with and without coating for all concentrations.

Figure 5.14. Comparison of P-V curves for polycrystalline solar cells with and without coating for all concentrations.

5.3.5.2 The Impact of ZnO/PMMA Nanocomposite Coating on The Power and Efficiency of The Polycrystalline Solar Cell.

To study the effect of ZnO/PMMA nano-coating on the power and efficiency, the coated polycrystalline solar cells were tested as mentioned previously to find the I-V curve, where the power and efficiency were measured and calculated for each of the solar cells coated with different concentrations of the ZnO/PMMA (3.375 wt%, 3.625 wt%, 3.875 wt%, and 4.125 wt%) and compared with the uncoated cells to see the amplitude of the effect of adding nano-coating to the top surface of the polycrystalline solar cells. The results showed the power and efficiency at the beginning of the test (at zero time) at the end of the test after one hour for each of ZnO/PMMA concentration (3.375 wt%, 3.625 wt%, 3.875 wt%, and 4.125 wt%), are precented in the table (5.6) while the power and efficiency of the polycrystalline solar cells without coating are precented in the table (5.6).

The effect of reducing the reflection by ZnO/PMMA nano-coating has increased the power and efficiency of the solar cell at the zero time of the test and according to the ZnO/PMMA concentration value of the coating used, and after one hour according to the additional nano-coating, the impact of raising the surface temperature of the solar cell and the action of the nano-coating on decreasing the cell temperature was obvious in enhancing the power and efficiency of the solar cell.

From the results shown in the table (5.6), it was found that the best concentration that was used was (3.875 wt%) as the power and efficiency increased from (140 mW, 16.32%) for the uncoated cell to (161 mW, 18.78%) at the beginning of the test (at zero time), and from (97.2 mW, 11.33%) for the uncoated cell to (131 mW, 15.22%) after one hour at the end of the test, and the amount of the increased power and efficiency was

(+33.8 mW) and (+3.8%) at the end of the test. This increase came as a result of reducing the visible light reflection from (35%) for the uncoated polycrystalline solar cell to (5.6%) for the solar cell coated with nano-coating at a concentration of (3.875 wt%), as well as reducing the surface temperature of the cell from (81.5 C) to (72.9 C).

Figures (5.15 and 5.16) show the power and efficiency graphs, while Table (5.6) shows the results of studies for all polycrystalline solar cells with various nanocomposite coatings and without coatings.

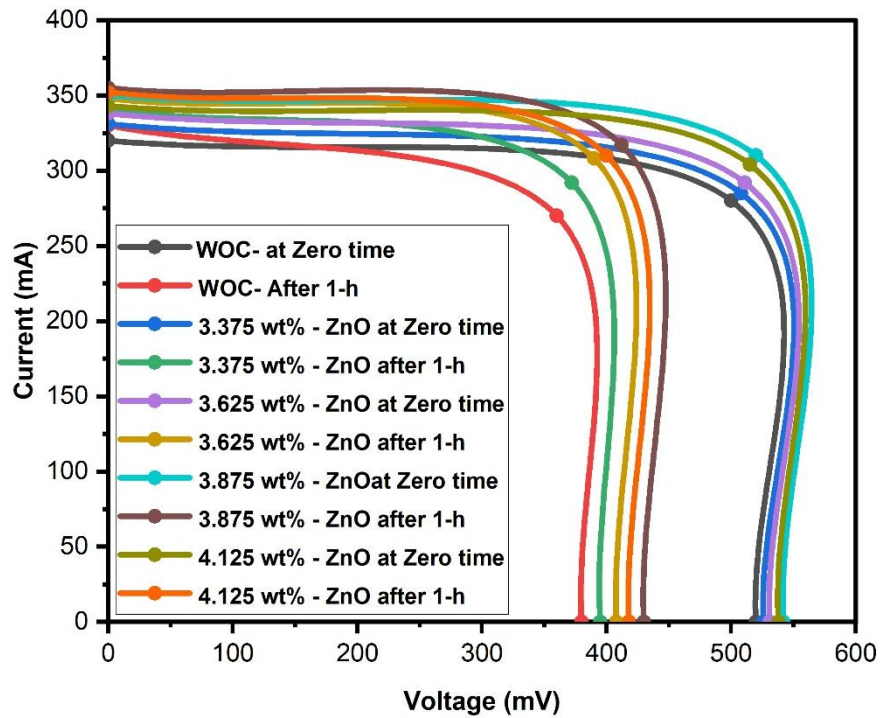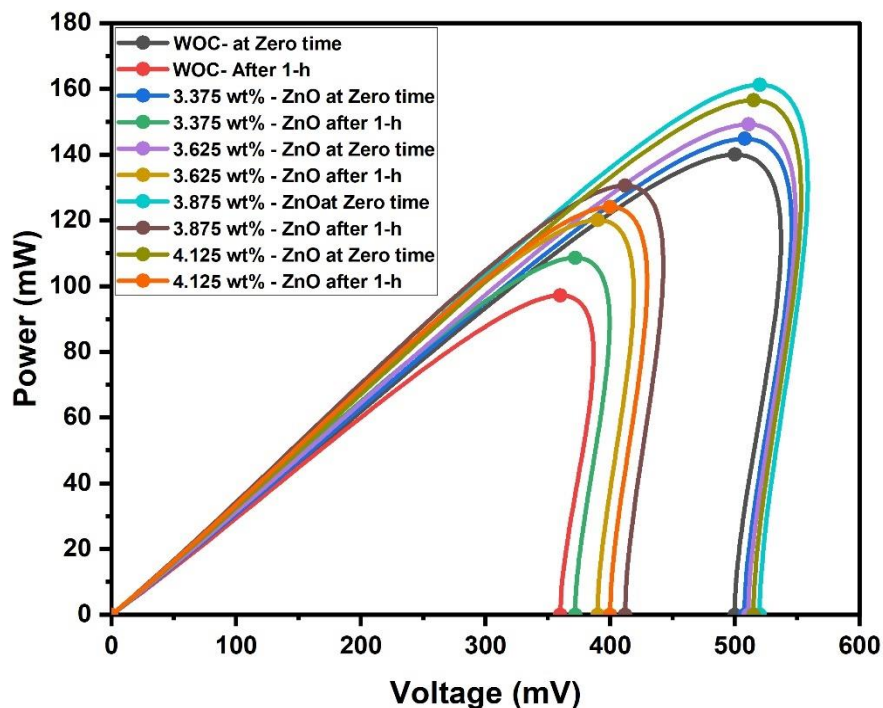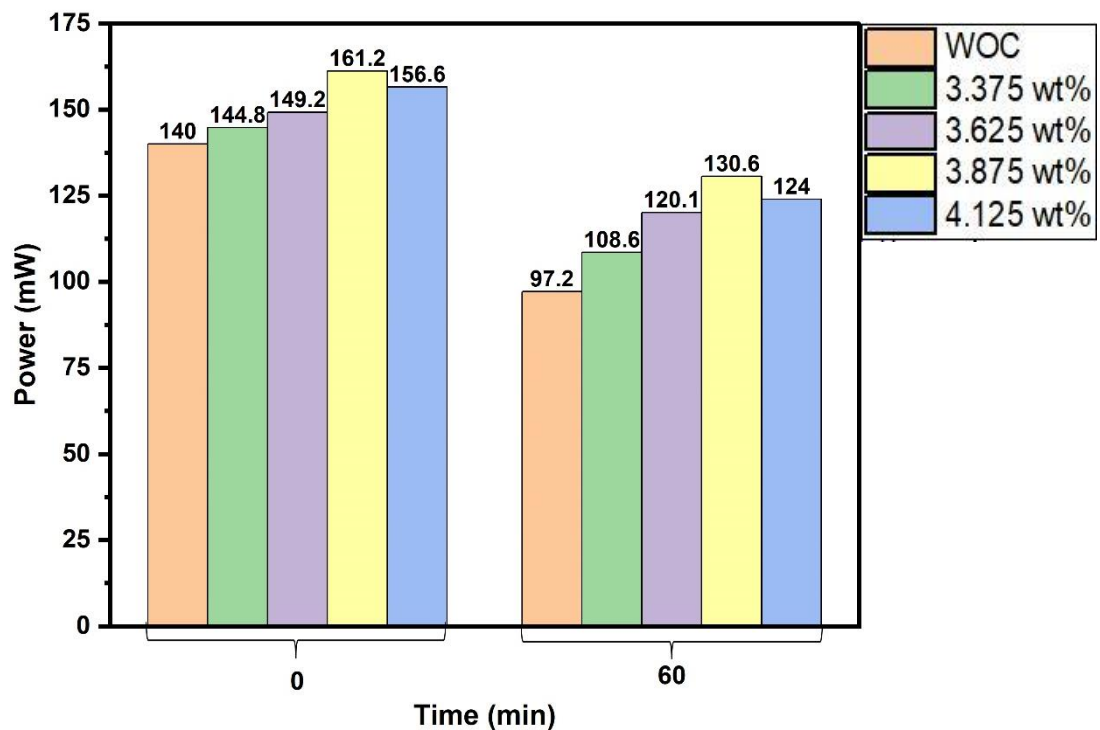Figure 5.15. Comparison of the power of polycrystalline solar cells with and without coating for all concentrations.

85
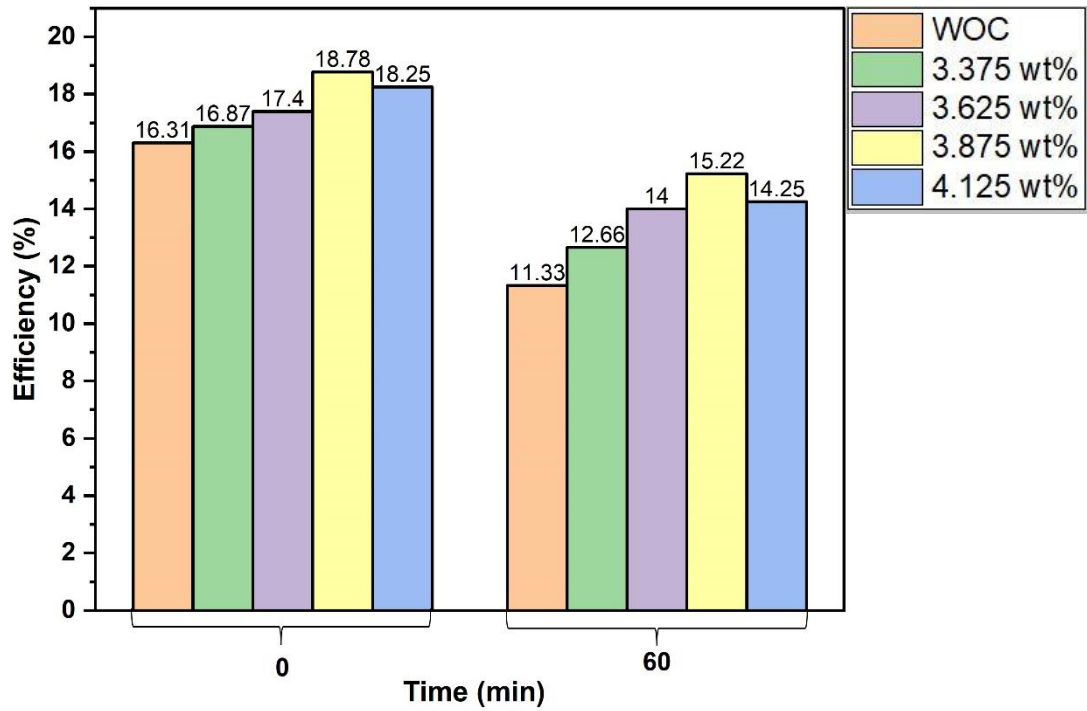
Figure 5.16. Comparison of the efficiency of polycrystalline solar cells with and without coating for all concentrations.

Table 5.6. Electrical properties and efficiency of polycrystalline silicon solar cells coated with different concentrations of ZnO/PMMA nanocomposite coating and without coating.

	Polycrystalline silicon solar cell without coating (WOC)		Polycrystalline silicon solar cell – Coated with 3.375 wt%-ZnO/PMMA		Polycrystalline silicon solar cell – Coated with 3.625 wt%-ZnO/PMMA		Polycrystalline silicon solar cell – Coated with 3.875 wt%-ZnO/PMMA		Polycrystalline silicon solar cell – Coated with 4.125 wt%-ZnO/PMMA	
Time test	Zero-time	After 1-h	Zero-time	After 1-h	Zero-time	After 1-h	Zero-time	After 1-h	Zero-time	After 1-h
Open-circuit voltage V_{OC} (V)	0.52	0.38	0.526	0.395	0.531	0.408	0.542	0.430	0.538	0.418
Short-circuit current I_{SC} (A)	0.32	0.33	0.331	0.341	0.338	0.348	0.350	0.355	0.343	0.352
Maximum power voltage V_{mp}(V)	0.5	0.36	0.508	0.372	0.511	0.390	0.520	0.412	0.515	0.40
Maximum power current I_{mp} (A)	0.28	0.27	0.285	0.292	0.292	0.308	0.310	0.317	0.304	0.31
Maximum power P_{max} (W)	0.140	0.097	0.145	0.108	0.149	0.120	0.161	0.130	0.156	0.124
Electrical efficiency (η)%	16.32	11.33	16.87	12.66	17.39	14	18.78	15.22	18.25	14.45

5.4 Test of Solar Cells Under Hot Weather Conditions

The solar cell was tested in hot weather to identify the effectiveness of the ZnO/PMMA nanocomposite coating in hot weather conditions. The coated polycrystalline solar cells with the best concentration obtained of 3.875 wt% of ZnO/PMMA with uncoated cells were placed in a special frame and an outer glass layer was added to simulate the commercial solar panels to compare the performance of the coated and uncoated cells in hot weather conditions. The electrical properties of each solar cell were tested individually under weather conditions (685 W/m^2 of solar radiation and ambient temperature of 44.8 °C). See figure (5.17).
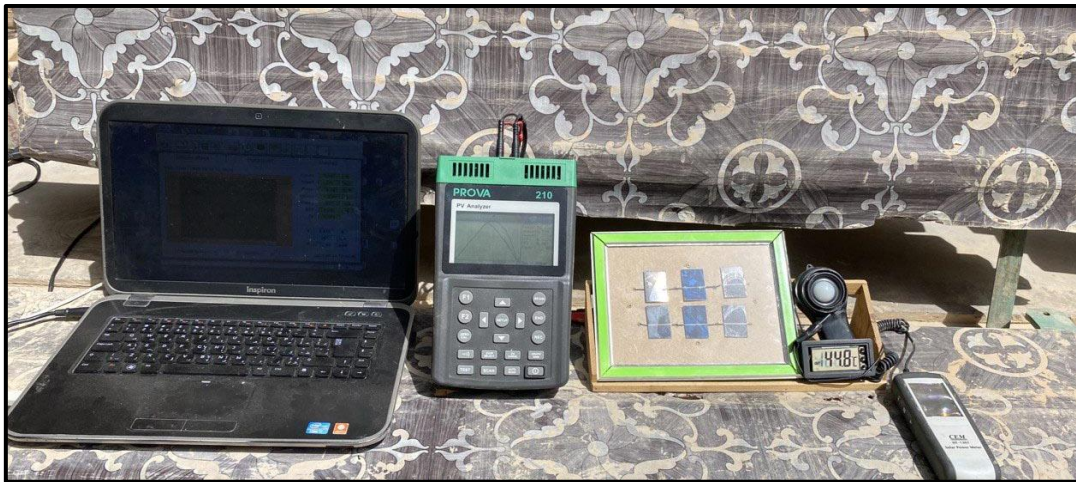
Figure 5.17. Testing of solar cells in hot weather conditions.

The electrical performance results of polycrystalline solar cells, figures 5.18 and 5.19, were (Isc=0.292A, Voc=0.441V, Imp=0.264A, and Vmp=0.403V) for the 3.875 wt% concentrations of ZnO/PMMA nanocomposite coating, and compared to the polycrystalline solar cell without coating that had (Isc=0.279A, Voc=0.412V, Imp=0.228A, and Vmp=0.381V). According to the data presented above, the effect of reducing the reflection and temperature by ZnO/PMMA nano-coating has increased the power and efficiency of the solar cell from (86.8 mW,

10.1%) to (106 mW, 12.4%), respectively. The amounts of the increased power and efficiency were (+19.2 mW) and (+2.3%).

The above reading was for the maximum efficiency achieved during the test that was conducted in Al-Najaf City-Iraq (32° 1' N / 44° 19' E) on 14th August at three different times as per the below table (5.7) that shows the electrical properties of PV solar cells coated and without coating.

Table 5.7. The Electrical properties of PV solar cells at three different times.

Time (AM)	I (W/m²)	Temp. (ºC)	PV solar cell	I_{SC} (A)	V_{OC} (V)	P_{max} (mW)	Efficiency (%)
09:00	664	40.3	Without coating	0.265	0.404	77.07	8.98
			With coating	0.280	0.411	85.27	9.93
10:00	673	41.7	Without coating	0.271	0.409	80.72	9.4
			With coating	0.284	0.425	94.38	11.0
11:00	685	44.8	Without coating	0.279	0.412	86.80	10.1
			With coating	0.292	0.441	106.0	12.4
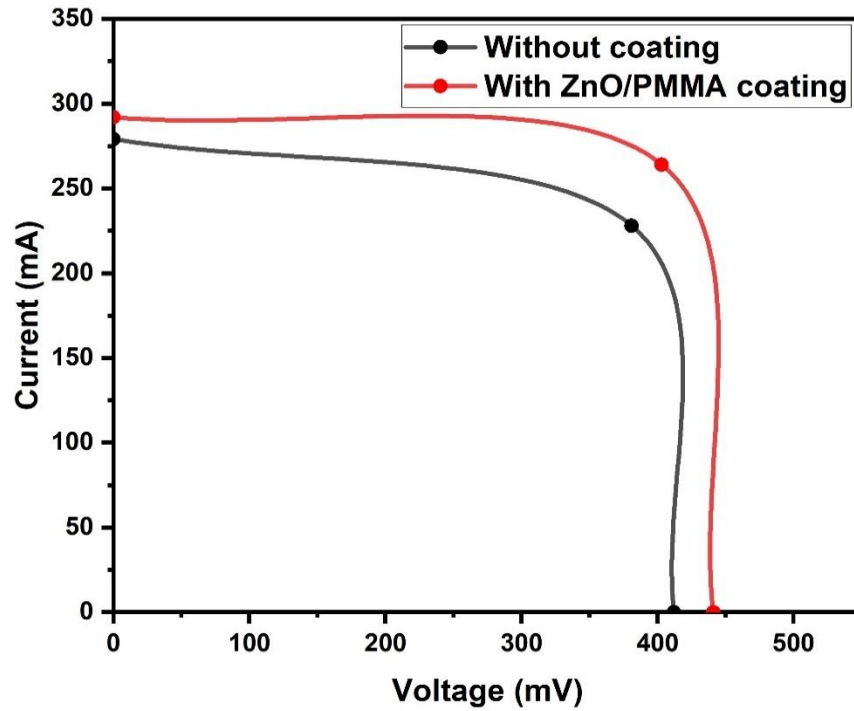
Figure 5.18. I-V Curves for polycrystalline solar cells with and without coating.
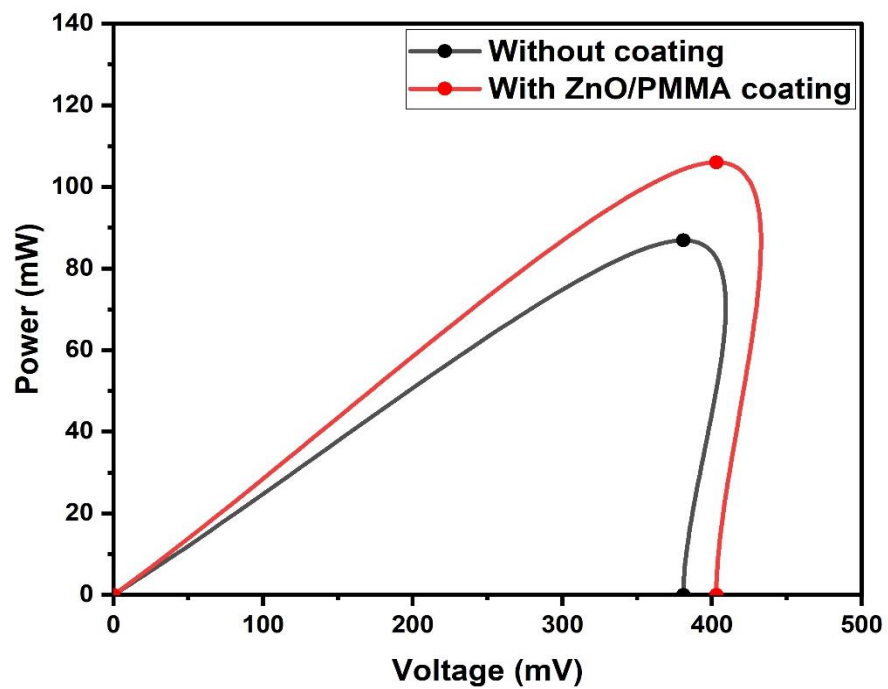
Figure 5.19. P-V Curves for polycrystalline solar cells with and without

coating.

5.5   Results Comparison

To confirm the behaviors, validity, and correctness of the data produced throughout the study's experimental portion, as indicated in the following sentences, the results acquired during this investigation were compared to those obtained by other studies.

5.5.1   Comparison of the UV-Vis Absorbance Results of Polymethyl Methacrylate (PMMA).

The results obtained from the UV-Visible test of the polymethyl methacrylate (PMMA) polymer used were compared to verify their validity, as the comparison was made with JM. I. Mohammed et al.[53], figure 5.20, within the same ultraviolet region wavelength of (200-400) and using the same polymer, where the results of the comparison showed a close match with more than 93%, which was the highest absorption (3.55 AU) at the wavelength (223 nm) for the comparative study[53], and the highest absorption (3.76 AU) at the wavelength (227 nm) for our experimental.
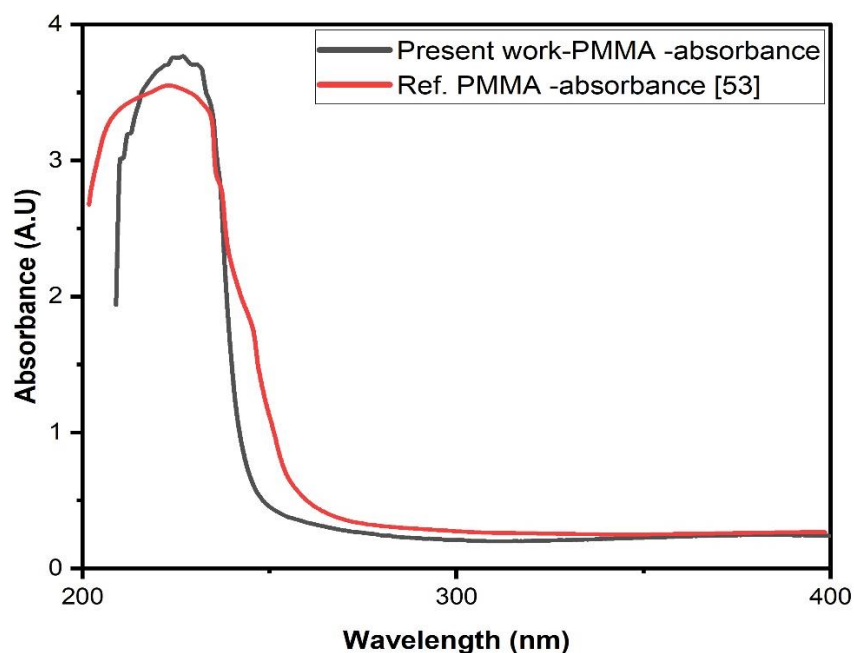
Figure 5.20. Comparison of the Absorbance Results of Polymethyl methacrylate (PMMA), present work, and JM. I. Mohammed et al. [53]

91

5.5.2   Comparison of the UV-Vis Absorbance Results of
   ZnO/PMMA Nanocomposite Coating

The UV-Visible results of the tests of the nanocomposite coating (ZnO/PMMA) used were validated to confirm their legality, as the comparison was made with J. Bagawade [54], in the same ultraviolet region wavelength of (200-400) and using the same nanomaterial coating, where the results showed a close match with about 98%. That was the greatest absorption (1.5 AU) at the wavelength (200 nm) for the comparative study [54]. The maximum absorption (1.86 AU) at the wavelength (205 nm) for the present experimental is shown below in figure 5.21, which shows the comparison between the reference and present work.
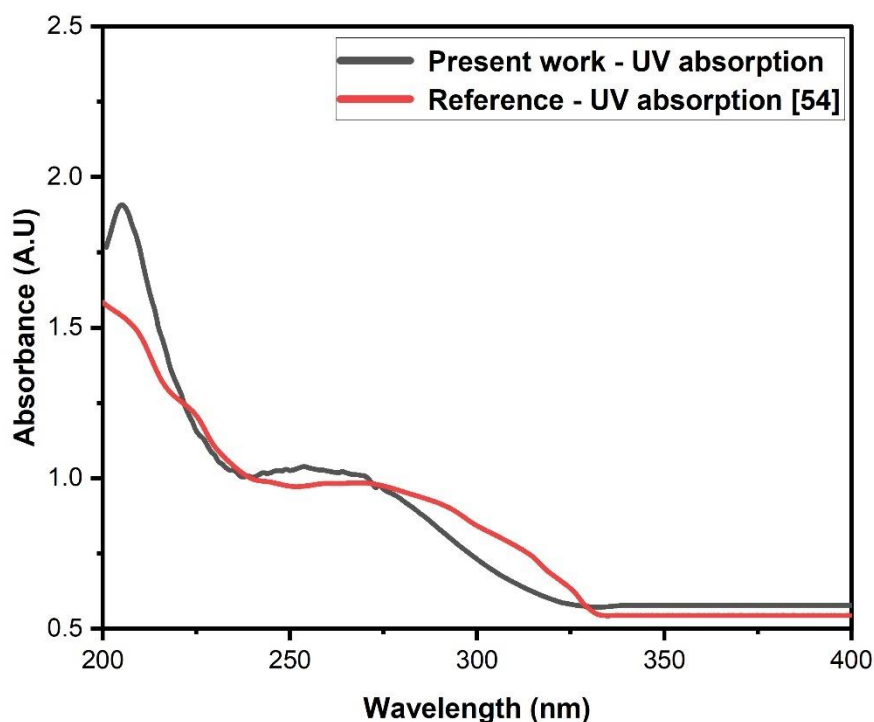
Figure 5.21. Comparison of the absorbance results of ZnO/PMMA nanocomposite coating, present work, and J. Bagawade [54].

5.5.3 Comparison of The Reflection and Transmittance Results of ZnO/PMMA Nanocomposite Coating

A comparison of the current study with the studies of some of the other authors must be carried out to ascertain the accuracy of the study. In terms of the reflectivity and transmission of visible light, the results of this study were compared to those of the researcher JM. I. Mohammed et al.[53]. In Ref. [53], the reflection was reduced from 35% to 7.3%, whereas in the current study, the reflection was reduced from 35% to 5.6%. Both the current study and the authors' studies use identical test settings. The test was carried out with a similar nano-material coating, zinc oxide. When comparing the two experiments in figure 5.22, the greatest inaccuracy has been estimated to be 1.7%.
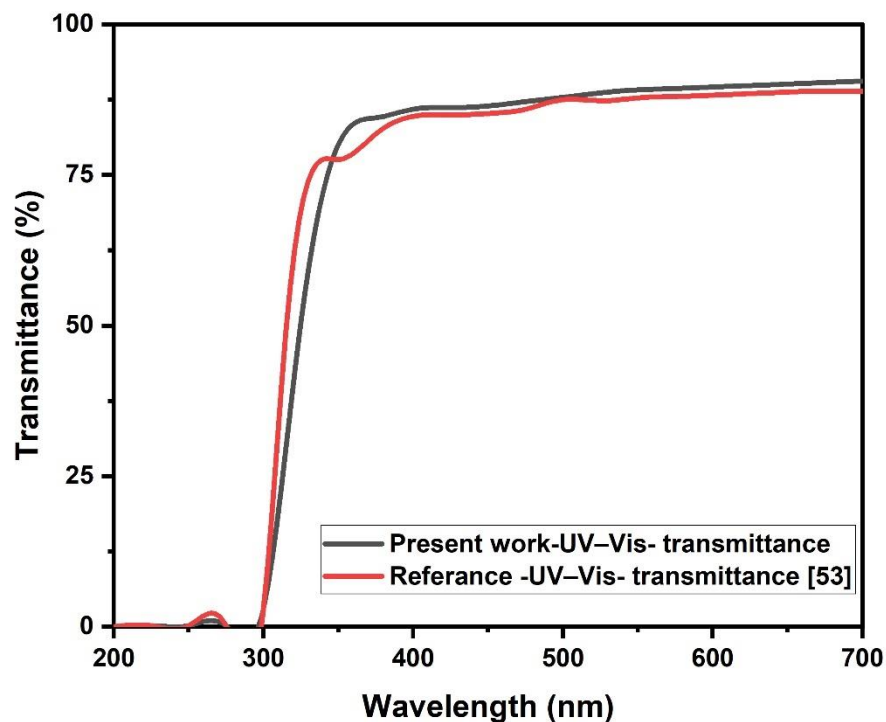
Figure 5.22. Comparison of the Transmittance Results of ZnO/PMMA nanocomposite coating, present work and JM. I. Mohammed et al.[53].

5.5.4 A Comprehensive Comparison of The Results Obtained with Previous Studies

To verify the validity and effectiveness of the current study, the results were compared with the latest studies that included the use of the same nanomaterials as nano-coating, to reduce reflection and reduce the temperature of the cell surface. As mentioned in the second chapter of previous studies in which most of the studies in this field were summarized, as per comparing it with the researcher H. Dhasmana et al.[25] who used ZnO as a nanomaterial, it was found that it could reduce the reflection of the silicon surface from 25 to 2.5% by using four layers of coating, while the researcher A. Jalali et al.[24] also using ZnO, the efficiency was increased from 5.29% to 9.19% and compared to the present experimental work, it was able to reduce the reflectance from 35% to 5.6% by using one layer of PMMA/ZnO coating, thus increasing its efficiency by (+3.8%). and as per the researcher A. Naser et. al.[35], used Titanium Dioxide/Polyvinyl Alcohol (TiO_2/PVA) as a nano-coating on the surface of the silicon cell, where it increased the efficiency by (+2.3%).

While the researchers Farah K. Mohd Zaini et al. [33], conducted an experimental study was conducted to apply a nanocomposite coating on the top surface of a photovoltaic (PV) solar cell to improve temperature-lowering and performance. The coating sample prepared from Methyltrimethoxysilane and 3-Amino Propyltriethoxysilane (MTMS/APTES) solution and TiO_2 nanoparticles scored the best temperature reduction, approximately 8.93 ℃ compared to without coating.

Comparing these results with the results obtained by using PMMA/ZnO in the present work, it is believed that the polycrystalline solar cell surface temperature was reduced by 8.6 °C, which represents a

good result and indicates promising results that can be used in the development of polycrystalline solar cells.

5.6 Feasibility and Cost-benefit Analysis

To determine the scope of a project's benefits and the definite returns it may provide relative to project costs, it is significant to perform an economic feasibility study.

This section of the chapter will show a feasibility study for creating a ZnO/PMMA nano-coating and applying it to the top surface of a commercial silicon solar cell to increase the solar cell's power to generate electricity. As a consequence of this study's findings, it was determined that the optimal ZnO/PMMA coating concentration is 3.875 wt%. Refer to table 5.8 below for the cost estimation for this coating.

Table 5.8. The material price of ZnO/PMMA nano-coating.

Type of material	Unite required	Price (USD)
Polymethyl methacrylate (PMMA) polymer	1.25 gram	0.0035 $
Zinc oxide (ZnO), nanoparticle 40-50 nm	0.3 gram	0.0705 $
Acetone solvent pure (99.5%)	80 ml	1.12 $
Nanocomposite coating	**Quantity (ml)**	**Total price (USD)**
ZnO/PMMA	100 ml	1.194 $

The amount required to cover the commercial solar cell (39×22) mm utilized in the experiment with one layer of ZnO/PMMA is 0.5 ml. As a result, efficiency is increased by +3.8%. And for one solar cell, the power generated by the coating effect is (+33.4 mW), see below table 5.9 for total power added by using ZnO/PMMA nanocomposite coating.

Table 5.9. The amount and cost of coating required for solar cells.

Number of solar cells	Quantity (ml)	Total coating price (USD)	Total power added
1-solar cell	0.5 ml	0.00597 $	0.0334 W
100-solar cells	50 ml	0.597 $	3.34 W
1000-solar cells	500 ml	5.97 $	33.4 W
1500-solar cells	750 ml	8.955 $	50.1 W

Since one commercial solar cell has an area of 858×10^{-6} m. From table 5.9, a solar panel with 1500 commercial solar cells will have a surface area of 1.287 m^2. It requires (750 ml) of ZnO/PMMA coating with a price of (8.955$) to fully coat all of the panels and the impact of the coating on the produced power is 50.1 W.

Depending on the average global electricity price [55]. The price of 1 kWh is 0.140 $ and 0.133 $ for household and business users, respectively.

Chapter Six

Conclusion & Recommendations

Conclusion and Recommendations

6.1 Introduction

A polymethyl methacrylate (PMMA) polymer was mixed with a (40-50) nm zinc oxide (ZnO) nanomaterial to produce a ZnO/PMMA nano-coating that passed several laboratory tests. It was used to coat the top surface of a commercial polycrystalline silicon solar cell (39×22), to investigate its efficacy in increasing solar cell efficiency by reducing reflection and lowering solar cell temperature.

6.2 Conclusion

1. As compared to an uncoated solar cell, the temperature of the solar cell decreased by 7.1 C when coated with PMMA polymeric coating and 8.6 C when coated with ZnO/PMMA nanocomposite coating. These are the best outcomes based on the concentrations utilized.

2. The PMMA polymeric coating absorbs ultraviolet rays and thus blocks UV rays from the solar cell, as it acts as a UV mask. The results that were achieved by using the PMMA are (2.1 AU, 2.3 AU, 3.2 AU, 3.7 AU, and 3.5 AU) by using concentrations (0.625 wt%, 1.25 wt%, 2.5 wt%, 3.125 wt%, and 3.75 wt%), respectively.

3. The ZnO/PMMA nanocomposite coating was used with different concentrations of 3.375 wt.%, 3.625 wt.%, 3.875 wt.%, and 4.125 wt.% which led to lower reflectance from 35% for the solar cell without coating to (13.2%, 10.3%, 5.6%, and 8.7%), respectively, for coated solar cells.

4. The ZnO/PMMA nano-coating was prepared to reduce the reflection by increasing the band gap of the light-facing surface of the solar cell, where the results showed an increase in the band gap from (1.1 eV) for the uncoated solar cell to (5.16 eV, 5.23 eV, 5.60 eV, and 5.50

eV) for the coated solar cell by concentrations of (3.375 wt%, 3.625 wt%, 3.875 wt%, and 4.125 wt%), respectively.

5. The outcome of the application of ZnO/PMMA nanocomposite coating on the polycrystalline solar cell was increased in its efficiency from (11.33%) to (15.22%), where the results of the electrical properties showed that the uncoated cell was ($I_{SC} = 0.33A$, $V_{OC} = 0.38V$, and $P_{max} = 97.2$ mW), while the results of the coated cell with the best concentration (3.875 wt%) were ($I_{SC} = 0.36A$, $V_{OC} = 0.43V$, and $P_{max} = 130.6$ mW).

6.3 Recommendations

Future research should incorporate some suggestions from this study to improve it because it was specifically focused on the usage of nanocomposite coating to enhance polycrystalline silicon solar cells.

1. Investigate how the size of nanoparticles affects the effectiveness of the nanocomposite coating layer by using different nanoparticles size.

2. Use various coating techniques, such as dip-coating or spin-coating, for coating solar cells and compare the results with the coating technology that was used in this experimental work.

3. Utilizing different kinds of nano-coatings and researching how they affect the performance of the solar cell.

References:

[1]   R. Singh, R. B. Choudhary, and R. Kandulna, "Optical band gap tuning and thermal properties of PMMA-ZnO sensitized polymers for efficient exciton generation in solar cell application," *Mater. Sci. Semicond. Process.*, vol. 103, no. June, 2019, doi: 10.1016/j.mssp.2019.104623.

[2]   B. Ashok Kumar, G. Sivasankar, B. Sangeeth Kumar, T. Sundarapandy, and M. Kottaisamy, "Development of Nano-composite Coating for Silicon Solar Cell Efficiency Improvement∗," *Mater. Today Proc.*, vol. 5, no. 1, pp. 1759–1765, 2018, doi: 10.1016/j.matpr.2017.11.273.

[3]   A. M. Elbreki *et al.*, "The role of climatic-design-operational parameters on combined PV/T collector performance: A critical review," *Renew. Sustain. Energy Rev.*, vol. 57, pp. 602–647, 2016, doi: 10.1016/j.rser.2015.11.077.

[4]   L. Zhu, A. Raman, K. X. Wang, M. A. Anoma, and S. Fan, "Radiative cooling of solar cells," *Optica*, vol. 1, no. 1, p. 32, 2014, doi: 10.1364/optica.1.000032.

[5]   E. Skoplaki and J. A. Palyvos, "On the temperature dependence of photovoltaic module electrical performance: A review of efficiency/power correlations," *Sol. Energy*, vol. 83, no. 5, pp. 614–624, 2009, doi: 10.1016/j.solener.2008.10.008.

[6]   K. Rakesh Tej Kumar, M. Ramakrishna, and G. Durga Sukumar, "A review on PV cells and nanocomposite-coated PV systems," *Int. J. Energy Res.*, vol. 42, no. 7, pp. 2305–2319, 2018, doi: 10.1002/er.4002.

[7]   A. H. A. Al-Waeli, H. A. Kazem, M. T. Chaichan, and K. Sopian, *Photovoltaic/thermal (PV/T) systems: Principles, design, and applications*. 2019.

[8]   A. A. F. Husain, W. Z. W. Hasan, and M. N. Hamidon, "A review of transparent solar photovoltaic technologies," *Renew. Sustain. Energy Rev.*, vol. 94, no. June, pp. 779–791, 2018, doi: 10.1016/j.rser.2018.06.031.

[9]   H. Zhang *et al.*, "A novel thermal-insulating film incorporating microencapsulated phase-change materials for temperature regulation and nano-TiO2 for UV-blocking," *Sol. Energy Mater. Sol. Cells*, vol. 137, pp. 210–218, 2015, doi:

10.1016/j.solmat.2015.02.018.

[10] L. El Chaar, L. A. Lamont, and N. El Zein, "Review of photovoltaic technologies," *Renew. Sustain. Energy Rev.*, vol. 15, no. 5, pp. 2165–2175, 2011, doi: 10.1016/j.rser.2011.01.004.

[11] A. K. Shukla, K. Sudhakar, and P. Baredar, "A comprehensive review on design of building integrated photovoltaic system," *Energy Build.*, vol. 128, pp. 99–110, 2016, doi: 10.1016/j.enbuild.2016.06.077.

[12] "Monocrystalline vs Polycrystalline Solar Panels | American Solar Energy Society." https://ases.org/monocrystalline-vs-polycrystalline-solar-panels/ (accessed Jul. 31, 2022).

[13] Y. Yang and P. Westerhoff, "Presence in, and release of, nanomaterials from consumer products," *Adv. Exp. Med. Biol.*, vol. 811, pp. 1–17, 2014, doi: 10.1007/978-94-017-8739-0_1.

[14] P. Sharma and M. Bhargava, "Applications and Characteristics of Nanomaterials in Industrial Environment," *Int. J. Civil, Struct. Environ. Infrastruct. Eng. Res. Dev.*, vol. 3, no. 4, pp. 63–72, 2013, [Online]. Available: http://www.tjprc.org/view_paper.php?id=2701.

[15] S. Amiri and A. Rahimi, "Hybrid nanocomposite coating by sol–gel method: a review," *Iran. Polym. J. (English Ed.*, vol. 25, no. 6, pp. 559–577, 2016, doi: 10.1007/s13726-016-0440-x.

[16] P. Dwivedi, K. Sudhakar, A. Soni, E. Solomin, and I. Kirpichnikova, "Advanced cooling techniques of P.V. modules: A state of art," *Case Stud. Therm. Eng.*, vol. 21, no. December 2019, 2020, doi: 10.1016/j.csite.2020.100674.

[17] S. M. Salih, O. I. Abd, and K. W. Abid, "Performance enhancement of PV array based on water spraying technique," *Int. J. Sustain. Green Energy*, vol. 4, no. 16, pp. 8–13, 2015, doi: doi: 10.11648/j.ijrse.s.2015040301.12.

[18] S. Duttagupta, F. Ma, B. Hoex, T. Mueller, and A. G. Aberle, "Optimised antireflection coatings using silicon nitride on textured silicon surfaces based on measurements and multidimensional modelling," *Energy Procedia*, vol. 15, no. 2011, pp. 78–83, 2012, doi: 10.1016/j.egypro.2012.02.009.

[19] A. Jannat, W. Lee, M. S. Akhtar, Z. Y. Li, and O. B. Yang, "Low cost sol-gel derived SiC-SiO 2 nanocomposite as anti reflection layer for enhanced performance of crystalline silicon solar cells,"

Appl. Surf. Sci., vol. 369, pp. 545–551, 2016, doi: 10.1016/j.apsusc.2016.02.098.

[20] D. Karthik, S. Pendse, S. Sakthivel, E. Ramasamy, and S. V. Joshi, "High performance broad band antireflective coatings using a facile synthesis of ink-bottle mesoporous MgF2 nanoparticles for solar applications," *Sol. Energy Mater. Sol. Cells*, vol. 159, pp. 204–211, 2017, doi: 10.1016/j.solmat.2016.08.007.

[21] V. Kaler, U. Pandel, and R. K. Duchaniya, "Development of TiO2/PVA nanocomposites for application in solar cells," *Mater. Today Proc.*, vol. 5, no. 2, pp. 6279–6287, 2018, doi: 10.1016/j.matpr.2017.12.237.

[22] J. Jung, A. Jannat, M. S. Akhtar, and O. B. Yang, "Sol–gel deposited double layer TiO2 and Al2O3 anti-reflection coating for silicon solar cell," *J. Nanosci. Nanotechnol.*, vol. 18, no. 2, pp. 1274–1278, 2018, doi: 10.1166/jnn.2018.14928.

[23] H. J. El-Khozondar, R. J. El-Khozondar, M. M. Shabat, and D. M. Schaadt, "Solar cell with multilayer structure based on nanoparticles composite," *Optik (Stuttg).*, vol. 166, pp. 127–131, 2018, doi: 10.1016/j.ijleo.2018.04.014.

[24] A. Jalali, M. R. Vaezi, N. Naderi, F. Taj Abadi, and A. Eftekhari, "Investigating the effect of sol–gel solution concentration on the efficiency of silicon solar cells: role of ZnO nanoparticles as anti-reflective layer," *Chem. Pap.*, vol. 74, no. 1, pp. 253–260, 2020, doi: 10.1007/s11696-019-00872-0.

[25] H. Dhasmana, V. Dutta, A. Kumar, A. Kumar, A. Verma, and V. K. Jain, "Hydrothermally synthesized zinc oxide nanoparticles for reflectance study onto si surface," *Mater. Today Proc.*, vol. 32, no. xxxx, pp. 287–293, 2020, doi: 10.1016/j.matpr.2020.01.374.

[26] S. A. Khan *et al.*, "Performance investigation of ZnO/PVA nanocomposite film for organic solar cell," *Mater. Today Proc.*, vol. 47, no. xxxx, pp. 2615–2621, 2021, doi: 10.1016/j.matpr.2021.05.197.

[27] A. E. H. B. Kashyout *et al.*, "Enhancement of the Silicon Solar Cell Efficiency by Spin-Coated Polythiophene Films Embedded with Gold or Palladium Nanoparticles on the Rear Contact," *ACS Omega*, vol. 6, no. 20, pp. 13077–13086, 2021, doi: 10.1021/acsomega.1c00761.

[28] H. A. Elsayed *et al.*, "Simple and efficient design towards a

significant improvement of the optical absorption of amorphous silicon solar cell," *J. Quant. Spectrosc. Radiat. Transf.*, vol. 275, p. 107890, 2021, doi: 10.1016/j.jqsrt.2021.107890.

[29] W. Li, Y. Shi, K. Chen, L. Zhu, and S. Fan, "A Comprehensive Photonic Approach for Solar Cell Cooling," *ACS Photonics*, vol. 4, no. 4, pp. 774–782, 2017, doi: 10.1021/acsphotonics.7b00089.

[30] A. Manasrah, A. Al Zyoud, and E. Abdelhafez, "Effect of color and nano film filters on the performance of solar photovoltaic module," *Energy Sources, Part A Recover. Util. Environ. Eff.*, vol. 43, no. 6, pp. 705–715, 2021, doi: 10.1080/15567036.2019.1631907.

[31] A. Kumar and A. Chowdhury, "Reassessment of different antireflection coatings for crystalline silicon solar cell in view of their passive radiative cooling properties," *Sol. Energy*, vol. 183, no. March, pp. 410–418, 2019, doi: 10.1016/j.solener.2019.03.060.

[32] A. Kumar and A. Chowdhury, "Advanced radiative cooler for multi-crystalline silicon solar module," *Sol. Energy*, vol. 201, no. February, pp. 751–759, 2020, doi: 10.1016/j.solener.2020.03.065.

[33] F. K. Mohd Zaini *et al.*, "Synthesis of nano-TiO2 coating systems for solar cell," *Pigment Resin Technol.*, vol. 49, no. 1, pp. 26–32, 2020, doi: 10.1108/PRT-02-2019-0010.

[34] D. M. Hachim, Q. A. Abed, and F. Kamil, "New eco-friendly coating for the higher temperature solar cell by nano-composite," *Energy Sources, Part A Recover. Util. Environ. Eff.*, vol. 43, no. 20, pp. 2456–2470, 2021, doi: 10.1080/15567036.2020.1860162.

[35] A. K. Naser, D. M. H. Al-shamkhee, and Q. A. Abed, "Enhanced Electrical Properties of Crystalline Silicon Solar Cells via Nano-Composite Polyvinyl-Alcohol / Titanium Dioxide," *Int. J. Des. Nat. Ecodynamics*, vol. 16, no. 5, pp. 557–564, 2021.

[36] V. K. Gobinath *et al.*, "Surface engineering of zinc sulphide film for augmenting the performance of polycrystalline silicon solar cells," *Chalcogenide Lett.*, vol. 18, no. 7, pp. 375–384, 2021.

[37] N. Shanmugam, R. Pugazhendhi, R. M. Elavarasan, P. Kasiviswanathan, and N. Das, "Anti-reflective coating materials: A holistic review from PV perspective," *Energies*, vol. 13, no. 10, pp. 1–93, 2020, doi: 10.3390/en13102631.

[38] A. R. Forouhi and I. Bloomer, "Optical Properties of Crystalline semicond," *Phys. Rev. B*, vol. 38, no. 3, pp. 1865–1874, 1988, [Online]. Available:

http://journals.aps.org/prb/abstract/10.1103/PhysRevB.38.1865.

[39] S. Hussain, "Investigation of Structural and Optical Properties of Nanocrystalline ZnO," *Dep. Physics, Chem. Biol.*, p. 93, 2008.

[40] N. T. Yaseen, "Design and Fabrication of Antireflection ZnO Thin Film by Using Different Techniques," *AL-Nahrain Univ.*, no. July, pp. 1–77, 2017.

[41] A. Höpe, *Diffuse Reflectance and Transmittance*, vol. 46. 2014.

[42] "Solar Cell Efficiency | PVEducation." https://www.pveducation.org/pvcdrom/solar-cell-operation/solar-cell-efficiency (accessed Jun. 25, 2022).

[43] O. Dupré, R. Vaillon, and M. A. Green, "Physics of the temperature coefficients of solar cells," *Sol. Energy Mater. Sol. Cells*, vol. 140, no. October 2017, pp. 92–100, 2015, doi: 10.1016/j.solmat.2015.03.025.

[44] C. G. Popovici, S. V. Hudişteanu, T. D. Mateescu, and N. C. Chereches, "Efficiency Improvement of Photovoltaic Panels by Using Air Cooled Heat Sinks," *Energy Procedia*, vol. 85, no. November 2015, pp. 425–432, 2016, doi: 10.1016/j.egypro.2015.12.223.

[45] M. N. Islam, M. Z. Rahman, and S. M. Mominuzzaman, "The effect of Irradiation on different parameters of monocrystalline photovoltaic solar cell," *Proc. 2014 3rd Int. Conf. Dev. Renew. Energy Technol. ICDRET 2014*, 2014, doi: 10.1109/icdret.2014.6861716.

[46] M. Azzouzi, D. Popescu, and M. Bouchahdane, "Modeling of Electrical Characteristics of Photovoltaic Cell Considering Single-Diode Model," *J. Clean Energy Technol.*, vol. 4, no. 6, pp. 414–420, 2016, doi: 10.18178/jocet.2016.4.6.323.

[47] F. A. Tuma, "The Optical Constants of Poly Methyl Methacrylate PMMA Polymer Doped by Alizarin Red Dye," *Am. Int. J. Res. Form. Appl. Nat. Sci*, vol. 16, no. 1, pp. 13–18, 2016.

[48] A. Naser, D. Hachim, and Q. Abed, "A review of Effect the Zinc Oxide deposition on Crystalline Silicon Solar Cells," *Eudl*, 2022, doi: 10.4108/eai.7-9-2021.2314810.

[49] R. A. Francis, "Through thick and thin: Some observations on dry film thickness of paint coatings," *49th Annu. Conf. Australas. Corros. Assoc. 2009 Corros. Prev. 2009*, pp. 846–856, 2009.

[50] C. A. De Caro, "UV / VIS Spectrophotometry," *Mettler-Toledo Int.*, no. September 2015, pp. 4–14, 2015, [Online]. Available: http://lcwu.edu.pk/ocd/cfiles/Chemistry/MSc/Chem-C-410/Fundamentals_UV_VIS.pdf.

[51] U. Jahn, M. Herz, and T. Rheinland, *Review on Infrared (IR) and Electroluminescence (EL) imaging for photovoltaic field applications*. 2018.

[52] N. M. Ravinder, P. Ganapathy, and J. Choi, "Energy gap-refractive index relations in semiconductors- An overview," *Infrared Phys. Technol.*, 2007.

[53] M. I. Mohammed *et al.*, "Enhancing the structural, optical, electrical, properties and photocatalytic applications of ZnO/PMMA nanocomposite membranes: towards multifunctional membranes," *J. Mater. Sci. Mater. Electron.*, vol. 33, no. 4, pp. 1977–2002, 2022, doi: 10.1007/s10854-021-07402-3.

[54] J. Bagawade, "Preparation and Characterization of Zinc Oxide (Zno)/ Polymethyl Methacrylate (PMMA) Nanocomposites," *Int. J. Curr. Sci. Res. Rev.*, vol. 04, no. 04, pp. 246–250, 2021, doi: 10.47191/ijcsrr/V4-i4-01.

[55] "Electricity prices around the world | GlobalPetrolPrices.com." https://www.globalpetrolprices.com/electricity_prices/ (accessed Jul. 02, 2022).

APPENDICES

Appendix-A. Zinc Oxide Certificate

This appendix is a copy of the HWNANO-COMPANY manufacturing certificate for Zinc Oxide (ZnO) nanoparticle characteristics. Figure A1 shows the characteristics of a nanoparticle, and Figure A2 shows a scanning electron microscope test (SEM) to confirm the grain's nano-size under a microscope.

HWNANO (宏武纳米)

Product Name	Zinc Oxide (氧化锌)	
Appearance	White powder, Dispersion	合符 Conform
Shape	spherical	合符 Conform
APS	40-50 nm	合符 Conform
Purity	99.8%	合符 Conform
Specific surface area	70 m²/g	合符 Conform
True Density	5.5 g/cm³	合符 Conform

For and on behalf of
HONGWU INTERNATIONAL GROUP LTD
宏武国际集团有限公司

Authorized Signature(s)

Tel: (86) 20-87226350, (86) 20-87748017
Website: www.xuzhounano.com   E-mail: hwnano@xuzhounano.com

Figure A1. Zinc Oxide certificate
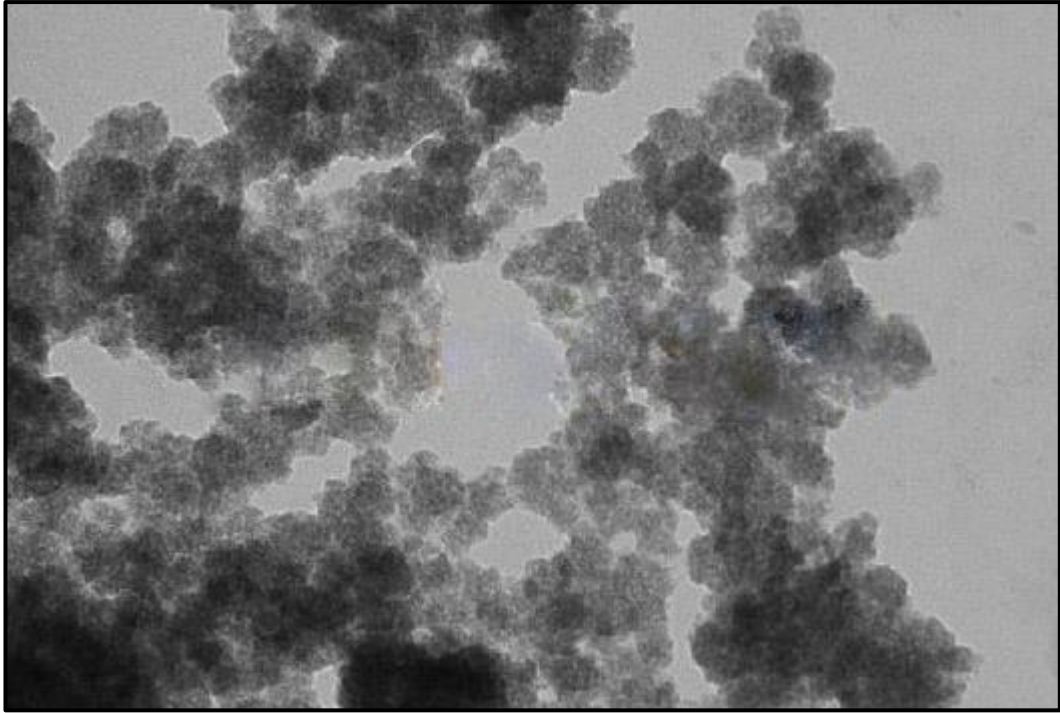
Figure A2. Zinc Oxide Scanning electron microscopy (SEM).

Appendix-B: Water Bath Ultrasonic Device (Elmasonic P-180H)

The main characteristics of the Elmasonic P180H Water Bath Ultrasonic device specifications are listed in this appendix, table B1.

Table B1. Ultrasonic water-bath properties

Property	Value
Electrical Characteristics	110/220 V (AC)
Frequency	37 / 80 kHz
Power consumption	1330W
Unit Dimensions L/W/H	39, 34, 32 cm
Basin dimension L/W/H	32, 30, 20 cm
Wight	8.5 kg
Volume tank	12 liters
Drain size	3/8"
Materials	Stainless steel V2A
Sound level (LPZ), (dB)	96 / 87

Appendix-C: Coating Thickness Gauge

Table C1. Coating thickness gauge properties

Property	Value
Temperature range	0 - 60 °C
Humidity	20% - 90% RH
Power source	12 V, 600 mA
Dimensions	270 mm ×86 mm ×47 mm
Weight	530 g
Probe-type	N-400
Coating thickness-range	0 - 400 μm

Appendix-D. Solar Meter Calibration

Table D1 and Figure D1. Shows the specifications of the solar meter (Pyranometer) and calibration**.**

Table D.1 solar meter characteristics (Pyranometer).

Property	Value
Model	DT-1307 (CME)
Range	1999 W/m^2, 634 BTU/(ft^2×h)
Resolution	1 W/m^2, 1 BTU/(ft^2×h)
Accuracy	± 10 W/m^2 (± 5%)
Sampling time	Approx 0.25 second
Humidity	<80% RH
Weight	176 g
Dimension H/W/D	162mm x 63mm x 28mm
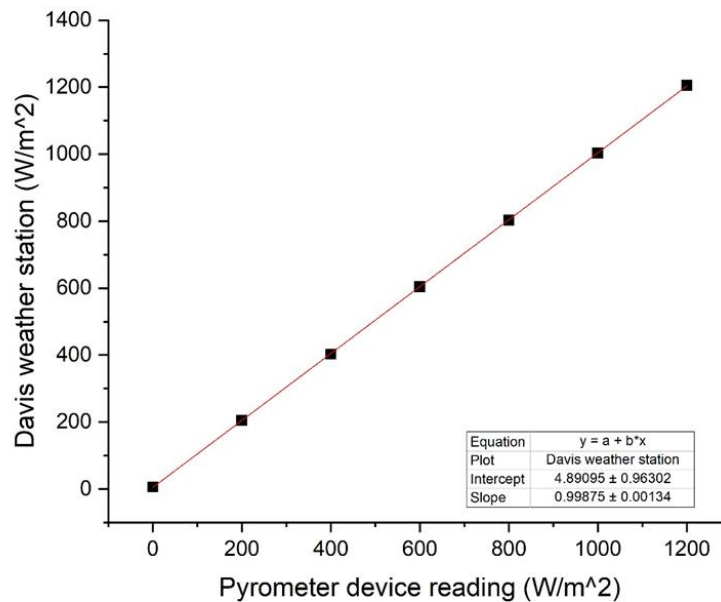
Figure D1. solar meter calibration (Pyranometer)

Appendix-E: Mini Dual-channel K/J Thermometer, UT-320D

Table E1. Specifications of Mini Dual-channel K/J Thermometer

Property	Value
Model	**UT-320D**
Working temperature	0 ºC- 40 ºC
Range of temp. Measurement (K)	-50 ºC – 1300 ºC
Range of temp. Measurement (J)	-50 ºC – 1200 ºC
Accuracy	$\pm (5\% +1)$
Sampling time	4 time/ second
Humidity	<80% RH
Power	3-batteries (1.5 V)
Weight	0.06 kg
Dimension H/W/D	120mm ×53mm ×28mm

Appendix-F: Thermal Imaging Infrared Camera, FLIR E-30bx

Table F1. Specifications of Thermal Imaging Infrared Camera.

Property	Value
Model	FLIR E-30bx
Temperature range	-20 ℃ - 120 ℃
Working temperature	-15 ℃- 50 ℃
Thermal sensitivity	0.1 ℃
Focal Plane Array detector	160 x 120 (19,200 pixels)
Accuracy	2%
Measurement modes	up to 3 moveable Spots

Appendix-G: Solar Module Analyzer, PROVA-200A

Table G1. Specifications of solar module analyzer

Property	Value
Model	**PROVA-2001**
Range (Voltage/ current)	60 V / 6 A
Resolution	± 0.1 %
Accuracy (Voltage/ current)	1% ± 0.09V /1% ± 9mA
Sampling time	4 time/ second
Power	AC 110V or 220V input
Battery Type	Rechargeable 2500mAh (1.2V) x 8
Weight	1160 g
Dimension L/W/H	257mm ×155mm ×57mm

Appendix-H: Thermocouples calibration system

This appendix represents the calibration process for K-Type thermocouples which was used in this work, figure H.1, 2, and 3 show the calibration data.

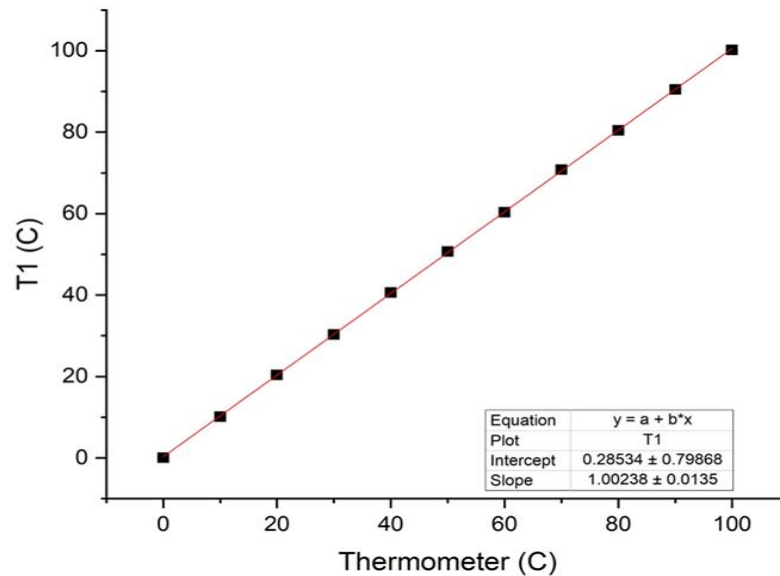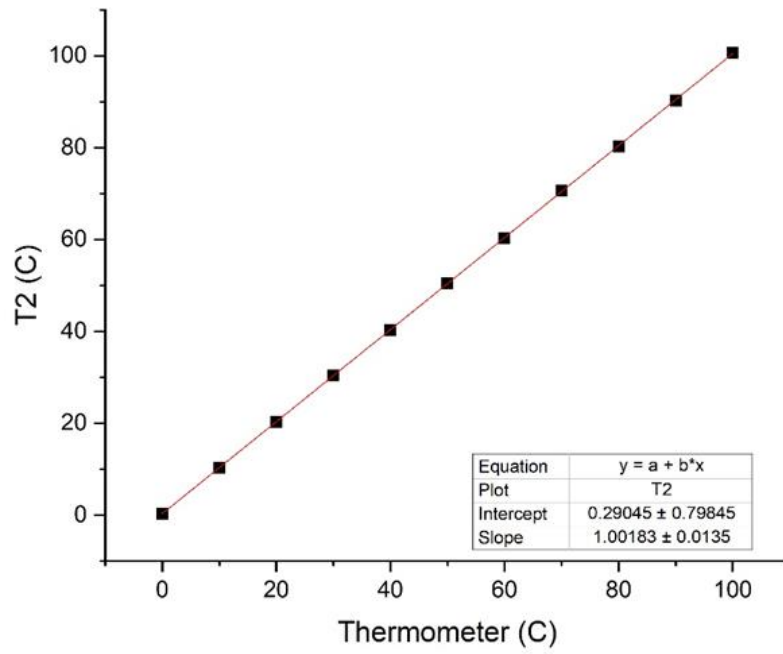| Equation	y = a + b*x
Plot	T1
Intercept	0.28534 ± 0.79868
Slope	1.00238 ± 0.0135

Figure H1. Temperature calibration T1

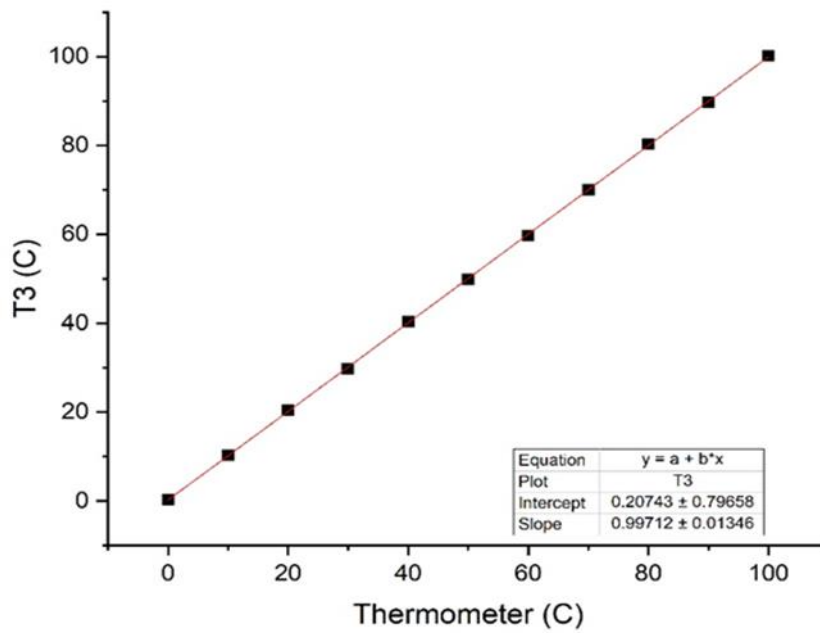Figure H2. Temperature calibration T2

Figure H3. Temperature calibration T3

Appendix. I-List of publications

1- Ali Majid Abbood, Qahtan Adnan Abed **" Using the Nanocomposite Coating Technology to Improve PV Solar Cell Performance: A review"** 1st International Conference on Achieving the Sustainable Development Goals (ICASDG-2022), Q4 Scopus Journal.

1st International Conference on Achieving the Sustainable Development Goals

(6th – 7th) June 2022 in Istanbul- Turkey

Final Acceptance Letter

Manuscript Number: 37

Dear: Ali Majid Abbood

Co-Authors: Qahtan A. Abed

Congratulations!

It's a great pleasure to inform you that, after the peer review process, your manuscript entitled

(Using the Nano-Composite Coating Technology to Improve PV Solar Cell Performance: A review)

had been **ACCEPTED** for participating in the **1st International Conference on Achieving the Sustainable Development Goals,** and considered for publication in **(AIP Conference proceeding).**

Thank you for your valuable participation in the ICASDG2022 conference.

Prof. Dr. Ahmed G. Wadday
ICASDG2022 Scientific Committee Chair | AIP Conference Proceeding Editor
6th – 7th June 2022 | Istanbul | Turkey

2- Ali Majid Abbood, Qahtan Adnan Abed "**Enhancing the Photovoltaic Cells' Efficiency by Controlling Surface Temperature with Polymethyl methacrylate (PMMA) Coating Thin Layer**"

4th International Conference on Sustainable Engineering Techniques (ICSET-2022), Q4 Scopus Journal.

4th International Conference on Sustainable Engineering Techniques (ICSET 2022)

Baghdad, Iraq, 5-6 October, 2022

Letter of Acceptance and Invitation   Ref: 25   Date: 27 / 6 / 2022

Paper ID: 29

Paper Title:

Enhancing the photovoltaic cells' efficiency by controlling surface temperature with polymethyl methacrylate (PMMA) coating thin layer

Dear Ali Majid Abbood , Qahtan A Abed

With heartiest congratulations I am pleased to inform you that based on the recommendations of the reviewers; your paper identified above has been accepted for publication and oral presentation by the 4th International Conference on Sustainable Engineering Techniques (ICSET 2022). Your paper will be published in the AIP Conference Proceedings.

Herewith, the Conference Organizing Committee sincerely invites you to present your paper at the conference to be held at the Middle Technical University / Engineering Technical College, Baghdad, Iraq, 5- 6 October, 2022.

We look forward to your participation in the ICSET 2022.

Yours sincerely,

Prof. Dr. Nabil Jamil Yasin

ICSET 2022 Organizing Committee, Baghdad, Iraq.

https://icset4.tecb.mtu.edu.iq/

الخلاصة

الطاقة الشمسية هي واحدة من أهم مصادر الطاقة المتجددة نظرًا لانها صديقة للبيئة وإمكانية الحصول عليها في نطاق واسع وتعد مصدرًا مهمًا للطاقة الخضراء وذلك لأنها على عكس الموارد الأحفورية التي ينبعث منها الكربون ، قابلة للتجديد ويمكن الوصول إليها بسهولة. من أكثر الطرق الواعدة والمنتشرة بكثرة استخدام الخلايا الشمسية الكهروضوئية (PVs) ، وهي عبارة عن أشباه موصلات تحول الطاقة الشمسية إلى تيار كهربائي باستخدام الفوتونات المنبعثة من الشمس لإثارة الإلكترونات فيها. فعند تعرض الخلية الشمسية الكهروضوئية للضوء ، يتم توليد الجهد والتيار. تعاني كفاءة الألواح الكهروضوئية من انخفاض ملحوظ في تحويل الطاقة الشمسية مع ارتفاع درجة حرارة سطح الخلية الشمسية ، حيث تنخفض الكفاءة بحوالي 0.45٪ لكل 1 درجة مئوية ارتفاع في درجة حرارة سطح الخلية الشمسية. بالإضافة إلى ذلك ان الخلايا الشمسية السليكونية تعكس ما يقرب من 35٪ من إجمالي كمية ضوء الشمس الساقط على سطحها، مما يؤدي إلى انخفاض الكفاءة الكهربائية للوحدات الكهروضوئية.

في هذا البحث على وجه التحديد تم العمل على خلايا (Polycrystalline silicon solar cell) لدراسة تأثير اضافة طبقة رقيقة من الطلاء النانوي على درجات الحرارة وخسائر الانعكاس على الخلايا الشمسية المصنوعة من السيليكون متعدد الكريستالات. حيث تم استخدام طلاء نانوي (Nanocomposite) لطلاء السطح العلوي للخلية الشمسية بأغشية رقيقة مصنوعة من بوليمر بولي ميثيل ميثاكريلات (PMMA) وجزيئات أكسيد الزنك (ZnO) ذات الحجم النانوي (40-50 نانومتر). تم استخدام تراكيز مختلفة من (ZnO) و (PMMA) (,0.25 wt%, 0.5 wt% و (0.75 wt%, and 1 wt%) و (0.625wt%, 1.25 wt%, 2.5 wt%, 3.125 wt%, and 3.75 wt%) على التوالي ، وذلك لغرض تحضير أربعة تراكيز من طلاء المركب النانوي(ZnO / PMMA) (4.125 ,3.375 wt%, 3.625 wt%, 3.875 wt%, and wt%). تم عمل الفحوصات المخبرية باستخدام جهاز المطياف (U-V spectrophotometer) و بناءً على اختبار كفاءة وقدرة الخلايا الشمسية باستخام جهاز (Solar-module analyzer)، اظهرت النتائج أن PMMA يؤثر على نظام حجب الأشعة فوق البنفسجية وبالتالي يقلل درجة حرارة سطح الخلية الشمسية ويعمل اوكسيد الزنك النانوي (ZnO) كمضاد للانعكاس من خلال زيادة فجوة الطاقة (Energy gap) وبالتالي يقلل من خسائر الانعكاس. سجل أفضل تركيز لـ PMMA هو (3.125 wt%) من حيث قدرته على امتصاص أكبر مقدار من الأشعة فوق البنفسجية. اما ZnO فان (0.75 wt%) هو أفضل تركيز تم اختياره من حيث قدرته على تقليل خسائر الانعكاس لذلك فان أفضل تركيز من الطلاء النانوي (ZnO / PMMA) هو (3.875 wt%). حيث سجلت النتائج ان 8.6 درجة مئوية هو اقصى فرق في درجة الحرارة مقارنةً بالخلية الشمسية بدون طلاء ، والحد الأدنى لخسائر الانعكاس التي تم الحصول عليها هي 5.6٪ مقارنةً بالخلية الشمسة بدون طلاء التي تعكس حوالي 35٪.وان مقدار التحسين في كفاءة الخلية الشمسية كانت بنسبة + 3.8٪.

طلاء مادة نانوي مركب لتحسين كفاءة الخلايا الشمسية في ظروف الطقس الحار

رسالة مقدمة الى

قسم هندسة تقنيات ميكانيك القوى في الكلية التقنية الهندسية – النجف – جامعة الفرات الاوسط التقنية كجزء من متطلبات نيل شهادة الماجستير في هندسة تقنيات ميكانيك الحراريات

تقدم بها

علي ماجد عبود

اشراف

الأستاذ الدكتور

قحطان عدنان عبد

محرم ١٤٤٤ه